

# PHYSICS, CHEMISTRY AND BIOGEOCHEMISTRY IN SOIL AND PLANT STUDIES

**MULTI-AUTHORS WORK**

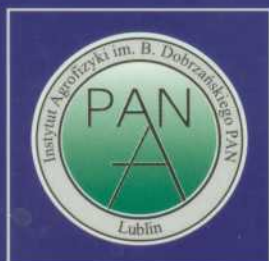
EDITED BY GRZEGORZ JÓZEFACIUK



**Centre of Excellence for Applied  
Physics in Sustainable  
Agriculture AGROPHYSICS**



**Institute of Physicochemical  
and Biological Problems in Soil  
Science  
Russian Academy of Sciences**



**Institute of Agrophysics  
Polish Academy of Sciences**

# **PHYSICS, CHEMISTRY AND BIOGEOCHEMISTRY IN SOIL AND PLANT STUDIES**

## **MULTI-AUTHORS WORK**

### SCIENTIFIC COMMITTEE

Ryszard Walczak

Grzegorz Józefaciuk

Józef Horabik

Valery Kudeyarov

Andry Alekseev

David Pinsky

### EDITOR

Grzegorz Józefaciuk

© Institute of Agrophysics PAS, Lublin

---

Print: Drukarnia *ALF-GRAF*, ul. Kościuszki 4, 20-006 Lublin

## **PREFACE**

Soil-plant-atmosphere system, our living environment.  
And its components: Soil – microbiologically active, extremely heterogeneous, multiphaseous, multicomponential, polydispersive; Plant – living organism with all its peculiarities; and Atmosphere within which everything is soaked. And extremely complex interrelations between these elements.

People wonder how science can deal with so complicated system. Fortunately some of them want to do this and like it. They study history and present, and try to predict the future. They find mechanisms and construct models to improve the system and protect it against degradation to leave it properly working for next generations. Sometimes they meet to exchange knowledge and experience, to discuss new ideas and place new hypotheses. To cooperate in research.

This issue contains some scientific results and opinions of such people, who met together during an international workshop hold in Puschchino, Russia 22-23 March 2004, organized by:

Grzegorz Józefaciuk, Andry Alekseev and Olga Khokhlova,  
in the frame of the scientific activity and with financial support of:

Centre of Excellence for Applied Physics in Sustainable  
Agriculture AGROPHYSICS

Institute of Physicochemical and Biological Problems in Soil  
Science of Russian Academy of Sciences

Institute of Agrophysics of Polish Academy of Sciences

SCIENTIFIC COMMITTEE

## *IN MEMORIAM*

### *Dr Ludmila Petrovna Korsunskaja*



**August 17, 1946**

**1966-1971** student of *Donetcky State University*,

**1972-2004** worker of *Institute of Physicochemical and Biological Problems in Soil Science of RAS*,

- junior researcher of *Physicochemical Laboratory* (1972-1982)
- researcher of the *laboratory of Bioproductivity of Agrocenoses* (1982-1988)
- senior researcher of the *laboratory of Mass- and Energy Transfer in Soils* (1988-2001)
- senior researcher of the “*Soil-Ecological Station*” laboratory (2001-2004)

**February 14, 2004**

*Participants of the workshop use the opportunity to sacrifice this page for Dr. Luda Korsunskaja, excellent soil physicist and chemist, and our best friend, who unexpectedly leaved us just few days ago. She will live in our memories.*

*Words are not suitable to describe the loss. Our memories will be helping us to imagine our caring, compassionate, energetic, and witty colleague and friend. Dr. L. P. Korsunskaja has made an important contribution in understanding and predicting solute transport in structured soil, which is the most difficult and challenging field in modern soil physics. She has advanced soil physics by applying fundamental advances and techniques of physical chemistry. It has been a pleasure to work with Luda as she was most reliable, knowledgeable, responsible, and helpful partner. The first thing to recall is her kindness, compassion and smile. This will stay with all of us and will help all of us.*

*Yakov Pachepsky  
Soil Scientist  
Agricultural Research Service  
United States of America*

## **MECHANISMS OF FORMATION AND OCCURRENCE OF IRON OXIDES IN SOILS – RELATIONSHIP TO VARIOUS ENVIRONMENTAL CONDITIONS.**

*Alekseev A.O., Alekseeva T.V., Maher B.A*

Iron oxides and hydroxides play an important role in soil science and environmental research. There are thirteen “iron oxides” known to date. The more important and predominant in soil science, mineralogy, geology Fe oxides are the following: goethite, hematite, lepidocrocite, ferrihydrite, maghemite and magnetite, akaganeite, ferrosityte. The significance of Fe- compounds and importance of Fe-oxides as suitable indicators of certain pedogenic environments has been recognized by many researchers. Fe-oxide minerals form under the influence of the common soil forming factors (temperature, moisture, pH, Eh, etc), and therefore reflect the pedoenvironmental conditions under which they have formed. In the modern literature, extensive material exists regarding the basic tendencies of formation and transformation of iron minerals in sediments and soils of different climatic zones. However, this kind of information for soils of the steppe and semi-desert zone is limited, as traditionally it was considered that in these geochemical conditions iron minerals are stable and, therefore, their indicative role for soil forming processes is not important. There are also a number of methodical difficulties of diagnostics of iron minerals, because of the rather small content of iron and its forms in soils of these climatic zones. Here, the results of analysis of steppe and semi- desert soils obtained with a range of magnetic and more traditional mineralogical methods are presented.

The most interest for our studies is the sensitivity of certain soil iron compounds to climate and environmental changes. Schwertmann (1988) demonstrated (mostly on the basis of bulk X ray diffraction analyses and chemical analyses) the response of haematite and goethite to different, climatically-driven pedogenic regimes. For example, the goethite-haematite ratio in soils varies systematically along climatic, hydrological and topographic transects.

Our data for steppe zone had shown the active role of the Fe in soil-geochemical processes (oxidation media, neutral and/or alkaline conditions) what permits to use its state as informative indicator of soil-geochemical processes under the impact of natural and anthropogenous factors. Obtained data demonstrate that iron state reflects environmental conditions not only on macro- (geochemical landscape), but on microscale (soil aggregates).

Environmental magnetism methods are now of wide use for the soils study .The magnetic properties of soils are often dominated by formation of the strongly

magnetic (ferrimagnetic) oxides, magnetite and maghemite – usually in concentrations undetectable by XRD but easily measurable by routine magnetic methods of analysis. Hence, magnetic analyses of soils provide an additional, sensitive window on soil iron and its response to climate.

Statistical examination of the relationships between magnetic properties of modern steppe soils from transect spanning the loess plain from the Caspian Sea to the North Caucasus and major climate variables identifies annual rainfall as the most significant factor ( $R^2 = 0.93$ ) (Maher et al., 2003). Soil formation in the steppe zone produces dispersed ferrimagnetic minerals (magnetite and maghemite) with particle size of predominantly  $\ll 0.1 \mu\text{m}$  which control the soil magnetic properties. The variety of shapes and sizes of magnetic particles, particularly the prevalence of grains of irregular, round, and oval shapes points to the predominantly soil genesis of these minerals. The quantitative content of ferrimagnetic minerals reflects the bioclimatic conditions of soil formation (Alekseev et al., 2003).

Environmental in situ production of magnetic minerals either through pedogenic or biogenic processes appears to be the major source of submicron magnetic particles. The production processes of these super dispersed ferrites in soil are debated.

Our mineralogical and microbiological investigation characterizes the nature of the carriers of the soil magnetic properties and identifies the possible mechanisms that lead to their formation.

Fe can act as an electron donor or receptor in microbial metabolism. And, in magnetite ( $\text{Fe}_3\text{O}_4$ ), Fe is a constituent of a sometimes biogenic mineral that may serve as a biosignature in soils and rocks from ancient Earth. Iron reducing bacteria (IRB) were determined in all studied steppe soils with up to  $10^5$  cells/g of soil. (Zavarzina et al., 2003). The formation of fine superparamagnetic ( $<10 \text{ nm}$ ) magnetite was observed in the soil samples after stimulating the growth of IRB. A comparison of the population of iron reducing bacteria in chestnut soils and chernozems shows the difference as in the variety of IRB as in the variety of “magnetic products” related to the type of soil and bioclimatic environment. This fact confirms previously obtained coupling between soil magnetism and climate.

The magnetic data ( $\chi$  susceptibility,  $\chi_{\text{ARM}}$  and SIRM) of the steppe soils are dominated by rather small concentrations of the ferrimagnets (magnetite/maghemite concentrations of 0.04 – 0.2%). The high-field remanence (HIRM) values indicate haematite concentrations of between  $\sim 0.08$  and 4 %. The climatically determined relationship in concentration of ferrimagnets and most oxitic iron oxides during soil development was observed. (Fig 1).

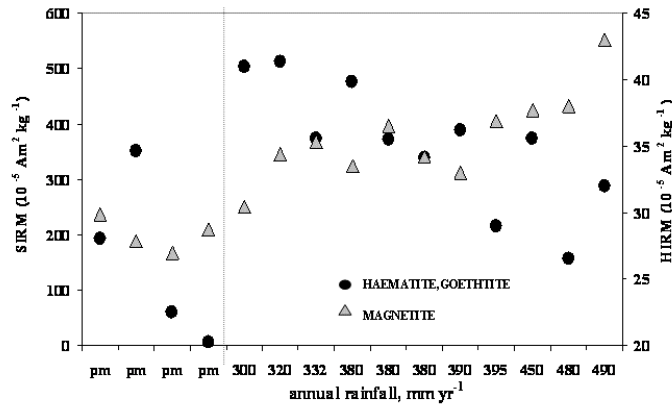


**Fig.1.** Iron Oxides Magnetic Mineralogy and climate relationship – SIRM(magnetite) and HIRM100mTaf (haematite, goethite) for parent materials (pm) and representative soil samples versus annual rainfall

The biogeochemical cycle of iron at neutral pH in steppe soils, with formation of secondary ferrimagnetic minerals may follow the following sequence: the flux of Fe from primary Fe bearing minerals to the microbiologically active zone as a function of intensity of weathering; poorly crystalline hydrous ferric oxide (ferrihydrite) formation by iron bacteria (*Gallionella sp.*; *Leptotrix sp.*, *Toxothrix sp.*) in oxidizing conditions. Higher oxidation rates, higher organic matter and lower pH (~ 4-6) predispose formation of goethite, whilst haematite is favoured by higher temperatures, decreased water activity and higher pH (~7-8) (Schwertmann, 1988). In soils, magnetite formation requires the initial presence of some Fe<sup>2+</sup> cations. Even in generally well-drained and oxic soils, like the steppe soils, Fe<sup>2+</sup> can be formed in soil micro-zones, made temporarily anoxic during periods of soil wetness, via the activity of iron-reducing bacteria (*Geobacter sp.*, *Shewanella sp.*, *et al*). In locally anoxic condition poorly crystalline hydrous ferric oxide will be reduced by iron reducing bacteria with formation of magnetite or siderite. Intermittent wetting and drying of soils will thus predispose formation of magnetite, in the presence of organic matter and a weathering source of iron. To produce a ‘constant’ grain size distribution (as in the steppe soils), magnetite formation must thus be initiated under ‘constant’ environmental conditions. Such constancy in the natural environment can be explained if the bacteria which produce the required Fe<sup>2+</sup> only operate within, and/or create via their metabolism, a certain set of pH, Eh and Fe conditions. In contrast to these optimal magnetite-forming conditions, longer periods of dryness, with increased oxidation rates and

reduced water activity, would favour formation of the more oxidic iron compounds, and goethite. Thus, a climatically determined, equilibrium magnetic value will be reached due to feedback between formation of ferrimagnets and their subsequent loss by oxidation.

The rate of formation of secondary ferrimagnetic minerals in soils is connected with the flux of Fe from primary Fe-bearing minerals. That is a function of the intensity and duration (time) of weathering. Once formed, Fe-oxides may be the subject to continual modification in an approach toward equilibrium with the changing soil environment. The investigation of sets of buried soils (a chronosequences spanning ~5000 years) from the steppe region does not confirm the fact that time is the main factor responsible for pedogenic enhancement of ferrimagnetic minerals concentration. Duration of the weathering determines the total pool of iron released from silicates and involved into formation of soil iron oxides in the connection with climatic conditions.

**Acknowledgements.** This research was supported by the Russian Foundation for Basic Research and the Program of Presidium of RAS for Basic Research

## REFERENCES

1. A.O. Alekseev, T. V. Alekseeva, and B. A. Maher Magnetic Properties and Mineralogy of Iron Compounds in Steppe Soils Eurasian Soil Science Vol. 36, No. 1, 2003 p. 59-70
2. Maher B.A., Alekseev A., Alekseeva T. Magnetic mineralogy of soils across the Russian steppe: climatic dependence of pedogenic magnetite formation. Palaeogeography, Palaeoclimatology, Palaeoecology. (2003), V. 201, N 3-4, P. 321-341
3. Schwertmann, U., 1988. Occurrence and formation of iron oxides in various pedoenvironments. In J.W. Stucki, B.A. Goodman and U. Schwertmann (eds.), Iron in Soils and Clay Minerals., D. Reidel, Dordrecht, NATO ASI Series C217, 267-308
4. Zavarzina D. G., Alekseev A. O., and Alekseeva T. V. The Role of Iron-Reducing Bacteria in the Formation of Magnetic Properties of Steppe Soils Eurasian Soil Science Vol. 36, No. 10, 2003,p.1085 -1094

## EFFECT OF EARTHWORMS BY SOIL INGESTION ON ATRAZINE ADSORPTION AND BIODEGRADATION

*Alekseeva T., Besse P., Binet F., Delort A-M., Forano C., Sancelme M.*

Atrazine (2-chloro-4-ethylamino-6-isopropylamino-1,3,5-triazine=AT) remains still nowadays one of the most widely used herbicide in corn growing areas. It is the most frequently detected herbicide in surface and groundwater, and its concentration often exceeds at least 10 to 100 fold the standard policy. High persistency of AT and its degradation products causes numerous environmental problems and makes the study of AT behavior of priority status.

The fate of pollutants in the ecosystems depends mainly on the processes in which they are involved in soils before the entering the ground and surface waters. Adsorption/desorption are the most important mode of interaction between soil components and pollutant that controls its availability towards microbial degradation, its retention or mobility through the soil profile. According to the studies, soil-sorbed organic compounds have been considered unavailable for biodegradation without prior desorption (Ogram *et al.* 1985; Crocker *et al.* 1995) or still degradable by microorganisms. The potential activity of herbicide degrading bacteria in soils can often be greatly modified, depending on the physico-chemical properties of the soil, but also on the interactions between herbicide and soil components (sorption, retention, formation of complexes), or on the interactions of bacteria with soil components .

Without doubt soil - biotic interactions have also to be considered to adequately estimate atrazine sorption and availability in soil, however little research have been undertaken to assess the role of soil fauna in these processes. Regarding the soil fauna, earthworms greatly disturb the soil structure and soil porosity by their casting and burrowing activities (Binet & Curmi 1992), leading to significant changes in physico-chemical and microbial soil properties. Earthworm casts differ from the surrounding soils because of the food selection made by worms and changes during soil gut transit (physico-chemical, enzymatical and microbial changes). Earthworms ingest preferentially the finest mineral soil particles (mostly clays) and the organic ones (leaf and root litter debris, fungal and bacterial cells). As a result, casts often have much higher contents of OM and nutrients and contain more fine-textured material than the surrounding soil. Therefore, earth worm casts seem particular the substrate wherein the adsorption of the molecules and their interactions with the soil matrix might be different than in un-ingested soil.

In this paper AT sorption by surface horizon of hydromorphous soil from natural riparian wetland (Brittany, France) was studied. Special attention has been paid to modifications of soil properties under the influence of earth worms (*Aporrectodea giardi*) by soil ingestion and their effect on atrazine adsorption. To investigate the effect of possible AT-soil interactions on bioavailability of AT and on kinetics of its biodegradation, laboratory experiments were performed under soil slurry conditions with a model well-characterized AT-degrading bacterium *Pseudomonas* sp. strain ADP (Mandelbaum *et al.* 1995). Worm casts were laboratory prepared by *Aporrectodea giardi* (Lumbricidae). Soil used for casts production was sampled from 20 cm top layer from studied soil profile (PF7). Deposited casts were sampled from the soil surface every 24 hs.

Carbon (total and organic) content in samples was determined with Shimadzu TOC-5050A equipment. Composition of humic substances was determined in the accordance with the method of Ponomareva & Plotnikova (1980). Cation exchange capacity and exchangeable bases content were obtained by ammonium acetate method with 1:10 solid: liquid ratio and pH 7. Mineralogical composition of bulk soil samples and their clay fractions was determined by X-ray diffractometry.

Atrazine (AT) stock solution of 30mg/l for adsorption experiments was prepared in mineral water (Volvic, France). Adsorption of AT was carried out using batch-equilibration technique at 25°C in darkness. 1 g of solid was agitated for 24h with 10 ml of 3, 6, 9, 12, 15, 18, 21, 24, 27 and 30 mg/l AT. After adsorption, supernatants were passed through solid phase extraction cartridges "Oasis" HLB, and AT was extracted with methanol.

For biodegradation experiments, *Pseudomonas* sp. strain ADP was grown in 100-ml portions of Trypticase Soy broth in 500-ml Erlenmeyer flasks incubated at 30°C at 200 rpm. The cells were harvested after 15 hs of culture. Extracts obtained from adsorption and biodegradation experiments were analyzed by HPLC analysis (Perkin Elmer series 200) with a UV detector ( $\lambda = 225\text{nm}$ ). A mixture of acetonitrile with acetate buffer was used as the mobile phase (30/70 V/V).

Earthworms change visibly the properties of the parent soil. Worm casts are characterized by lower pH, are enriched in organic carbon, clay fraction, have larger CEC and exchangeable Ca content. Bulk cast sample is higher in C, HA, HA/FA ratio, degree of humification ( $\Sigma C_{\text{HA}}/C$ ) in a comparison with parent soil. Clay fraction of cast sample contains less C, lower proportion of humic acids, and is characterized by smallest HA/FA ratio and degree of humification in a comparison with clay fraction separated from parent soil. This is, probably, connected to the preferential ingestion of slightly decomposed organic fragments.

Both soil and cast are characterized by similar mineralogical composition of clay fractions: predominantly muscovite (30-45 %) – kaolinite (35-40 %)

association and absence of minerals with swelling lattice (smectite type). Parent soil sample contains lepidocrocite ( $\gamma$ -FeOOH). The presence of lepidocrocite confirms the prevailing of reductomorphic conditions, which favour the formation of Fe II - required precursor for lepidocrocite synthesis. Casts in a comparison with parent soil they do not contain lepidocrocite. The fast dissolution of lepidocrocite (the age of casts was about 24 hs) can be caused by the activity of iron reducing bacteria and worms' enzymes or enhancement of CO<sub>2</sub> production in casts.

Adsorption isotherms were linear and best described by Freundlich equation. The mean amounts of adsorbed AT for concentrations 3-30 mg/l were 18 % for the soil and 34 % for the cast. Distribution coefficients,  $K_d$ , expressed as the ratio of the amount of AT adsorbed per unit mass of sorbent ( $x/m$ ) to the amount of pesticide in the equilibrium solution ( $C_e$ ) were  $22 \cdot 10^{-4}$  and  $52 \cdot 10^{-4}$ . Kinetics of AT biodegradation in the presence of parent soil sample, cast and its fractions is presented on Fig. 1. Worm casts had a greater effect on biodegradation than the corresponding soil: AT has completely disappeared within 5hs of incubation instead of 9hs for soil.

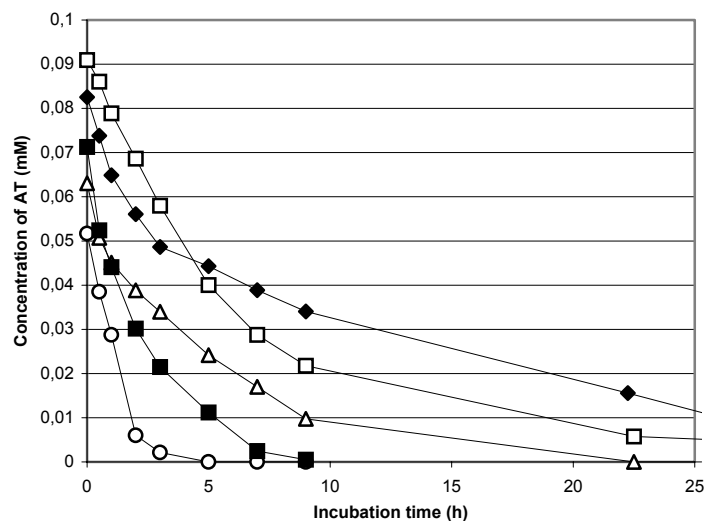


**Fig. 1.** Kinetics of AT biodegradation in the absence (◆) or in the presence of solid: (■) soil PF7 0-20 cm bulk; (○) worm cast bulk; (△) worm cast clay; (□) worm cast bulk OM free (NaOH treated).

Organic carbon content and its parameters such as humic acids content, humic/fulvic acids ratio plays the primary role in AT adsorption. Good correlations

were obtained with clay content, pH, exchangeable Ca. Non-swelling layer silicates and iron-hydroxide (lepidocrocite) sorb negligible quantity of AT. Worm cast demonstrates larger capacity for AT adsorption than parent soil due to higher OC and HA content, HA/FA ratio and, probably, additional AT adsorption on slightly decomposed OM, microbial or fungal biomass and specific compounds like proteins, polysaccharides (intestinal mucous) excreted during gut transit. The presence of natural solids (both soil and worm cast) greatly stimulates AT biodegradation. The effect seems to be linked to the content and composition of OM, but also to other parameters: granulometry, desorption rate, bacterial cell characteristics like attachment to the solid matrix particles, chemotaxis towards AT, etc.

**Acknowledgements.** This research is part of TRANZAT project which was supported by CNRS/ Programme “Environnement, Vie et Sociétés / Ecosystèmes et Environnement”.

#### REFERENCES.

1. Binet, F. & Curmi, P. 1992. Structural effects of *Lumbricus terrestris* (Oligochaeta, Lumbricidae) on soil/organic matter system: micromorphological observations and autoradiographies. *Soil Biology and Biochemistry*, 24, 1519-1523.
2. Crocker F.H. , Guerin W.F. & Boyd S.A. 1995. Bioavailability of naphtalene sorbed to cationic surfactant-modified smectite clay. *Env. Sci. & Techn.*, 29, 2953-2958.
3. Mandelbaum R.T. , Allan D.L. & Wackett L.P. 1995. Isolation and characterization of a *Pseudomonas* sp. That mineralizes the s-triazine herbicide atrazine. *Applied and Env. Microbiology*, 61, 1451-1457.
4. Ogram A. V., Jessup R.E., OU L.T., & Rao P.S.C. 1985. Effects of sorption on biological degradation rates of (2,4-dichlorophenoxy)acetic acid in soils. *Applied and Environmental Microbiology*, 49, 582-587.
5. Ponomareva, V.V. & Plotnikova, T.A. 1980. Humic substances and soil formation. Leningrad, Nauka, 220 (in Russian).

## USING PETROGRAPHIC AND MAGNETIC METHODS FOR THE SOILS PARENT MATERIAL ORIGIN INDICATION

*Alekseeva V.A.*

Data from quartz grain micromorphology were compared with those obtained from magnetic and heavy mineral analysis for two sections of Pleistocene sediments in the Upper Oka River Basin (central part of the Russian Plain). The aim of the study was to compare the particularities of depositional processes and sediment provenance for the Early-Middle Pleistocene alluvial sediments, two horizons of the Middle Pleistocene moraines, which are divided by the complex of fluvial-glacial and lacustrine sediments, and the Late Pleistocene cover loams on the top surfaces, which are the soil's parent rocks (Complex analysis ..., 1992).

The published heavy mineral data suggests the one primary source from Scandinavia for two separate moraine layers, thus the difference in the relative content of material derived from Scandinavian source was noticed (Complex analysis ..., 1992). The increase in content of hornblende, garnet and epidote and decrease of staurolite, tourmaline, glauconite and siderite content is characteristic for younger moraine layer and can be explained by the gradual loss of influence of the underlying, carbonate-rich bedrocks and greater input of Scandinavian material. The data obtained by magnetic measurements show the largest differences between the pre-glacial alluvial sediments of Early-Middle Pleistocene age and the complex of glacial sediments of Middle Pleistocene age (Alekseeva, Hounslow, in prep.). The lowest values of magnetic mineral abundance characterize pre-glacial sediments and can be explained by fluvial reworking of the carbonate-rich bedrocks. The glacial sediments contain up to 16 times larger amounts of magnetic material with the maximum values for the younger moraine layer and cover loams. Such a difference between the two moraine complexes is probably a reflection of the greater Fe-oxide content in sediments from the Scandinavian source.

The study of the quartz surface grain micromorphology by scanning electron microscope (SEM) is a tool for help in differentiating ancient sedimentary environments and potential transport mechanisms (Krinsley and Doornkamp, 1973; Higgs, 1979). This methodology assumes that grain shape and surface features reflect the environmental history of the discrete particles. Abrasion of quartz produces mechanical surface textures, which are characteristic for specific environments. Features due to chemical action can also be distinguished by means of the SEM and a number of criteria are available to separate these mechanical and chemical textures (Krinsley and Doornkamp, 1973).

In present investigation the quartz surface grain micromorphology was studied on the 0.25-0.5 mm sand fraction. The complex of 13 quartz surface microtextures of mechanical and chemical origin was observed, which had been described previously in many studies (Krinsley, Doornkamp, 1973; Higgs, 1979). They are, angular and rounded outlines, conchoidal fractures, straight steps, fracture plates, parallel striations, straight and curved scratches and grooves, V-shaped indentations, upturned plates, oriented etch pits, adhering particles, solution pits and crevasses (Alekseeva, 2003). The special combination of these microtextures allowed conclusions to be made about the likely transport histories of the clastic grains (Higgs, 1979; Krinsley, Donahue, 1968; Krinsley, Doornkamp, 1973). The analysis of surface micromorphology of quartz grains from studied sediments allowed separating the three main grain groups:

A) The mostly subangular grains show the prevalence of conchoidal fractures, fracture plains and straight steps, which are the result of the weathering processes or glacial transport (Krinsley, Doornkamp, 1973; Fig. 1-A). A considerable number of grains with such a suite of surface textures have more rounded outlines, V-shaped indentations and curved grooves overprinted on their surfaces and indicate that these quartz grains were transported by water either prior to, during, or after the glacial transport.

B) The subrounded and rounded grains show the presence of small conchoidal fractures, V-shaped indentations, straight and curved grooves and scratches, which are considered to be the product of high-energy fluvial transport in coastal or riverine settings (Higgs, 1979; Fig. 1-B).

C) The grains with subrounded and rounded outline, small conchoidal fractures, upturned plates and dish-shaped concavities were formed during the aeolian transport (Krinsley, Doornkamp, 1973; Fig. 1-C).

The sediments of different origin show the difference in the content of quartz grains of the groups mentioned. The grains with water transport traces absolutely dominate in alluvial sediments. Grains from weathered rocks and aeolian material appear in glacial sediments. Fluvial-glacial sediments vastly have processed the moraine deposits and differ from them by bigger contents of grains with traces of water processing that can be explained by the existence of more dynamic conditions during the glacier retreating. The lacustrine sediments between two moraine layers contain a lot of aeolian grains. The cover loams deposits inherit the composition of glacial sediments; the increasing of the contents of grains with traces of water conversion in contrast with moraine was observed.

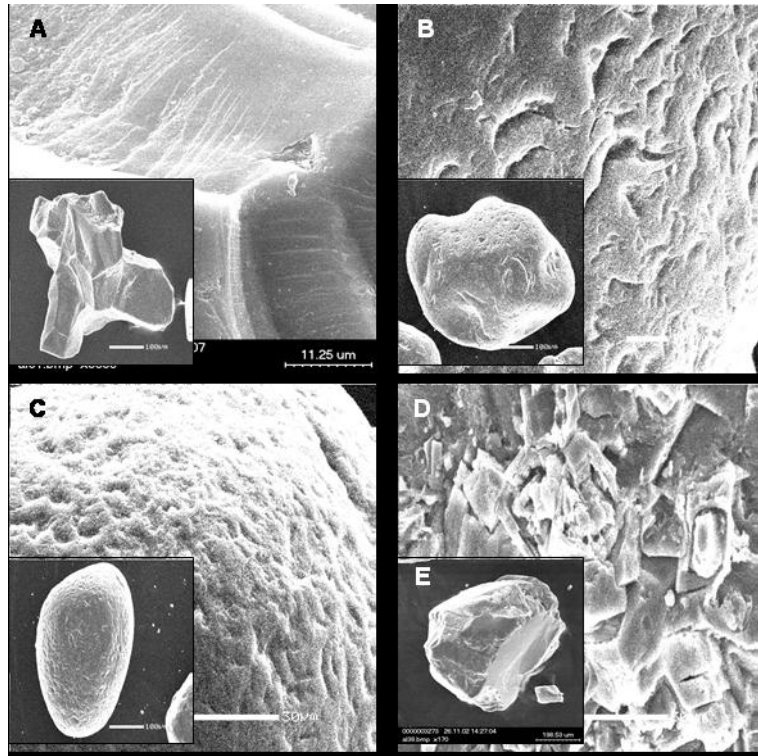


**Fig.1.** Micromorphology of quartz grains from the Pleistocene sediments in the Upper Oka River Basin: A – grains formed as a result of glacial transport; B – grains with the traces of water reworking; C – grains with the traces of wind reworking; D – adhering clays particles as a result of diagenesis; E – traces of cryogenetic weathering.

Commonly present on the majority of studied grains, are adhering clays particles forming accumulations of different thickness both on the exposed grain surfaces and within the fracture planes and depressions (Fig. 1-D). They are perhaps the result of diagenesis (Krinsley, Doornkamp, 1973). Solution pits and crevasses are probably the result of *in situ* chemical weathering. The content of grains with such surface features increases in cover loams deposits and can be explained by the activity of soil processes. Many grains carry the traces of cryogenic weathering, which is reflected in the presence of fresh conchoidal fractures on the grains surface (Rogov, 2000; Fig. 1-E).

Hence, the micromorphology suggests that the quartz grains of the studied sediments have an unexpectedly heterogeneous origin of aeolian and fluvial processes, as well as the anticipated glacial origin. The content of these grains groups varies for the sediments of different origin. The heavy minerals and magnetic data provide information about provenance differences and reflect the influence of the Scandinavian sources but not the transport processes as surface micromorphology data.

The data obtained characterize the historical-genetic sequence of events of glacial morpholithogenesis that can be considered as a certain trend of the change in properties of sediments of different origin. These sediments (predominantly cover loams on the top surfaces) are the parent rocks for soils and can provide important information for palaeoenvironmental reconstructions.

## REFERENCES

1. Alekseeva V.A. 2003. Data on the transport and diagenetic transformation of quartz grains and their palaeogeographical interpretation (in the Upper Don River Basin). *Vestnik Moskovskogo Universiteta, ser. 5 Geography*, 4, 40-46 (in Russian).
2. Alekseeva V.A., Hounslow M.W. Sediment provenance determination using discrete and included magnetic particles: a comparison with petrographic methods (in pres.).
3. Complex analysis of the quaternary sediments of the Satino practice territory (ed. by G.Rychagov and S.Antonov). 1992. Moscow State Univ. Press, Moscow, 18-19, (in Russian).
4. Higgs R. 1979. Quartz-grain surface features of Mesozoic-Cenozoic sands from the Labrador and Western Greenland continental margins. *Journal of Sedimentary Petrology*, 49, 599-610.
5. Kinsley D.H.; Donahue J. 1968. Environmental interpretation of sand grain surface features by electron microscopy. *Geol.Soc.America Bull.*, 79, 743-748.
6. Kinsley D.H.; Doornkamp J.C. 1973. *Atlas of quartz sand surface textures*, Cambridge, Cambridge Univ. Press.
7. Rogov V.V. 2000. The peculiarities of morphology of particles of cryogenic weathering products. *The Earth's Cryosphere*, vol.IV, 3, 67-73 (in Russian).

## OXYGEN STRESS IN THE ROOT ZONE AND PLANT RESPONSE (SOME EXAMPLES)

*Balakhnina T.I., Bennicelli R.P., Stepniewska Z., Stepniewski W.*

One of the essential negative consequences of the soil flooding is oxygen deficiency in the tissues of the submerged plants. Oxygen deficiency effects the intensity and the direction of a number of physiological and biochemical reactions and induces oxidative stress in the plant cells (Bennicelli et al. 1998, Blokhina et al., 1999; Hunter et al., 1987; Yan et al., 1996, Zakrzhevsky et al. 1995).

Under optimal conditions the content of reactive oxygen species (ROS) maintains, with the help of antioxidative defence system, at a level which is safe for the organism (Larson, 1988). Enzymes of superoxide dismutase and ascorbate – glutathione pathway eliminate the excess of H<sub>2</sub>O<sub>2</sub> in chloroplasts, in the cytoplasm and in non photosynthesizing tissues (Foyer and Halliwell, 1976). Under stress conditions the formation of ROS can exceed the antioxidative potential of the cell and cause an oxidative damage (Halliwell, 1984).

The plant capability to activate the defense system against oxidative destruction may be a key link in the mechanism of plant tolerance to unfavorable conditions. Changes in the activity level of one or more antioxidative enzymes are connected with the plant resistance to stressor action (Allen, 1995). The aim in this paper was to show response of stomatal resistance (R<sub>d</sub>) on the examples of some plants: *Triticum aestivum L.*, *Triticale L.*, *Zea mays L.*, *Pisum sativum L.* reaction planted on unfavorable soil conditions through hypoxia to anoxia conditions. As the indicators of soil aeration conditions Oxygen Diffusion Rate (ODR) and redox potential (Eh) were used as described by Gliński and Stepniewski (1985).

### MATERIALS AND METHODS

The experiments were performed with the use of *Triticum aestivum L.*, *Triticale L.*, *Zea mays L.*, *Pisum sativum L.* under growth chamber in plastic pots, 5.9 dm<sup>3</sup> in volume, filled with soil material from the Ap horizon of a brown loess soil (Orthic Luvisol) of pH in H<sub>2</sub>O - 7.3 (pH in KCl - 7.1) containing 0.89% C<sub>org</sub>, 15% of 1 -0.1m fraction, 80% of 0.1-0.002 mm fraction, and 5% clay. Each pot contained 6.2 kg of soil (dry mass basis) packed to a bulk density 1.35 Mg m<sup>-3</sup> corresponding to total porosity 48% v/v .

The air temperature was kept at 23±2°C and 12±2°C during the day and night, respectively. The day period was 12 hours with the light intensity of 190 Wat m<sup>-2</sup>. The relative air humidity in the growth chamber was 45±5% during the day and 70±5% during the night.

As the indicators of soil aeration conditions the air-filled porosity (Eg), Oxygen Diffusion Rate (ODR) and redox potential (Eh) were used as described by Gliński and Stepniewski (1985).

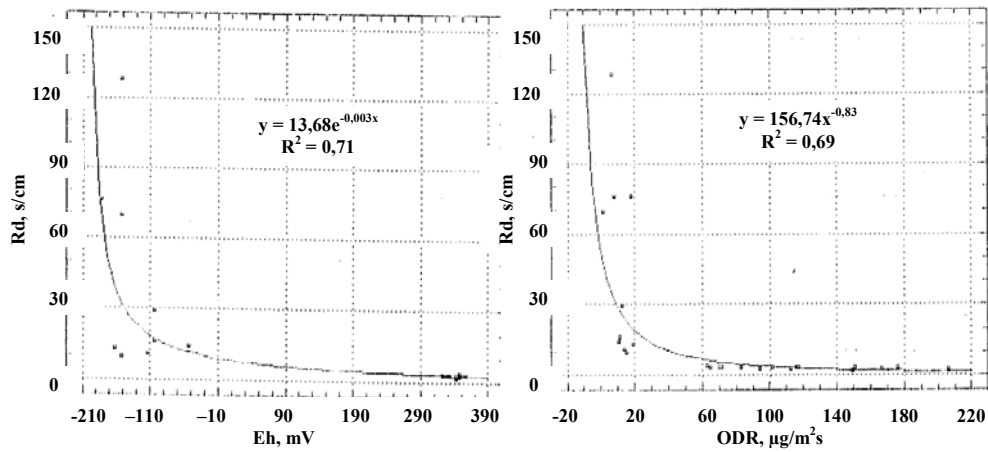


**Fig. 1.** Leaf stomatal resistance ( $R_D$ ) of *Pisum sativum* L. as a function of Eh i ODR of the soil after 12 days of oxygen stress.

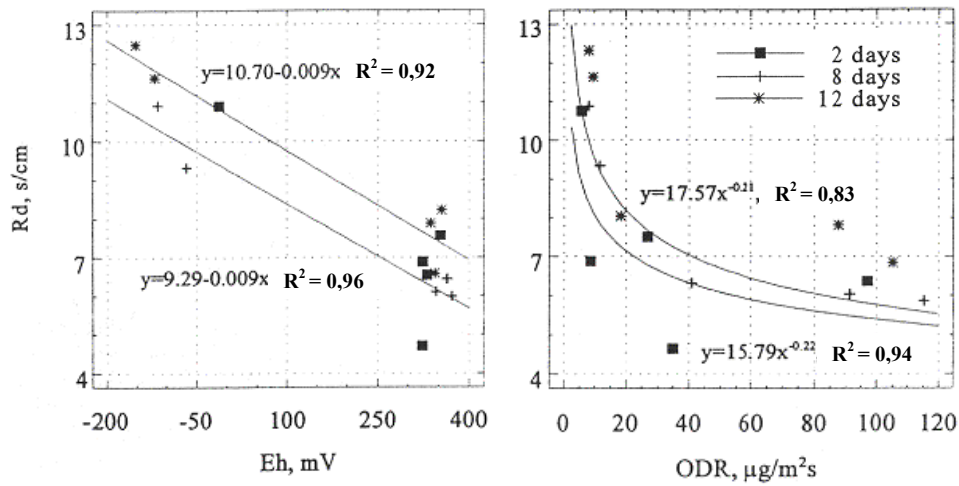


**Fig 2.** Leaf stomatal resistance ( $R_D$ ) of *Zea Mays* L. as a function of Eh i ODR of the soil after 12 days of oxygen stress.

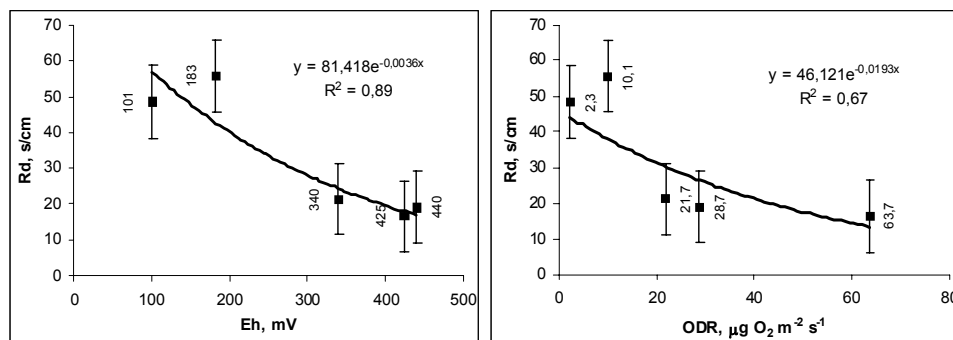


**Fig. 3.** Changes of stomatal diffusive resistance ( $R_d$ ) in relation to  $E_g$ , ODR and  $E_h$  (*Triticum aestivum* L.). Mean value  $\pm$  standard deviation.

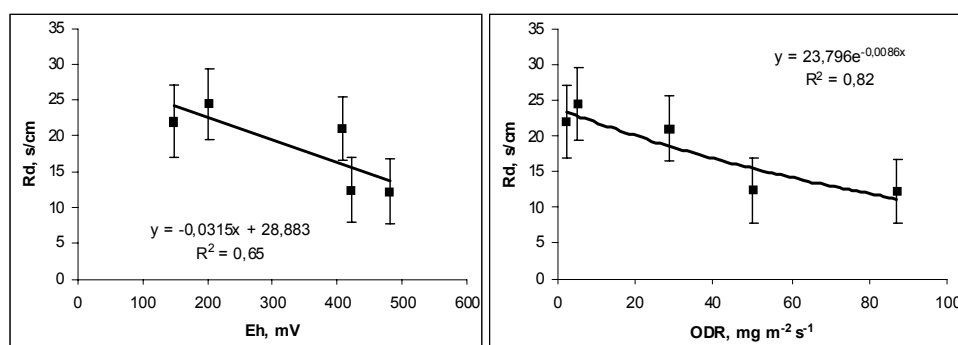


**Fig. 4.** Changes of stomatal diffusive resistance ( $R_d$ ) in relation to  $E_g$ , ODR and  $E_h$  (*Triticale*). Mean value  $\pm$  standard deviation.

## RESULTS

After 12 days of growth under unfavorable conditions of aeration the availability of oxygen to roots ODR were change from 210 to 2  $\mu\text{g m}^{-2} \text{ s}^{-1}$  and  $E_h$  from 490 to -180 mV.

Under oxygen deficiency conditions experienced by the plant roots during the 12 days of flooding the soil a generalized adaptive response took place in the leaves, which were in the normal aerobic conditions (Zakrzhevsky et al., 1995; Yan et al., 1996). The root hypoxia resulted in an increase of the value of leaf stomatal diffusive resistance up to 130 and 60 s/cm in *Pisum sativum* L. as well *Triticum aestivum* L- non tolerant of oxygen stress plant; and up to 25 and 13 s/cm in the case of *Triticale* L. and *Zea mays* L - less sensitive to the effect of unfavorable factors plants.

Stomatal diffusive resistance of the leaves (Fig.1-4) express relations between soil and plant parameters in relation to soil aeration. In each tested plant increased of  $R_d$  was observed under hypoxia or anoxia conditions. This relation can be describe by linear or curvilinear relationships with high correlation coefficients at  $R^2 = 0.65-0.96$  for redox potential and at  $R^2=0.67- 0.94$  for oxygen diffusion rate. From results obtained Eh is seems to be more effective parameter of soil aeration status.

## REFERENCES

1. Allen RD (1995) Dissection of oxidative stress tolerance using transgenic plants. *Plant Physiol* 107: 1049-1054.
2. Bennicelli RP, Stepniewski W, Zakrzhevski DA, Balakhnina TI, Stepniewska Z, Lipiec J (1998) The effect of soil aeration on superoxide dismutase activity, malondialdehyde level, pigment content and stomatal diffusive resistance in maize seedlings. *Environ and Experim Bot* 39: 203-211.
3. Blokhina OB, Fagerstedt KV, Chirkova TV (1999) Relationships between lipid peroxidation and anoxia tolerance in a range of species during post-anoxic reaeration. *Physiologia Plantarum* 105: 625-632.
4. Foyer CH, Halliwell B (1976) The presence of glutathione reductase in chloroplasts: a proposed role in ascorbic acid metabolism. *Planta* 133: 21-25.
5. Glinski J, Stepniewski W (1985) *Soil Aeration and its Role for Plants*. CRC Press. Boca Raton, USA.
6. Halliwell B (1984) Oxidative damage, lipid peroxidation and antioxidant protection in chloroplasts. *Chem. Phys. Lipids* 44: 327-340.
7. Larson RA (1988) The antioxidants of higher plants. *Phytochemistry* 27 : 969 – 978.
8. Yan Bin, Qiujie Dai, Xiaozhong Liu, Shaobai Huang and Zixia Wang (1996) Flooding-induced membrane damage, lipid oxidation and activated oxygen generation in corn leaves. *Plant and Soil* 179: 261-268.
10. Zakrzhevsky DA, Balakhnina TI, Stepniewski W, Stepniewska S, Bennicelli RP, Lipiec J (1995) Oxidation and growth processes in roots and leaves of higher plants at different oxygen availability in soil. *Fiziol Rast*: 42: 272-280. *Russian Plant Physiol* 42: 242-248.

## AEROBIC CONDITIONS AND ANTIOXIDATIVE SYSTEM OF *AZOLLA CAROLINIANA* IN THE PRESENCE OF Hg IN WATER SOLUTION

*Bennicelli R.P., Balakhnina T.I., Stepniewska Z., Szajnocha K.,  
Banach A.*

### INTRODUCTION

High concentration of heavy metals effects like other stress conditions in plants a number of physiological and biochemical reactions and induces oxidative stress in the plant cells (Noctor and Foyer 1998, Blokhina et al., 1999; Hunter et al., 1987; Yan et al., 1996). Formation of reactive oxygen species (ROS) takes place in the cells of all the plants and is a consequence of normal aerobic metabolism. Under optimal conditions the content of ROS maintains, with the help of antioxidative defense system, at a level which is safe for the organism (Larson, 1988). Thus superoxide dismutase scavengers superoxide anion - radical ( $O_2^-$ ) in the cytoplasm, chloroplast and mitochondria (Bowler et al., 1992). Under stress conditions the formation of ROS can exceed the antioxidative potential of the cell and cause an oxidative damage (Halliwell, 1984).

The plant capability to activate the defense system against oxidative destruction may be a key link in the mechanism of plant tolerance to unfavorable conditions. Changes in the activity level of one or more antioxidative enzymes are connected with the plant resistance to stressor action (Allen, 1995). Previously we found (Bennicelli et al., 1998) that maize response to soil aeration conditions (as evaluated by biomass production and stomatal diffusive resistance) and the advancement of destructive processes (as assessed by malondialdehyde content) as well as the antioxidant system status (expressed by SOD activity) were related to soil oxygen availability as measured by oxygen diffusion rate (ODR). Similar dependences of growth and oxidative processes to soil aeration parameters was also shown for pea known as flood intolerant plant (Zakrzhevsky et al, 1995).

The aim of the paper was to investigate the response of *Azolla caroliniana* Willd. defense system in the presence of different concentration of Hg and availability of oxygen in water solution.

### MATERIALS AND METHODS

The studies were performed under model laboratory conditions with the use of aquatic fern *A. caroliniana*. The air temperature was kept at  $25 \pm 2^\circ\text{C}$  and 18/6 photoperiod was applied. The relative air humidity was on the level  $70 \pm 5\%$ . As the

indicators of soil aeration conditions Oxygen Diffusion Rate (ODR) was used as described by Gliński and Stepniewski (1985).

Plant defense system was characterized by superoxide dismutase (SOD) measurements by spectrophotometric method of Paoletti et al (1986), based on oxidation of NADH by superoxide anion radicals. The enzyme extract was diluted 20-fold before the analysis. As a unit of SOD activity, 50% inhibition of NADH oxidation rate was used. Analyses were performed from the crude homogenates and enzyme extracts from control and treatment plants. All the results were calculated per one gram of leave dry mass.

Three replications of each experimental treatment were done. The variability of treatments was analysis by ANOVA test. The relationship between ODR or SOD activity and time (day) of prolonged experiment is expressed by correlation coefficient ( $R^2$ ) and by correlation equation.

## RESULTS

The availability of oxygen to roots of *A. caroliniana* plants differentiated in the wide range what was indicated by changes of the control ODR values  $20\text{-}30\mu\text{g m}^{-2}\text{s}^{-1}$  to  $50\mu\text{g m}^{-2}\text{s}^{-1}$  under higher Hg concentration (Fig. 1). In the presence of  $30\text{ mg Hg dcm}^{-3}$  adaptation time (1-4 days) for *A. caroliniana* plants was needed. After this time increasing values of ODR were observed. The level of the availability of oxygen (ODR) indicated the release oxygen by roots *A. caroliniana* to water medium. Release of oxygen from the roots of *Typha latifolia* at the level of  $0.12\text{-}0.20\text{ mmol O}_2\text{ DW h}^{-1}$  was described by (Jespersen et al. (1998).

The SOD activity (Fig. 2) in the leaves of the control plants was during the experimental period within the normal physiological range 1800-3000 u. In the presence of Hg(II) in water solution increasing of SOD activity in plant tissue was observed up to 4000 u what indicates the sensitive response of defense system of *A. caroliniana* to environmental stress.

This reaction is comparable to adaptive response of plant under oxygen deficiency conditions experienced by the plant roots during the period of flooding the soil and took place in the leaves, which were in the normal aerobic conditions (Zakrzhevsky et al., 1995; Yan et al., 1996).

Under these conditions limitation of the amount of final electron acceptor in electron transport chain –  $\text{NADP}^+$  favors functioning of oxygen as an alternative acceptor of electrons. Induction of such reactive oxygen species as superoxide radical ( $\text{O}_2^-$ ) and hydrogen peroxide ( $\text{H}_2\text{O}_2$ ) initiates processes of lipid peroxidation and leads to a serious damage of cells and of the entire organism. (Egneus et.al.,1975). Increase of the rate of  $\text{O}_2^-$  and  $\text{H}_2\text{O}_2$  generation in leaves of plant under soil hypoxia was correlated with lipid peroxidation (Yan et al., 1996).

Protection of plants from oxidative destruction is associated with active functioning of SOD activity in roots and leaves under waterlogging conditions (Zakrzhevsky et al., 1995).

Many plants are able to survive stress conditions when antioxidative enzymes is not the long - term and the active functioning of enzymes-detoxicators i.e. SOD is effective.

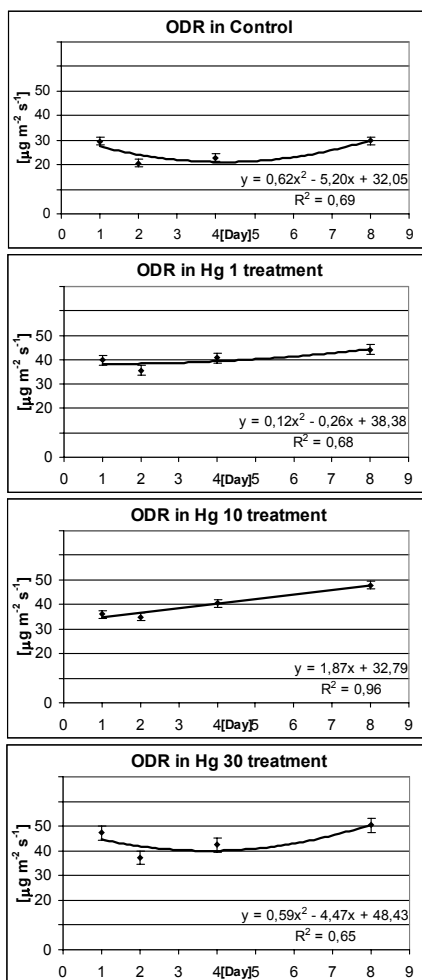


**Fig. 1.** Dynamic of Oxygen Diffusion Rate in the soil at different experimental treatments.

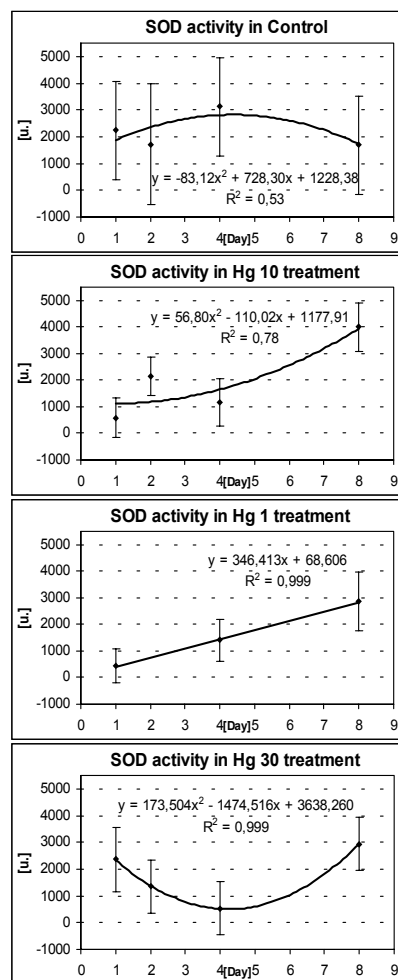


**Fig. 2.** The Superoxide Dismutase activity in plant tissues at different experimental treatments.

## REFERENCES

1. Allen RD (1995) Dissection of oxidative stress tolerance using transgenic plants. *Plant Physiol* 107: 1049-1054
2. Bennicelli RP, Stepniewski W, Zakrzhevski DA, Balakhnina TI, Stepniewska Z, Lipiec J (1998) The effect of soil aeration on superoxide dismutase activity, malondialdehyde level, pigment content and stomatal diffusive resistance in maize seedlings. *Environ and Experim Bot* 39: 203-211
3. Blokhina OB, Fagerstedt KV, Chirkova TV (1999) Relationships between lipid peroxidation and anoxia tolerance in a range of species during post-anoxic reoxygenation. *Physiologia Plantarum* 105: 625-632
4. Egnéus H, U Heber, M Kirk (1975) Reduction of oxygen by the electron transport chain of chloroplasts during assimilation of carbon dioxide. *Biochim Biophys Acta* 408: 252-268
5. Halliwell B (1984) Oxidative damage, lipid peroxidation and antioxidant protection in chloroplasts. *Chem Phys Lipids* 44: 327-340
6. Hunter MIS, Hetherington AM and Crawford RMM (1983) Lipid peroxidation – A factor in anoxia intolerance in *Iris* species. *Phytochemistry* 22: 1145-1147
7. Jespersen DN, Sorrell BK, Brix H (1998) Growth and root oxygen release by *Typha latifolia* and its effects on sediment methanogenesis. *Aquatic Botany* 61: 165-180
8. Noctor G and Foyer CH (1998) Ascorbate and glutathione: keeping active oxygen under control. *Ann. Rev. Plant Physiol. Plant Mol. Biol.* 49: 249-279
9. Yan B, Dai Q, Liu X, Huang S, Wang Z (1996) Flooding-induced membrane damage, lipid oxidation and activated oxygen generation in corn leaves. *Plant & Soil* 179: 261-268
10. Zakrzhevsky DA, Balakhnina TI, Stepniewski W, Stepniewska S, Bennicelli RP, Lipiec J (1995) Oxidation and growth processes in roots and leaves of higher plants at different oxygen availability in soil. *Fiziol Rast.* 42: 272-280. *Russian Plant Physiol* 42: 242-248

## PROBLEM OF STANDARDIZATION OF SOIL PHYSICS METHODS.

*Bieganowski A., Walczak R.T.*

One of the most important criteria, enabling a comparison of the results, obtained in various laboratories is the standardization of research methods. It is especially important in reference to the studied media, which are characterized with high variability in time and space. Surely, it is possible to rate soil among such media.

The specificity of agrophysical measurements of soils is connected with the fact, that soil is an object in which continuous physical phenomena and chemical reactions take place. These phenomena and reactions, connected with changing external conditions (e.g. changes of temperature, rainfall, etc.) as well as with life processes of microorganisms and organisms living in the soil, cause the variability of soil properties in time. Additionally, the variability and large heterogeneity of soil properties in space gives the view of difficulties, to be faced by physicists dealing with measurements performed in the soil environment.

International Standardization Organization (ISO) has perceived the problems of measurements, realized in the soils. The confirmation of this fact is the output of the Technical Committee TC 190 "Soil quality". This committee, which is divided into 6 sub-committees, has elaborated 70 standards\* till now:

- TC 190/SC 1 "Evaluation of criteria, terminology and codification" (6 standards)
- TC 190/SC 2 "Sampling" (5 standards)
- TC 190/SC 3 "Chemical methods and soil characteristics" (32 standards)
- TC 190/SC 4 "Biological methods" (15 standards)
- TC 190/SC 5 "Physical methods" (9 standards). The whole breakdown of SC 5 standards is presented in Table 1.
- TC 190/SC 7 "Soil and site assessment" (3 standards)

Taking into consideration the numbers of officially published standards, concerning the chemical and biological methods, it should be stated that the number of standardized physical methods is relatively small.

---

\*<http://www.iso.ch/iso/en/stdsdevelopment/tc/tclist/TechnicalCommitteeDetailPage.TechnicalCommitteeDetail?COMMID=4381>. State actual on 10/02/2004.

Table 1. Breakdown of numbers and titles of standards elaborated by TC190/SC 5 “Physical methods”

ISO 10573:1995	Soil quality - Determination of water content in the unsaturated zone - Neutron depth probe method
ISO 11272:1998	Soil quality - Determination of dry bulk density
ISO 11274:1998	Soil quality - Determination of the water-retention characteristic - Laboratory methods
ISO 11276:1995	Soil quality - Determination of pore water pressure - Tensiometer method
ISO 11277:1998	Soil quality - Determination of particle size distribution in mineral soil material - Method by sieving and sedimentation
ISO 11277:1998/Cor1:2002	
ISO 11461:2001	Soil quality - Determination of soil water content as a volume fraction using coring sleeves - Gravimetric method
ISO 11508:1998	Soil quality - Determination of particle density
ISO 16586:2003	Soil quality - Determination of soil water content as a volume fraction on the basis of known dry bulk density - Gravimetric method

Before the international standard is finally accepted by ISO, the procedure of standards elaboration provides several intermediate stages. Particular projects of a given standard, which are the effect of the work performed in a stage, are accordingly denoted at the standard’s number. For instance:

- ISO/CD denotes Committee Draft and is the result of work done in a working group. This is the first proposition to formulate this problem in the form of a standard. A possibility exists to publish several CDs.
- ISO/DIS denotes *Draft International Standard* and is the effect of consultation and discussion, which took place outside the working group.
- ISO/FDIS denotes *Final Draft International Standard* and is the last version of the document, proceeding an official publication.

One of working groups - SC SC5, in the second half of the 90-ies, led to publishing ISO/CD 12229 „Soil Quality – Determination of soiling water content volume fraction – Time Domain Reflectometry (TDR) and Time Domain Transmissometry (TDT) Methods”.

The procedure of standard’s elaboration is a little bit arduous and prolonged in time. It requires that the experts from various countries were engaged in the working group. Therefore, particular persons can resign of different motives from

participation in a working group and the quorum is not preserved. In such case the work on a given standard are suspended.

Such situation took place in case of the standard ISO/CD 12229. The decision of ISO/TC 190/SC 5 WG 3 “Water content” from 7/11/2000, suspended the work on further elaboration of the standard.

Taking into consideration that the normalization of the soil water content measurement with application of TDR technology is really needed by the users, the Institute of Agrophysics PAS in Lublin in the frame of the Center of Excellence “Agrophysics” has made a trial to reactivate the works on that standard.

To strengthen our efforts we would like to prompt the participants of this conference to support this work. This support can consist in making the national standardization committees in particular countries interested in joining this issue.

## MORPHOLOGICAL AND PHYSICOCHEMICAL PROPERTIES OF STEPPE PALEOSOILS AS A BASIS FOR RECONSTRUCTION OF NATURE IN THE PAST

*Borisov A.V., Alekseev A.O., Alekseeva T.V., Demkin V.A.*

During the past few decades investigations of ancient barrows have been carried out in close cooperation by archaeologists and environmental scientists. The objects of their investigations are paleosoils buried under archaeological monuments. The main points of such investigations are as follows: (1) the kurgans are not only monuments of ancient history but also monuments of nature; (2) the properties of the soils of past epochs preserved under kurgan embankments retain information about the climatic conditions of their formation and development. Comparative analysis of paleosols buried under the kurgan mounds in different historical epochs, enables one to obtain information about the dynamics of soil properties and thus to reconstruct the climatic changes and pedogenesis regularities in the area.

This paper concerns with the transformation of soil properties influenced by the climate changes as well as the soil forming condition development. To answer the questions five paleosoils of different ages buried under the kurgan as well as modern background soils in the southeastern part of the Russian Plain have been studied. According to  $^{14}\text{C}$ -dating the kurgans were created  $5100\pm 50$ ,  $4410\pm 100$ ,  $4260\pm 120$ ,  $4120\pm 70$  and  $3960\pm 40$  years BP (the Mayckop Culture, the, Early and Developed period of the Katakomb Culture). The paleosoil studies of archaeological monuments were conducted in the southern part of the Ergeny Upland, in the neighborhood of Iki-Burul (the Republic of Kalmykia).

The most ancient paleosoil is dated back  $5100\pm 50$  BP, Cal. 3966-3803 BC. The paleosoil had differentiated profile with prismatic structure of the solonetz horizon B. The thickness of humus horizon was 36 cm (Fig.1.); HCl reaction began at the depth of 30 cm. The thickness of carbonate accumulation zone was about 50 cm, with the impregnation forms of carbonate neoformations prevailing in the upper part whereas the nodule forms prevailing in the lower one. The carbonate content in the accumulation zone was 13-14%; the middle value in the layer 0-50 cm was 4.4% (Fig.3). The content of the easily soluble salts and gypsum did not exceed 0,6% (Fig.2). The upper boundary of the salt accumulation zone was on the depth 60 cm. There were many Fe-Mn- oxide neoformations in the horizons B1, B2, and BC. On the whole, the morphological and chemical properties of the paleosoil are close to those of modern soils.

Next paleosol is dated back 4410±100 BP, Cal. 3304-2911 BC. The paleosol properties are also close to these of modern soils. But some soil parameters indicate that the climate in the middle of the third Millennium BC differed from that of present days. In particular, the salt concentration in the buried soil was virtually

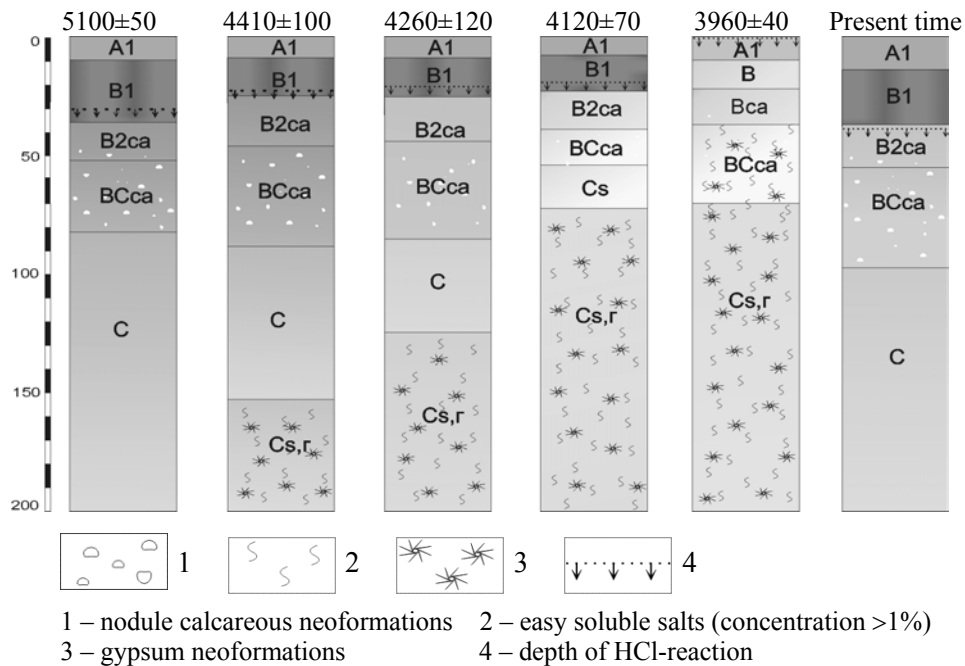


**Fig. 1.** Stratigraphy morphology of the paleosols and modern surface soils

higher, with the content of chloride in the upper part of soil profile exceeding 600 ppm. Evidently, this kind of soil salinity was due to increasing the salt transfer by the wind, sodium chloride, in the first place, from the Caspian Sea, the process occurring when the climate becomes more arid. On the other hand, the HCl-reaction begun at the depth of 28cm, the thickness of carbonates accumulation zone reached 63cm, with the calcareous new formations in the nodule form prevailing. The gypsum content was less than 1% (Fig.2.). The Illuvial horizon B had prismatic structure with signs of solonetzic process developing. The upper part of the soil-forming rock had been leached from the easily soluble salts and gypsum. It is typical of the paleosol to contain many Fe-Mn oxide neoformations in the form of thin pellicles and coatings on the soil particle surface in the horizons B1, B2 and BC. Fe and Mn are known to immobilize at Eh exceeding 450 mv. Such an ambiguity of the soil properties indicates that comparatively humid climate

conditions, existing at the first part of the third Millennium BC, had been changed by more arid ones not long before the soil been covered by kurgan embankment.

About 150 years later the soil salinity increased. In the profile of the paleosol buried under the kurgan embankment  $4260 \pm 120$  BP, (Cal. 3016-2628 BC) the  $\text{SO}_4$  content became three-five times higher, while the chloride content remained high as well. The thickness of the carbonates accumulation zone reduced but the carbonate content in the upper 50 cm layer grew up 6,5%. The morphological forms of the  $\text{CaCO}_3$  neoformations changed too. The size of calcareous nodules decreased, with impregnation forms prevailing. The Fe-Mn oxide neoformations were not observed in the soil as well as in all paleosols described below. The prismatic structure of the paleosol illuvial horizon B became less prominent, which is evidence of solonetzic process extinction under the condition of intensive water evaporation. Increasing the gypsum content also indicates the intensification of ascending migration of water-soluble components in the soil profile, which is typical of drought periods.

During the next one and a half century both the easily soluble salts and gypsum evidently rose up gradually resulting in the formation of their accumulation zone with the upper boundary at 70 cm deep at the end of the third Millennium BC. The gypsum content in the paleosol buried  $4120 \pm 70$  BP (Cal. 2871-2508 BC) was 2,4%. The sulphate concentration in the layer of 70-200 cm reached 1300-1400 ppm. The chloride concentration in the lower part of the soil profile considerably increased. This can be due to either the salt re-distribution in the soil profile or the ground water chemistry composition change with the ground water salinity increasing. The great amount of soil carbonates moved to the upper 0-50 cm layer, in which the average  $\text{CaCO}_3$  content was 8,4% (Fig.3). All carbonates were in impregnation form.

Development of climate aridization resulted in forming unusual soils, which are not found within the modern soil cover of dry and desert steppe zones. Whereas the modern background soils are light-chestnut soils with differentiated profile and solonetzic horizon, the paleosols at the turn of the third and the second Millennium BC ( $3960 \pm 40$  BP, Cal. 2490-2409 BC) are characterized by undifferentiated profile with indistinct boundaries between soil horizons, uniform color of soil-ground mass, and considerable salinity. We proposed to refer these soils as "chestnut-like soils". In contrast to the paleosols described above in this soil the thickness of the humus horizon reduced until 7 cm, resulted from, most likely, activation of the wind erosion. The textural differentiation of the soil profile disappeared. The HCl-reaction was observed at the level of the soil surface. The soil salinity considerably increased, with the easily soluble salts forming another accumulation zone in the horizon B. The upper border of the easily soluble salts accumulation zone was on

the depth only 25 cm. It should be noted, that sulphate content in this horizon grown to about 2000 ppm. The complex of such soil properties indicates extremely drought conditions existed at the turn of the 3-d and 2-d Millennium BC.

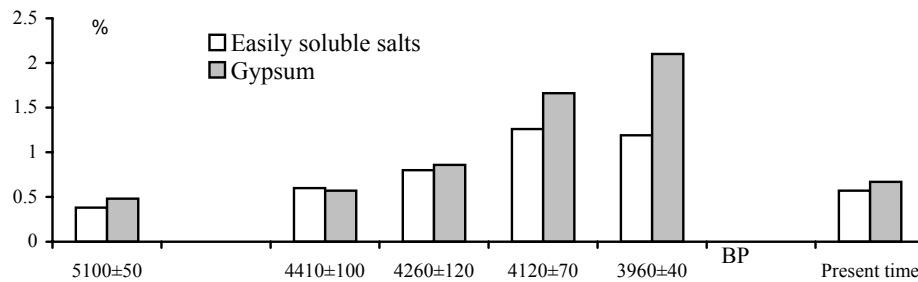


**Fig.2** The dynamics of easily soluble salts and gypsum contents in the profiles of buried paleosoils and modern background soils

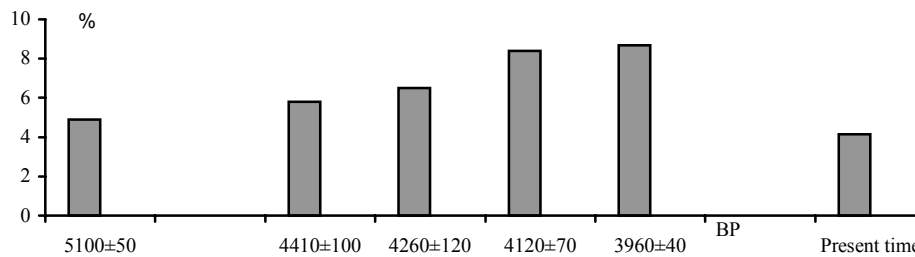


**Fig. 3** The dynamics of carbonate contents in the layer of 0-50cm in paleosoils and modern background soils

Thus, the soil data obtained allowed us to propose the following concept of the climate development and soil forming conditions changes during the 3-d Millennium BC. At the first part of the 3-d Millennium BC the climate in the area under investigation was moderately dry, and the atmospheric precipitation was close to than of the present. During the whole second part of the 3-d Millennium BC the climate aridization was gradually increasing. The heaviest droughts occurred at the turn of the third and second Millennium BC resulting in disastrous wind erosions, increase of the concentration of water-soluble components (easily soluble salts, gypsum, carbonates), and deflation of the upper horizon of the watershed area soils.

**Acknowledgements.** This research was supported by the Russian Foundation for Basic Research and the Program of Presidium of RAS for Basic Research (directive 4)

## INFLUENCE OF TEMPERATURE ON WATER PROPERTIES OF URBAN SOIL

*Bowanko G., Hajnos M., Witkowska-Walczak B.*

Effect of addition of various amount of rubble to the soil and influence of cyclic changes of temperature on water properties of the resulting mixtures was studied. One-week freezing (-20°C) and one-week de-freezing (30°C) cycles were performed at constant soil moisture (25w/w%) during 18 weeks. For samples collected before the cycles (control) and after 6<sup>th</sup>, 12<sup>th</sup> and 18<sup>th</sup> week of the cycles, water potential vs. moisture dependencies (pF curves) were measured. From these curves amounts of gravitational, plant available, and non-accessible water as well as porosity of the studied materials were calculated.

### INTRODUCTION

As a result of human activity area of anthropogenic soils, including urban soils, expands every year. In urban soils complete destruction of natural soil profile is a common phenomenon. Buildings or roads cover the significant portion of urban areas, which makes proper circulation of air and water impossible. Engineering works leave different kinds of building materials in the soil, which corrode under atmospheric and soil environment factors, leading to long-term changes in soil properties, particularly in soil structure thus affecting gases, water and nutrients retention and transport.

Soil structure depends on granulometric composition, amount and mineralogy of clay fraction, and quantity of humus, as well as on climatic conditions, soil biota, fertilizers and meliorations thus this is very sensitive to human building activities. Among climatic factors, the temperature is of primary importance as this influences soil structure due to alteration of soil colloidal properties, consolidation and deformation and movement of soil particles.

The aim of this work was to find how the addition of building materials into the soil affects its water properties under the influence of cyclic changes of temperature.

### MATERIALS AND METHODS

The upper 0-25 cm layer of a leached brown loessial soil was used. The soil material was mixed with a rubble, composed from equal quantities of concrete, brick, foam concrete and mortar. Soil and rubble were ground and screened by 1mm sieve. Mixtures of soils and rubble were prepared in 9:1; 8:2; 7:3; 6:4 and 5:5

w/w ratios, moistened with distilled water to 25% w/w and subjected to cyclic changes of temperature. One cycle consisted of one-week treatment at -20°C following by one-week treatment at 30°C. The material for investigations was taken after 6<sup>th</sup>, 12<sup>th</sup> and 18<sup>th</sup> week.

Water retention vs. moisture dependencies (pF curves) were measured using laboratory set LAB 012 produced by Soil Moisture Equipment in a range of soil water potential from 0 Jm<sup>-3</sup> (pF 0) to 1,5·10<sup>6</sup> Jm<sup>-3</sup> (pF 4,2). Prior to the measurements the studied samples were placed in stainless steel cylinders (1.8 cm radius and 1 cm height) and subjected to several cycles of 48h wetting (capillary rise) and 48h (40°C) drying to stabilize the structure i.e. until differences in sample bulk densities were insignificant. Changes in granulometric composition and bulk density of the soil and mixtures were measured, as well.

From the above dependencies, the quantity of gravitational water, plant available water and non-accessible water were estimated. Quantity of large pores ( $\phi > 18,5 \mu\text{m}$ ), medium pores ( $18,5 \mu\text{m} > \phi > 0,2 \mu\text{m}$ ) and small pores ( $\phi > 0,2 \mu\text{m}$ ) were estimated also.

## RESULTS AND DISCUSSION

Figure 1 shows dependencies of moisture on water potential (pF-curves) for initial samples and after cyclic changes in temperature.

First cycle of freezing-defreezing (6 weeks) lead to significant increase in water retention for all samples. During next cycles the water retention decreases consecutively reaching after third cycle (18 weeks) lower values than the initial samples. The above phenomena suggest changes of soil structure during freezing-thawing periods. Initially the compact structure of artificially prepared soil and mixtures is obtained. This structure markedly loosened after first 3 cycles of freezing and thawing indicating that most probably larger soil aggregates were formed. These aggregates may brake during further cycles and the soil structure becomes more stabilized.

After third cycle when the structure seems to be most stabilized, the water retention is higher in all mixtures than in the soil itself. This is due to higher water capacity at low pF values i.e. in the range of coarser pores. However, in higher pF range (smaller pores), the water retention seems to be smaller in the mixtures than in the soil. This may be connected with an increase in silt and loam fractions, resulting most probably from dispersion of coarser rubble fractions by water during cyclic changes of temperature.

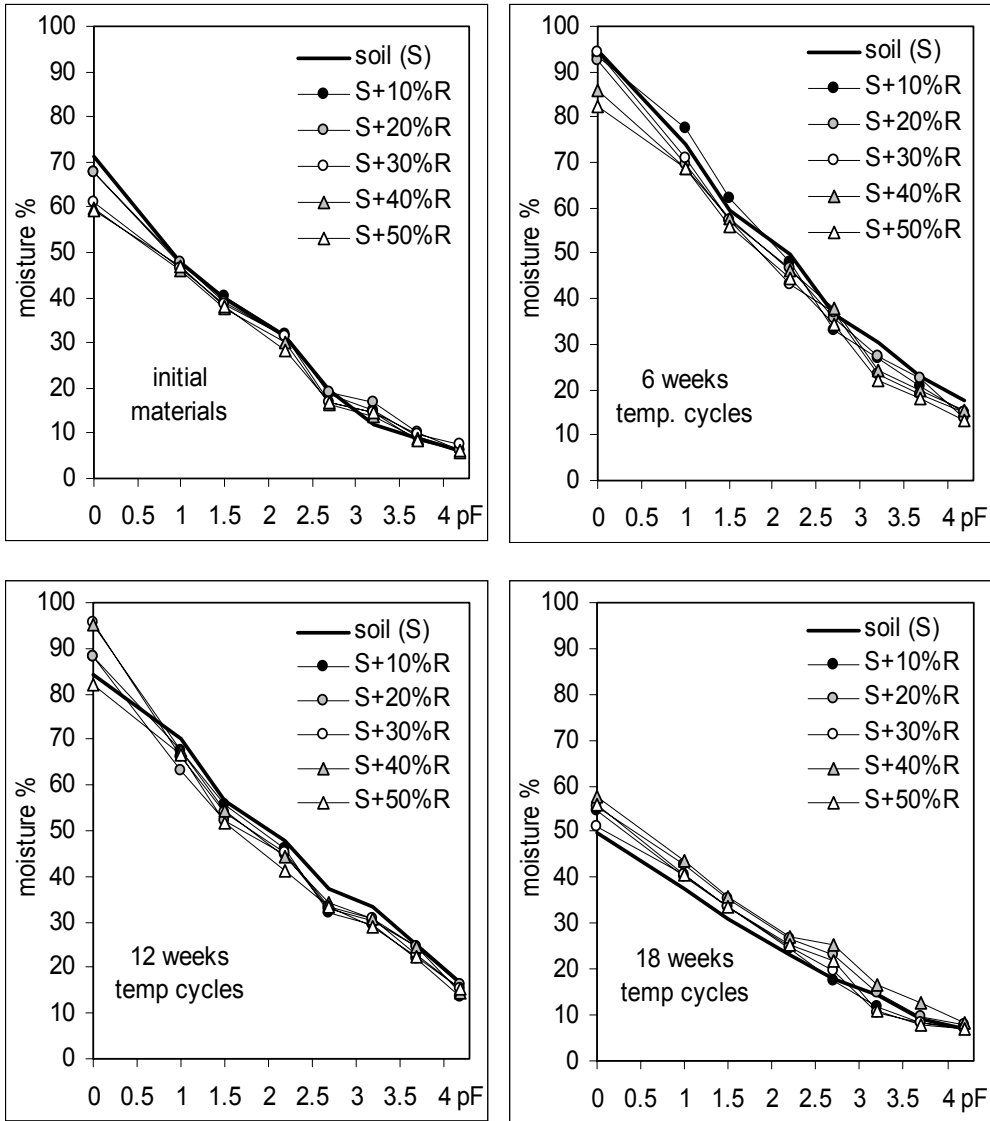


**Fig. 1.** Dependencies of moisture on water potential for the studied samples.

Figure 2 shows changes in amount of pores of various sizes during the temperature cycles for the soil and its mixtures with 10% and 50% of the rubble.

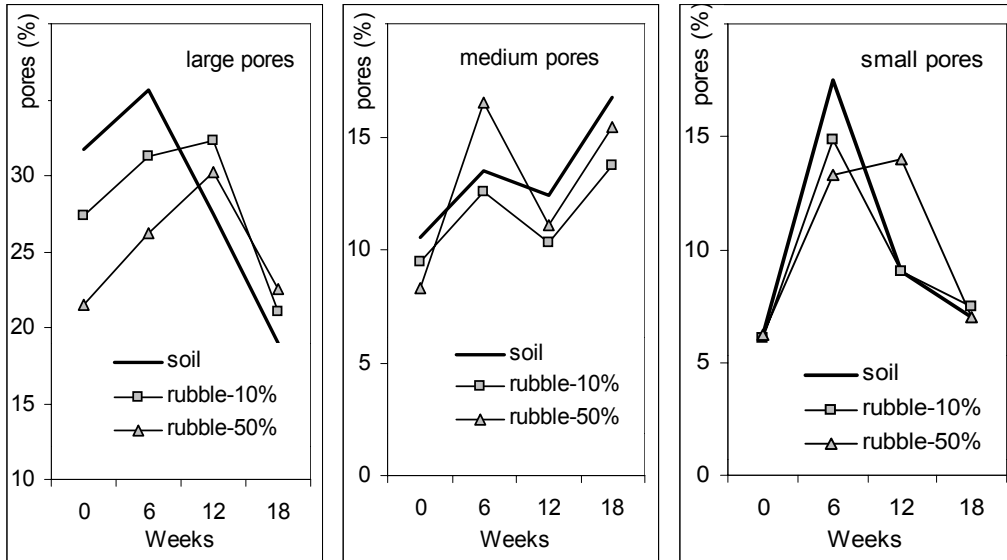


**Fig. 2.** Effect of temperature cycles on porosity in soil and soil-rubble mixtures.

As mentioned previously, the temperature cycles affects the porosity of the soil and its mixtures with rubble. The differences in porosity between the studied materials are the least after 18 weeks of thermal cycles.

The addition of the rubble to the soil influences the porosity of the resulting mixtures, particularly during the course of stabilization of the structure i.e. during first 12 weeks of the thermal treatment. After 18 weeks of the thermal treatment the amount of large pores was higher in soil mixtures with rubble than in the soil, whereas the amount of medium size pores decreased. Amount of small pores was similar in soil and its mixtures with rubble.

## CONCLUSIONS

Thermal cycles caused initial increase in water retention of soil and its mixtures with rubble, which consecutively decreased during further freezing-thawing periods. After 18 weeks of thermal cycles when the soil structure seems to be most stabilized, the water retention and porosity of soil mixed with rubble was higher than in the natural soil due to increase in the amount of large pores. The amount of medium pores was lower in the mixtures than in the soil.

## STATE OF MICROBIAL COMMUNITIES IN MODERN AND BURIED SOILS AS INDICATOR OF CHANGING SOIL-FORMING CONDITIONS

*Demkina T.S., Borisov A.V., Demkin V.A.*

Soil microbial community is an important part of soil. Practically all soil processes are going on with the participation of soil microorganisms. Therefore the state of microbial community is one of the most important indicators of pedogenesis conditions. Paleosols buried under kurgans retain their properties from the time of kurgan building and, consequently, the environmental conditions of that time should be reflected in the properties of microbial community. The earliest our investigations have demonstrated the existence of active microorganisms in the buried soils. This microorganism grown well after the soil-water suspension was sowed on the nutrient medium. Using various nutrient mediums it is possible to appreciate the trophic groups, quantity, and biomass of microorganisms. These data allowed us to reconstruct the pedogenesis conditions in the past.

At present there is little evidence of these microorganism's ages and of the diagenesis changes of microbial communities in paleosols. Not numerous data show that  $^{14}\text{C}$  age of bacteria from marine sediments varies from  $985\pm 85$  to  $7480\pm 80$  years (1). Studying microbial properties of ancient paleosols buried under sediments dated back 1-4 million years it was shown that on the depth of 50-60 m the paleosols enriched by organic carbon had a higher population of culturable heterotrophs, a greater glucose mineralization potential, a higher microbial diversity, and a more than 20-fold higher concentration of ATP than the weakly developed paleosols (2). To the author's opinion, the survival of microorganisms over geologic time periods would be dependent on their ability to prevent cell death imposed by desiccation contaminant nutrient limitation. A second adaptive strategy for long term survival is the ability to enter a resting state characterized by a lack of metabolism or very slow utilization of endogenous energy reserves at low matric water potential. The complex of fungi in cultural layers of medieval archaeological sites was shown to be similar to that of modern city soils (3).

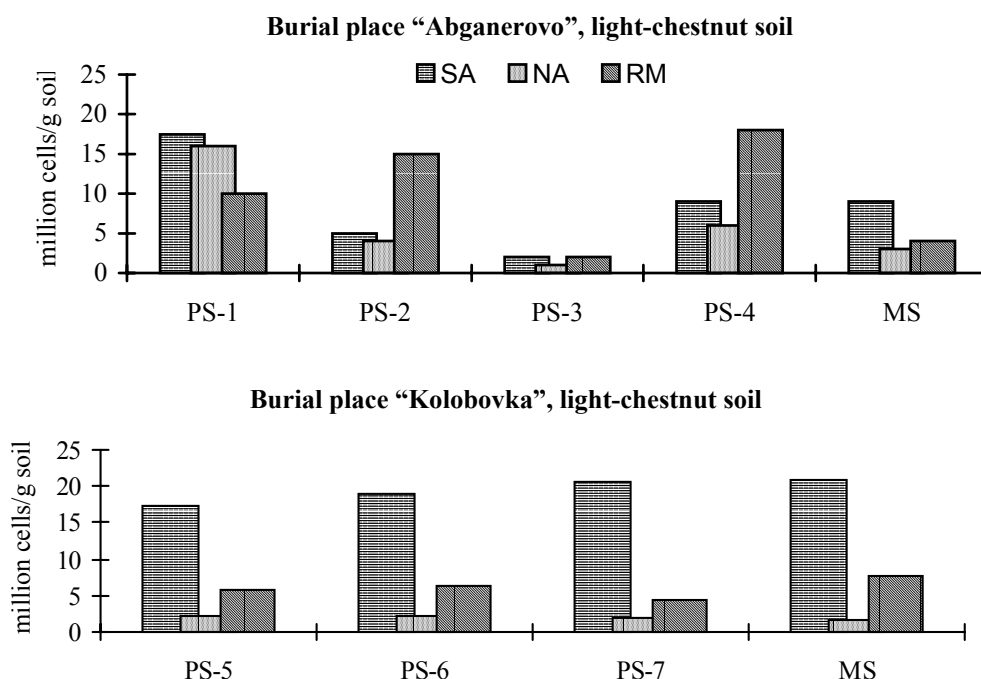
Dispersion analysis of microbiological data of buried and modern soils allowed us to establish intensity of diagenetic changes of microbial parameters and to appreciate whether the characteristics of microbial community of the paleosols can be used to reconstruct soil-forming conditions in the past. It was established that during 3000-4000 years the diagenetic changes of microbial community in the horizon B2 of the paleosols were not going on. Hence the state of microbial community in this horizon reflects the soil-forming conditions in the past.

We performed microbiological investigation of several dozens of kurgans created at Eneolith Epoch, Bronze Epoch, Early Iron Age and the Middle Ages within the dry and desert steppe zone. Using the complex of microbiological methods the information about microbial biomass, populations of microorganisms of different trophic groups and fungal colony-forming units, and microbial respiration rate was obtained and some original coefficients were calculated.

For the first time the distribution of microorganisms in a kurgan embankment and buried paleosol was investigated. The quantity of microorganisms of different trophic groups in the horizon A1 of the paleosols is 10-fold higher than that in the kurgan embankments. The values of microbiological parameters in modern soils decrease downward. In the buried paleosols the distribution of microorganisms is either similar to that in the modern soils or increase downward depending on the digenetic changes, lithology, and climate conditions in the past.

In order to establish the relationship between the state of microbial communities and modern soil-forming conditions the comparative analysis of microbial communities of modern light-chestnut soils and solonchaks within the dry and desert zones in the Lower Volga region has been performed. It was established that microbial characteristics are mainly depend on the local peculiarities of pedogenesis. Within the same soil type the microbial communities vary significantly subject to the lithological and geomorphologic conditions, as well as the location in the landscape. And vice versa, the microbial communities in different soil types are often similar if the soils have similar location in the landscape, soil forming rocks and depth of ground water. Therefore we suppose the state of microbial community at certain historical period depends on the regularities of soil evolution and climate changes in concrete area.

The dynamics of microbial community states in the various paleosols has also been studied. It was shown that during some historical periods the variability of microbial community characteristics was considerable (burial places "Abganerovo": the turn of the IV-III Millennium BC (PS-1), XIX-XVII cc. BC (PS-2), III-IV cc. AD (PS-3), IV c. AD (PS-4) (Fig.1); "Malyaevka": the turn of the III-II millennium BC, XVI-XV cc. BC, III-IV cc. AD, XIII-XIV cc. AD, and during other ones it was not great (burial place "Kolobovka" the first part of the I c. AD (PS-5), I-II cc. AD (PS-6), II-III cc. AD (PS-7). The data obtained are evidences of variability of microbiological parameters caused by natural condition changes. Predominance of the microorganisms, consuming an easily available organic matter, high values of ratio of microbial population consuming plant residues to that consuming humus substances, and low index of oligotrophicity allows one to suppose high amount of organic matter entering into the soil, the process occurring in conditions of high precipitation norm. And vice versa, the drought increasing leads to



SA – soil agar (microorganisms consuming nutrient elements from poor environment)  
 NA – nitrite agar (microorganisms consuming humus substances)  
 RM – rich medium (microorganisms consuming an easily available organic matter)

**Fig. 1.** Quantity of microorganisms of various trophic clusters in the horizon B2 in the paleosols (PS) and modern surface soils (MS)

reduction of the first and second parameters, whereas the index of oligotrophicity grows up. This index expresses the ability of microbial community to use nutrient elements from poor environment: the poorer nutrient conditions are the higher index of oligotrophicity is.

The temporary and spatial variability of trophic structure of soil microbial community in several regions of the steppe zone has been described. For instance, during the last 3600 years in the saline chestnut soils in the river Esaulovsky Aksay valley the microorganisms consuming nutrient elements from poor environment prevailed (74-97%) (Table 1). These microorganisms also prevailed (69-77%) in the light-chestnut soils developed on the saline loams in the Lower Volga region under more arid climate. In the light-chestnut soils, developed under conditions of less saline soil-forming rocks and higher precipitation on the watershed areas of Ergeny Upland the microorganisms growing on the rich organic medium prevailed.

**Table 1.** The temporary and spatial variability of microbial communities in paleosols and modern surface soils.

Burial places		Aksay <sup>1</sup>	Abganerovo <sup>2</sup>	Malyaevka <sup>2</sup>	Kolobovka <sup>2</sup>	
Microbial biomass*	MS	546	406	107	35	
	PS	16-112	20-42	11-19	0.4-3	
Quantity of microorganisms**	MS	66	57	17	44	
	PS	8-48	4-47	7-10	25-27	
Populations of microorganisms of different trophic groups***	SA	MS	74	58	66	70
		PS	74-97	21-58	28-66	69-77
	NA	MS	8	15	4	6
		PS	0-8	18-36	4-32	6-8
	RM	MS	18	35	30	24
		PS	4-18	25-61	25-43	16-28

MS – modern soil, PS – buried soil <sup>1</sup> – chestnut soil, <sup>2</sup> – light-chestnut soil  
SA – soil agar, NA – nitrite agar, RM – rich medium  
\* - µg C/g soil \*\* - million cells/g soil, \*\*\* - %

It should be noted, that pedogenesis reconstructions obtained on the base of microbiological methods are in full accord with those obtained with the help of traditional morphological-genetic analysis of the soils. Moreover, being more sensitive to soil-forming condition changes, the data of microbial community state allows to specify and work out in detail the morphological-genetic analysis data.

**Acknowledgements.** This research was supported by the Russian Foundation for Basic Research and the Program of Presidium of RAS for Basic Research (directive 4)

## REFERENCES

1. Eglinton T. I., Benitez-Nelson B.C., Pearson A., McNichol A.P., Bauer J.E., Drufel E.R.M. (1997) Variability of Radiocarbon Ages of Individual Organic Compounds from Marine Sediments. *Science*. Vol.277. 796-799.
2. Brockman F.J., Kieft T.L., Fredricson J.K., Bjornstad B.N., Shu-mei W. Li, Spangenburg W., Long P.E. (1992) Microbiology of Vadose Zone Paleosols in South-Central Washington State. *Microbial Ecology*. 23. 279-301.
3. Marphenina O.E. Gorbatoovskaya E.V. Gorlenko M.B. Microbial characteristics of cultural layers in medieval Russian archaeological sites. *Pochvovedenie*. 2001. Vol.70. 855-859.

## THE INFLUENCE OF COMPOSITION AND PROPERTIES OF SOILS CONTAMINATED BY LEAD ON THE OAT GROWTH

*Dmitrakov L.M., Dmitrakova L.K., Abashina N.A., Pinsky D.L.*

The problem of geochemical stability of the soils and ecosystems to technogenic pollution is still requiring great attentions of soil scientists. The results of investigations was shown that in 3-10 fold excess of natural concentration of metal in soil triggers negative influence on production process in plants. Thus many researches have been carried out using substrates and nutritious solutions polluted by soluble salts of heavy metals (HM). At the same time, the analysis of both available in the literature and our data demonstrate the existence of the contradictions in estimated influence of low and average levels under lead soil pollution. In particular there are quite often no precisely expressed factors of negative influence on plants under doses Pb up to 1000 mg/kg soil. Consequently, lead presence in plants being greatly dependent on durability of lead binding with soil and, hence, on soils compositions and properties.

The behavior and functions of Pb (II) in the system soil - plant in a series of pot experiments with the soils and substrates having various composition and properties have been studied.

### OBJECTS AND METHODS

Pot experiments were carried out in plastic vessels in the KTLK-1250 chamber under constant light exposure, temperature, humidity and extent light day. In the experiments with samples from top horizons and parent rock of Soddy-podzol and Leashing Chernozems were used. Besides substrates obtained by mixing of soil top horizons with parent rock and washed quartz sand were used. Initial agrochemical characteristics of the soils (0-20 sm) have been determined using standard techniques : for Soddy-podzol -  $\text{pH}_{\text{KCl}}$  - 6.4; C org. - 0.93; CEC - 17.72 mg-eq /100g, particles < 0.01 mm - 33.84; particles < 0.001 mm - 14.48; for Leashing Chernozems -  $\text{pH}_{\text{KCl}}$  - 5.8; C org. - 3.48; CEC - 33.78 mg-eq /100g; particles < 0.01 mm - 46.92; particles < 0.001 mm - 22.75. As a test-plant oat (*Avena sativa* L.) was chosen as steadiest culture to action of HM for experiments. In the first experiment as a substrate: top horizon (TH) of Soddy-podzol (1), mix of TH with parent rock in the ratio 1:1 (2), parent rock (3), mix TH with sand in the ratio 1:1 (4) and sand (5) were used. In all cases the control (Ca) was used with addition and in three variants the control (K) - without addition of  $\text{Ca}(\text{NO}_3)_2$ . The duration of plants vegetation was made 30 days. In the second experiment as a substances: 1a - top horizon of Leashing Chernozems (TH), 2a – mix of TH with parent rock (1:1),

3a - mix TH with parent rock (1:3), 4a - parent rock, 5a - mix of TH with sand (1:1), 6a - mix of TH with sand (1:3) were used. In all cases the control (K) was used without addition of  $\text{Ca}(\text{NO}_3)_2$ . The vegetation duration has made 60 days. In both experiments  $\text{Pb}(\text{NO}_3)_2$  in a doze of 2000 mg/kg in a dry kind (Pb) were added in substrates and after grinding and careful mixing were placed in vessels. Substrates have been placed in the chamber and incubated during a month. After incubation of the substrates 5 sprout of oat was planted in vessels, it was done 3 times. Temperature of light day (16 hours / day) was kept within 23-24<sup>0</sup>C. In all experiments during the vegetation of oat have been made phenological: the rates of plants growth have been estimated their height by measuring, transpiration of moisture – by weight method, plants shoot and root biomasses has been determined as well. Mathematical statistics was used when analyzing the results.

## RESULTS

The results of our research in the series of pot experiments showed that the oppressing influence of pollutants in Pb doses up to 2000 mg/kg soil on growth of plants was insignificant and reached the maximal value by 20-30 days of vegetation. Then the plants overcame stress caused by soil pollution, but jet failed to overcome some morphometric differences. In a number of cases more intensive growth of plants was observed at low levels of soil pollution by  $\text{Pb}(\text{NO}_3)_2$  than in controls (Fig. 1). The edition of  $\text{Ca}(\text{NO}_3)_2$  into the soil for alignment of nitric nitrogen background influences plants development similarly to  $\text{Pb}(\text{NO}_3)_2$ . Biomass of plant root and shoot was effected by level of soil pollution by  $\text{Pb}(\text{NO}_3)_2$  and  $\text{Ca}(\text{NO}_3)_2$  during of oat vegetation in comparison with plants growth.

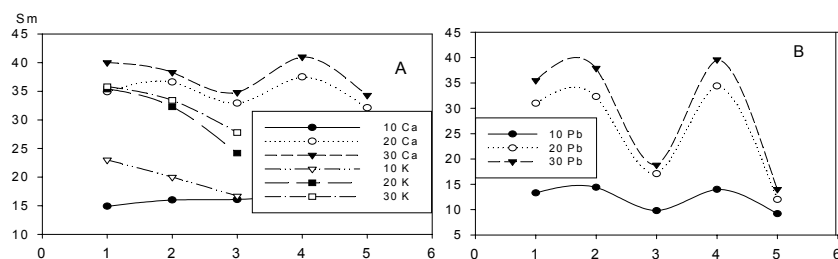


**Fig. 1.** Dynamics of oat growth on control (A) and polluted substrates (B).

The influence Pb on oat biomass was more considerable in comparison with Ca in parallel variants (Fig. 2). As shown by the data presented, influence of substrate composition on plants growth is typically change depending not only on kind of cation, but also on duration of vegetation. Substrate influence lines polluted by Ca and Pb are not in agreement with control variants. Control plants during the first 10

days grew faster than on substrate polluted by  $\text{Ca}(\text{NO}_3)_2$  and  $\text{Pb}(\text{NO}_3)_2$ . However by 30-th day of vegetation control plants have lagged in growth behind not only plants on substrate polluted by calcium, but also the plants on substrate polluted by lead. Probably, it is connected either with stimulating action of low HM concentration on plants, or with reception of an additional nutrition of metals nitrogen salts by plants.

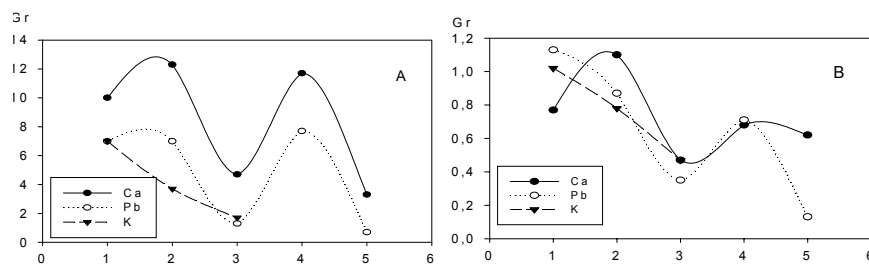


**Fig. 2.** Shoot(A) and root(B) biomass.

In model experiment with Leashing Chernozems samples the behavior of oat plant was similar. For the first 20 days of vegetation the negative influence of lead on plants was more considerable, than substrates properties (Fig. 3).

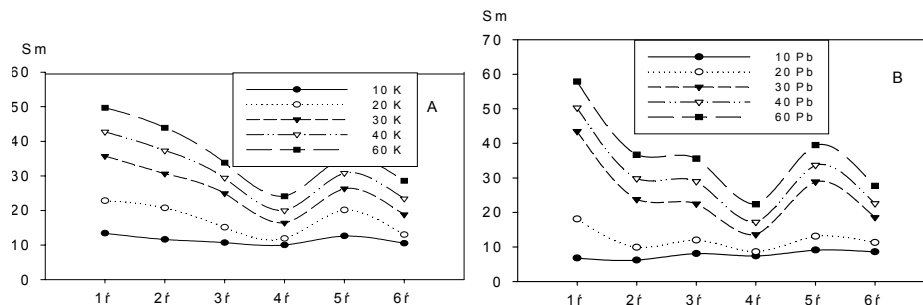


**Fig. 3.** Dynamics of oat growth on control (A), and polluted substrates (B).

By 30-ty days of vegetation the oat height on polluted substrates practically had leveled with control plants and by the end of experiment it even overtook in some variants. Finally composition and properties of substrate rendered the most essential influence on growth and development of oat. The height of stalks was decreasing (from 100 up to 49 % on the control and from 100 up to 39 % on polluted substrate) and sand (from 100 up to 58 and 48 % accordingly) process of growth of parent rock content.

Biomass of shoot oat (from TH to parent rock decreased from 100 up to 22 on the control and to 8 % on polluted substrate) and roots (from 100 to 24 and 28 % accordingly) reacted even more sharply to composition and properties of substrate. The influence of  $\text{Pb}(\text{NO}_3)_2$  had various effects on shoot oat biomass being greater on polluted substrates than on control ones, the root biomass in all the variants with lead (except for TH + sand 1: 1) was 56 - 85 % from those on the control (Fig.4).

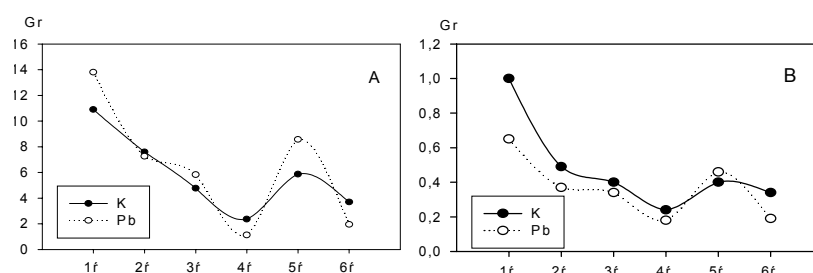


Fig. 4. Shoot(A) and root(B) biomass.

The results of experiment of soil conditions modeling testify to complex influence properties of soil and concentration of metal -pollutant on growth and development of plants. Presence pollutant and its concentration right at the beginning of oat vegetation caused the most negative influence on plants. In the further most essential distinctions in growth and biomass were shown as a result of influence of composition and physico-chemical properties of soil - the humus contents, exchange capacity, pH and other factors.

## CONCLUSION

As a whole, analyzing obtained by us and literary data it is possible to make conclusions, that nitric lead produced dual influence on morphometric parameters of oat plants: contained in salt nitrate nitrogen facilitates growth processes, and lead cations in the doses exceeding 2000 mg/kg soil inhibit them. Rather low doses Pb (up to 1000 mg/kg soil) fail not only negative influence on development of plants owing to high buffer capacity soils in relation to HM, but even in a number of cases stimulate their development. According to sensitivity to  $\text{Pb}(\text{NO}_3)_2$  influence morphometric parameters form: height of plants < shoot biomass < roots biomass < brunching. Collateral action on development of oat plants render also  $\text{Ca}^{2+}$  cations, added soil with  $\text{Ca}(\text{NO}_3)_2$  in order to balance nitrate background. This action as a whole has the same  $\text{Pb}^{2+}$  cation orientation, as it should be taken into account when using nitrogen metal salts in pot experiments.

Study supported by the Russian Foundation for Basic Research (project no. 02-04-48970).

## SOIL SALINITY AND CLIMATE CHANGES IN THE PAST

*Eltsov M.V., Borisov A.V., Demkin V.A.*

During the 2001-2002 years the research workers of the Institute of Physicochemical and Biological Problems in Soil Science RAS have carried out the field investigations of burial places disposed in the Volgograd region. The basic method of research was the method of archaeological pedology. This method consists in joining investigation of modern soils and paleosols of archaeological monuments constructed at different periods of history.

Paleosols of different ages (the beginning of the 3-d Millennium BC, the first part of the III Millennium BC, the turn of the III-II Millennium BC, first century AD, the II-III centuries AD, the first part of the XIII century AD) buried under burial mounds as well as modern surface soils have been investigated. These soils are chestnut and chestnut-like calcareous saline soils.

All studied soils have great carbonate content, with the carbonate neoformations in the form of nodules and impregnation prevailing. In the layer of 0-200 cm the carbonate content was not changed. The depth of HCl-reaction varied from 21 to 33 cm. The carbonate content in the soil layer of 0-50 cm was highest in the soils of the turn of the III-II Millennium BC; the lowest one was in the medieval paleosols.

It was established, that during the last 4500 years the salt content in the soils under investigation varied significantly. For the second part of the III Millennium the soil salinity increased more then by 50%, with the upper boundary of the salt accumulation zone replacing from the depth of 130 cm to 55 cm. The lowest salinity (0.54%) observed in the paleosols buried at I century AD. But already by the III-IV centuries AD the soil salinity increased in about three times (the salt content was 1.3%). The medieval paleosols were leached from the easily soluble salts and gypsum due to the strong increasing precipitation occurred at the XIII-XIV centuries AD.

It is typical of the paleosols of all historical periods the presence of gypsum accumulative horizon. The gypsum content did not vary significantly and only paleosols of the turn of the III-II Millennium AD had more than 1% of gypsum. During the next epochs the leaching gypsum from the soil and accumulation of it in the soil-forming rocks occurred.

The temporary changes of the soil salinity described above were mainly caused by climate condition changes in the past.

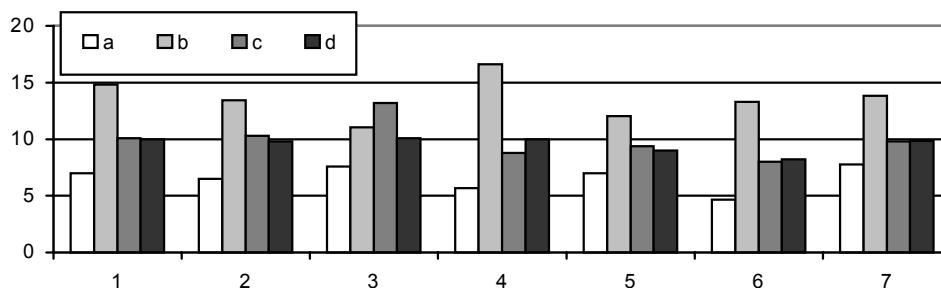


**Fig.1.** Soil carbonate content (%) in the layers: 0-50 cm (a); 0-100 cm (b); 100-150 cm (c); 0-200 cm (d).

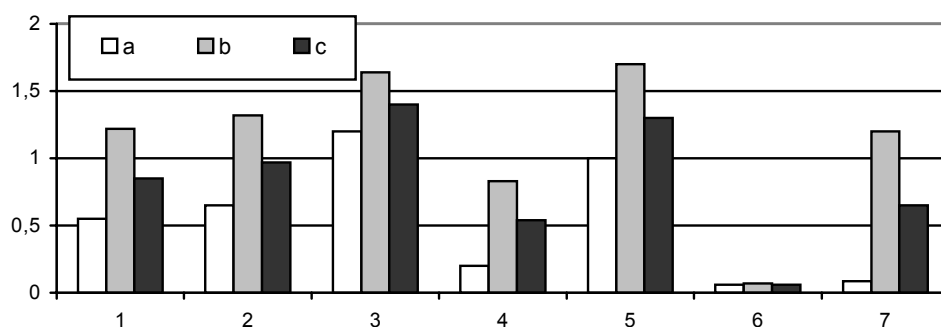


**Fig.2.** Soil salinity (%) in the layers: 0-50 cm (a); 100-200 cm (b); 0-200 cm (c)

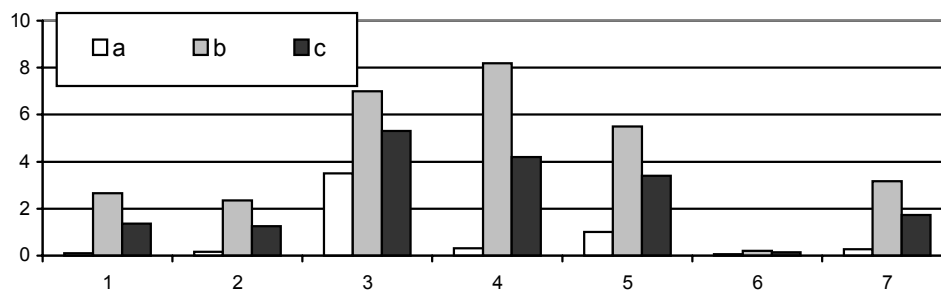


**Fig.3.** Gypsum content the layers: 0-50 cm (a); 100-200 cm (b); 0-200 cm (c)

Abbreviations for the Figures: 1 – the beginning of the III Millennium BC, 2 – the first part of the III Millennium BC, 3 – the turn of the III-II Millennium BC, 4 – first century AD, 5 – the II-III centuries AD, 6 – the first part of the XIII century AD, 7 – the present time

**Acknowledgements.** This research was supported by the Russian Foundation for Basic Research and the Program of Presidium of RAS for Basic Research (directive 4).

## POROUS STRUCTURE OF NATURAL BODIES

*Hajnos M., Świeboda R.*

Porosity is one of more important parameters characterizing porous bodies. The solid phase of a given body may be either nonporous (cast, monolyte) or may contain pores - spaces filled by liquid or gas phases. The pores may be open and/or closed, may have different shape, may be available or nonavailable from the surface of the body, may have very different sizes. So, the porosity is defined as the occurrence of internal spaces in solid body. A measure of the porosity is a volumetric ratio of all free spaces to the bulk of the body. The latter value is called absolute porosity ( $m^3/m^3$ ). The other definition, relative porosity ( $m^3/m^3$ ), is a ratio of a volume of available (open) pores only to the bulk volume of the body. Both porosity values may be expressed also as percentage or, which is frequently used, as volume of pores in a mass unit of the body ( $m^3/kg$ ).

Porous structures may be formed in several ways:

- As a result of connection of smaller nonporous units (grains) into larger aggregates. The porous structure is thus formed from internal spaces between the grains and the grains themselves form the structure skeleton. Such materials have granular structure.

- As a result of the removal of some part of the solid from monolytic body (e.g. leaching, dissolution). Such materials have a sponge structure.

- As a result of both processes together.

For most porous materials one can distinguish the intergranular porosity (between the grains) which is called bed porosity and intragranular porosity (inside the individual grains). Solid bodies may have also a geometrically irregular surface, which is difficult to distinguish from "real" pores. The pore is thus defined by a convention as the surface cavity having larger depth than the half of its average size (e.g. the radius for cylindrical pore).

The pores may be classified according to different criteria:

According to their availability from outside one distinguishes:

Unavailable pores (totally closed, isolated) – having any connection with surface of the solid body (e.g. occluded gas or liquid bubbles in rocks). Such pores are not detected by most porosimetric methods, however they influence among others the measurements of solid phase density, shear stresses under high pressures and may be responsible for a collapse of a solid under high external forces.

Available pores – connected with the surface either indirectly or via other pores (channels). These pores are subdivided on several groups:

- pores available from one side (one-side open)

- pores available from two sides (two-side open),
- connected pores,
- pore nets or clusters – systems of interconnected pores (channels, voids, cavities).

The shape of natural pores is usually nonuniform. Their complicated build-up for calculation purposes is usually approximated by selected geometrical models. Among many models (slit-like, ink-bottle, conical, globular etc.) the most frequently used is a cylindrical pore model.

According to the dimension of pores, that is connected with the method of their measurement, one distinguishes:

From point of view of capillary condensation process, Dubinin proposed the following classification:

- macropores: more than 200 nm in radius; in such pores no capillary condensation occurs but they may be important in diffusion transport of molecules,
- mesopores: 2 - 200 nm in radius; in these pores capillary condensation occurs,
- micropores: less than 2 nm in radius; in these pores no capillary condensation occurs, but volumetric filling with adsorbate vapor.

A popular soil science classification (Luxmoore) is based on water retention (pF curve) in soils and is related to plant water availability. One distinguishes capillary and noncapillary (aeration) pores. The boundary between the above is 20  $\mu\text{m}$  in diameter (pF = 2,2). In pores larger than 20  $\mu\text{m}$  (macropores) the water is passed through with gravitational force.

Less than 20  $\mu\text{m}$ , capillary pores are divided on criteria of water availability for plants:

- storing easily available water,  $d = 20 - 3 \mu\text{m}$  (pF = 2,2 - 3)
- storing difficult available water,  $d = 3 - 0,2 \mu\text{m}$  (pF = 3 - 4,2)
- storing unavailable water, microcapillary pores,  $d < 0,2 \mu\text{m}$  (pF > 4,2).

Smart classified pores according to image resolution:

- for an eye - larger than 200  $\mu\text{m}$
- for microphotography – larger than 6  $\mu\text{m}$
- for optical microscopy – larger than 0,2  $\mu\text{m}$ .

Geenland had distinguished:

- bonding pores (<5 nm), important for menisci forces connecting primary soil aggregates;
- residual pores (5 - 500 nm), important for soil reactions on molecular level;
- water storage pores (0,5 - 50  $\mu\text{m}$ ), storing water available for soil organisms;
- transmission pores (50 - 500  $\mu\text{m}$ ), important for water movement and roots penetration

These nonuniform classification systems lead to misinterpretations of porosity. Therefore the International Union of Pure and Applied Chemistry (IUPAC) recommends use of the following terms:

- micropores – of radii less than 2,0 nm
- mesopores - between 2,0 and 50 nm
- macropores – larger than 50 nm.

### **MEASUREMENT OF ABSOLUTE AND RELATIVE POROSITY**

Total (absolute and/or relative) porosity may be estimated from measurements of the bedvolume (or bulk density) and the solid phase density. The open pores volume may be estimated pycnometrically basing on Boyle-Mariotte gas law.

Total porosity value is of less importance for characteristic of porous materials because provides no information on pore dimensions and number. The same total porosity can result from small number of large pores and large number of small ones despite both above materials have quite different properties. More important pore characteristic is than a function relating pore volume and dimensions within defined pore size class (pore size distribution).

### **MEASUREMENT OF PORE SIZE DISTRIBUTION**

Pore size distribution is determined using so called direct and indirect methods. Direct methods are usually used for investigation of larger than 30  $\mu\text{m}$  pores and indirect methods for studying of smaller pores. Direct methods are based on an analyze of cross sections of porous bodies: niontransparent sections in reflected light and transparent ones in transmitted light microscopy. Soil cross sections are useful for determination of pore shapes. Image analyze of XRD and NMR scanning photographs is used, as well. Indirect methods determine pore size distributions basing on measurements of other physicochemical parameters related to pore sizes and volumes as for example gas, vapor or liquid volume and pressure present within and over the sample of porous body in equilibrium. The gas or vapor condensed in a pore or liquid filling the pore form a lens-shaped surface, called meniscus. The pressure difference across the meniscus (inside and outside the pore),  $\Delta P$ , is related with the curvature of the meniscus  $r$  (and so the pore dimension) according to Young-Laplace equation:

$$\Delta P = \frac{2\gamma}{r}$$

where  $\gamma$  is a surface tension of the liquid (condensate) present in a pore.

The curvature of the meniscus is dependent somehow with the pore dimension. One relates these two values using any convenient pore model, which is selected

either operationally or basing on a knowledge of the sample structure. As far as the model pore shape may not reflect the real pore shape, the pore dimensions calculated using models are called equivalent dimensions. The pore size distributions coming from indirect measuring methods do not include closed, nonavailable pores.

Among most frequently used indirect porosimetric methods one can list mercury intrusion, nitrogen or water vapor sorption and water retention. The ranges of (equivalent /cylindrical model) pores detected by the above methods are:

- from water vapor desorption isotherms: 1,6 to 60 nm;
- from mercury intrusion porosimetry: 3,7 to 7500 nm;
- from water retention (pF) curves: 95 to 150000 nm.

### MERCURY INTRUSION POROSIMETRY TECHNIQUE

Mercury intrusion porosimetry is widely used for characterizing mesopore structure of various porous materials: soils, minerals, sorbents, ceramics, building materials, as well as for plats and food products.

The mercury intrusion porosimetry involves forcing of mercury into soil samples at increasing hydraulic pressure. Because mercury does not adhere to most of solids (the contact angle is higher than 90 degs), it enters the pores only when an external pressure ( $p_m$ ) is applied (for example water of contact angle close to 0 degs enters the pores spontaneously). The higher the pressure, the mercury is force to narrower pores. The pores should be empty at the beginning and so the sample is outgassed at a vacuum prior to the mercury intrusion. The mercury intrusion porosimetry apparatus registers the volume  $V$  of the mercury forced into the sample against the intrusion pressure  $V = V(p_m)$ .

The volume  $V$  of the mercury forced into the pores is related directly to the pore volume and the intrusion pressure may be related to the (equivalent) pore radius using Washburn equation:

$$r_0 = -2\gamma_m \cos \theta_m / p_m$$

where:  $\gamma_m$  - is a mercury surface tension,  $\theta_m$  - is mercury – solid contact angle (for soils this equals to 141,3 degs).

The volume of pores having radii less than say  $r_0$  is calculated as:

$$V(r < r_0) = V_0 - V_s - V(p_m)$$

where:  $V_s$  - is a volume of sthe solid phase of the porous body,  $V_0$  - is a volume of all pores before the intrusion of mercury and  $V(p_m)$  -the volume of the intruded mercury at a pressure  $p_m$ .

Mercury intrusion data are plotted either in a form of cumulative curve showing total pore volume vs. pore size (Fig. 1.) or in a form of a derivative curve (Fig 2.) showing volumetric fractions of pores of different sizes.

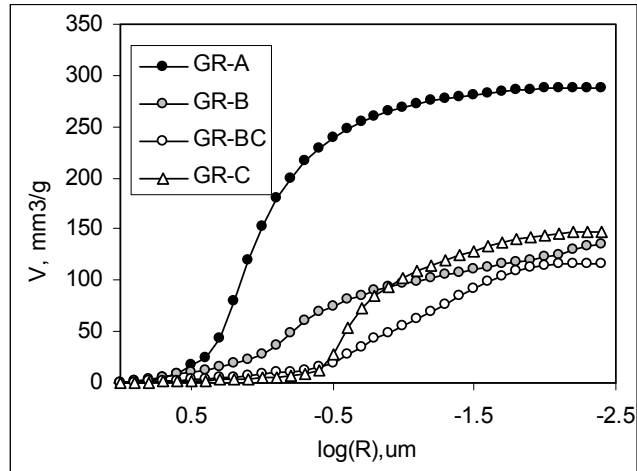


**Fig.1.** Cumulative porosimetric curves for exemplary soil samples.  $V$  - pore volume,  $R$  – pore radius

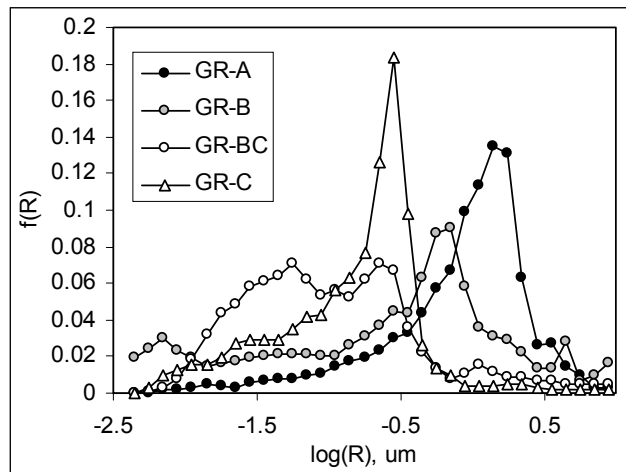


**Fig. 2.** Differential porosimetric curves for the above soil samples.  $f(R)$  is fraction of pores of radii  $R$

## STRENGTH PARAMETERS OF FOOD POWDERS

*Horabik J., Molenda M.*

The strength characteristics of food powders were examined. Experiments were performed using the Jenike shear tester according to the Eurocode 1 recommendations. The tester was 60 mm in diameter and the displacement velocity was 0.03 mm·s<sup>-1</sup>. A reference normal stress ranging from 30 to 100 kPa was applied. The following strength parameters were determined: the effective angle of internal friction, the angle of internal friction, the cohesion and the flow index. There was no clear influence of the consolidation pressure on the effective angle of internal friction and the angle of friction. In the case of fine milk, agglomerated milk and potato starch a significant shear stress vibration was observed. The frequency of these vibrations were found to decrease with an increase in normal stress. Two components of the total strength were considered: the physical friction strength and the extra component of strength due to dilation.

### INTRODUCTION

Automation and increased scale of operation in the food industry in recent decades has led to an increase in the amount of raw materials, ingredients and food products used in a more convenient granular form. At the same time handling bulk solid materials is one of the least understood areas associated with solid processing plants. An important part of powder production and processing is maintaining the consistency of the product such that in-plant powder flow problems which could effect packaging or the use of die-filling machine do not occur. Strength characteristics of powders and flow behaviour are essential for better design of those type of processes [6]. To explain the fundamentals of particulate solids consolidation and flow behaviour a reasonable combination of particle and continuum mechanics are frequently used. This behaviour depends on the nature of the acting binding mechanisms at the contact areas among particles [8].

Jenike's [5] publication is the best known work on determining the strength and flowability characteristics using shear strength testing. This technique is the most popular and widely accepted by researchers and knowledgeable practitioners as a definitive mean of flowability characterisation. Eurocode 1 [3] recommends using the Jenike shear tester to determine the strength of granular materials. The objective of this study was to compare shear strength parameters of typical food powders.

## METHOD AND MATERIALS

The shear strength parameters of food powders were determined according to the Eurocode 1 [3] recommendations using the Jenike [5] shear tester. The effective angle of internal friction  $\delta$ , the angle of internal friction  $\varphi$ , the cohesion  $c$  and the flow index  $i$  were determined from experiments performed in the tester of 60 mm in diameter. A displacement velocity was equal to  $0.03 \text{ mm}\cdot\text{s}^{-1}$ . The sample was consolidated under the reference normal stress  $\sigma_n$  of 30, 60, 80 and 100 kPa. In the case of powders which reveal the tangent stress oscillation the reference normal stress was enlarged to about 200 kPa to verify the influence of the consolidation pressure. The standardized twisting of the top plate of the shear box were applied to consolidate the sample. Two shear tests were carried out for each variant of experiments. One sample was sheared when loaded to the reference stress. The other was sheared at half of the reference stress after pre-loading to the reference stress (Fig. 1). Tests were performed in the controlled temperature ( $20^\circ\text{C}$ ) and air relative humidity (65%) laboratory. Tests were performed for 12 grocery food powders: products of cereal grain, milk, sugar and kitchen salt.

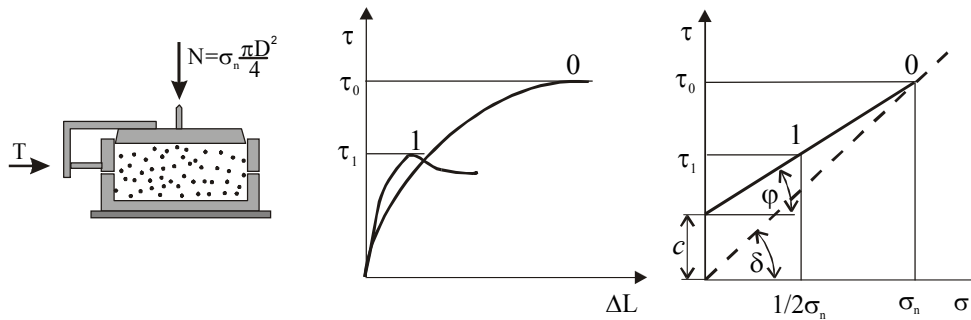


*Fig. 1. Jenike shear tester and procedure of the strength testing [3].*

## RESULTS

The effective angle of internal friction  $\delta$  of all tested materials was found to be in the range of 30-35 deg. mainly (Table 1). There was no clear influence of the consolidation pressure. The largest value of the effective angle of internal friction (approx. 40 deg.) was obtained for potato starch and agglomerated milk for the lowest value of the consolidation pressure. The smallest was for coarse wheat flour (27 deg.) for the highest value of the consolidation pressure. About twice higher standard deviation of the effective angle of internal friction for coarse sugar as

compared to other materials indicates that the simplified procedure applied in this study may be not enough accurate for some materials. The angle of internal friction  $\phi$  was smaller than the effective angle of friction  $\delta$  of no more than 5 deg.

The angle of natural repose  $\theta$  of coarse food powders (groats, durum wheat flour, agglomerated milk and corn meal) was found to be close to the effective angle of internal friction  $\delta$  while for fine powders  $\theta$  was larger than the angle  $\delta$ . Only in the case of NaCl salt the angle of natural repose  $\theta$  was significantly smaller than the effective angle of friction  $\delta$ . This confirms the opinion that the angle of repose does not coincide with the angle of internal friction.

Within the range of consolidation stress applied in this study the food powders tested were determined to have the flow index which would classify them as free ( $i < 0.1$ ) or easy ( $i < 0.25$ ) flowing powders. The largest value ( $i = 0.2$ ) was obtained for the agglomerated milk.

Three types of the tangent stress-displacement relationships were observed in this study: smooth curve typical for wheat flour and groats, irregular vibration typical for corn meal and NaCl salt, and saw blade curve typical for fine milk (Fig. 2). In the case of three tested materials: the fine milk, the agglomerated milk and the potato starch very regular oscillations of the shear stress occurred while approaching the maximum strength of the material. This saw-tooth pattern resulted in large variation in the shear stress for very small displacements.

The amplitude of the oscillation was found to be proportional to the normal stress. To cheque whether this relationship is valid also for higher pressures the tests were performed in extended range of the normal stress (Fig. 3). The pitch oscillation was determined to increase for an increase in normal stress (Fig. 4). The pitch of oscillation was the highest for the agglomerated milk (approx. 0.5 mm) and the lowest for the potato starch (approx. 0.1 mm). The pitch of oscillation is a fraction of the mean grain diameter (0.2 and 0.16) in the case of the agglomerated milk and the fine milk and equals to approx. 3 grain diameter in the case of the potato starch. Therefore, it is possible that for this two group of powders two different mechanisms of the shear stress oscillation participate. Maksimovic [7] indicates four components related to the angle of maximum shearing strength: the angle of physical friction, the angle of degradation, the angle of reorientation, and the angle of dilation. All four components are of different significance for different types of granular solids. The angle of physical friction depends on the material. This value is recorded only as combined with the values of angles of degradation and reorientation. It seems the most possible that in the case of the agglomerated milk and the powder milk a grain degradation contributes the strongest the shear strength oscillation while in the case of the potato starch a component related to the grain reorientation participates the strongest in this process.

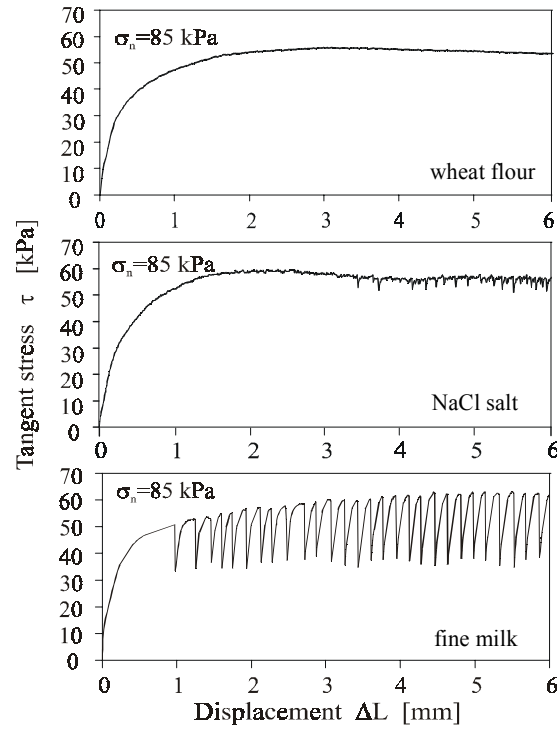


**Fig. 2.** Comparison of the tangent stress-displacement relationships: smooth curve for wheat flour and groats, irregular vibration for NaCl salt, and saw blade curve for fine milk.

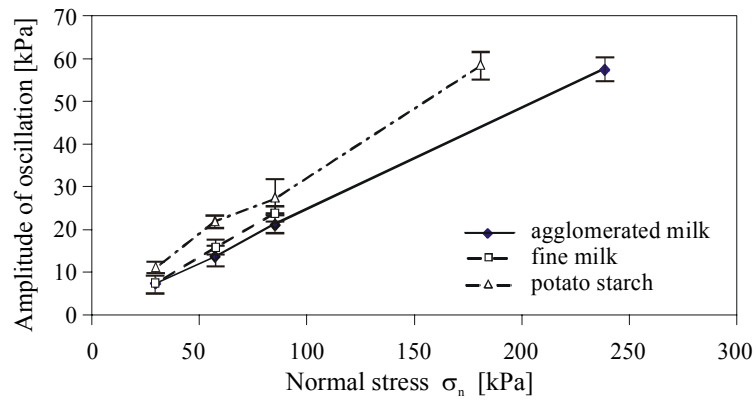


**Fig. 3.** Amplitude of the tangent stress oscillation as affected by normal stress.

Some powder materials exhibit tendency to change volume during shear, known as dilatancy. Strength and resistance to slow deformation can be profoundly affected by dilation [1,2,4]. Sequences of compaction-dilation events were thought to be the most probable source of the shear stress oscillations. Oscillation can be considered as part of a sequence of compaction-dilation events occurring around the area of shear zones developing in the material. Compaction of the particulate material resulted in an increase in material strength and the ability to withstand higher shear loads. When the maximum strength of the particulate material is exceeded dilation in the shear zone occurs resulting in a sharp decrease in the shear load. This leads to limiting mechanisms of slow dilatant plastic shear deformation.

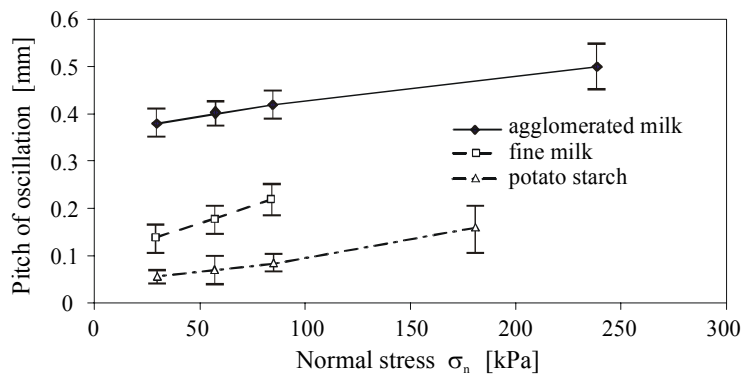


**Fig. 4.** Pitch of the tangent stress oscillation as influenced by the normal stress.

Based on the saw blades model of dilatancy proposed by Bolton [1] the two following strength components were determined from the tangent stress – shear displacement relationships: the physical friction strength and the extra component of strength related to dilation. It was assumed that the minimum value of tangent stress during oscillation corresponds to a critical state of the sample with zero dilation. Contribution of the stress oscillation to the total strength was approximately 30% for the agglomerated milk, 35% for the fine milk and 45% for the potato starch.

## CONCLUSIONS

The effective angle of internal friction  $\delta$  of all tested materials was found to be in the range of 30-35 deg. There was no clear influence of the consolidation pressure. The angle of internal friction  $\varphi$  was smaller than the effective angle of friction  $\delta$  of approximately 0.2-5 deg.

The shear experiments revealed two different types of the shear stress-displacement relations of food powders: smooth curve in the case of wheat flour and groats and a considerable shear stress vibration in the case of fine milk, agglomerated milk and potato starch. The most probable reason of the vibrations is dilation and hardening of the material during slow deformation. The frequency of these vibrations were found to decrease as normal stress increased. Two components of the total strength were suggested: the physical friction strength and the extra component of strength caused by dilation.

## REFERENCES

1. Bolton M.D. The strength and dilatancy of sands. *Géotechnique*, 36(1), pp. 65-78, 1986.
2. Dunstan T., Arthur J.R.F., Dalili A., Ogunbekun O.O., Wong R.K.S. Limiting mechanisms of slow dilatant plastic shear deformation of granular media. *Nature*, 336, pp. 52-54, 1988.
3. Eurocode 1. Basis of design and actions on structures. Part 4. Actions in silos and tanks. European Committee for Standardization. Rue de Stassart 36, B-1050 Brussels, 1996.
4. Gephart H. Scherversuche an leicht verdichteten Schüttgütern unter besonderer Berücksichtigung des Verformungsverhaltens. Verein Deutscher Ingenieure, VDI-Verlag GmbH Düsseldorf 3, 68, 1982.
5. Jenike A.W. Storage and flow of solids. Bull. 123, Eng. Expt. Station, Utah State Univ., 1964.
6. Lubert M., de Ryck A., Dodds J.A. Evaluation of the mechanical properties of powder for storage. The Third Israeli Conference for Conveying and Handling of Particulate Solids, Israel, pp. 3.93-3.98, 2000.
7. Maksimovic M. A family of nonlinear failure envelopes for non-cemented soils and rock discontinuities. *The Electronic Journal of Geotechnical Engineering*, 1, pp. 1-15, 1996 (<http://geotech.civen.okstate.edu/ejge/ppr9607>).
8. Molerus M. Theory of yield of cohesive powders. *Powder Technology*, 12, pp. 259-275, 1975.

## **SURFACE CHARGE OF SOILS AND PLANT ROOTS**

*Józefaciuk G.*

Electric charge of natural materials may be divided onto two general types: permanent charge and variable charge. The permanent charge results from a substitution of higher valence cations by lower valence cations in the atomic (macromolecular or crystal lattice) structure, and a variable charge resulting from dissociation and/or association of protons by surface acidic groups (Van Olphen, 1993).

Prevalence of permanent charge exposed on basal planes of the particles is a common feature of most clay minerals. Variable charge occurs on surfaces of most soil solid phase constituents: organic matter, aluminum, iron and silicon oxides, edges of clay minerals and on plant roots surfaces, as well. Variable charge dominates also on kaolinites that is located both on the edges and on the basal Al and Si sites of the mineral (Ward and Brady, 1998). Contrary to the permanent charge, the magnitude of the variable charge depends on the composition of the soil solution (pH, concentration, ionic composition). The variable charge originates from dissociation and association of hydrogen ions (protons) from/to surface functional groups of acidic, basic or amphoteric character.

### **MINERAL SOIL CONSTITUENTS**

The permanent charge of clay minerals originates from that higher valence cations in the crystal lattice (for example silicon in the silica layers) are substituted by lower valence cations (for example by aluminum) during the genetic processes. This results in the “unsaturation” of oxygen bonds and excess of the negative charge. The substituting cation should be of similar size to this being replaced, therefore this process is called isomorphic substitution. Frequently the summational amount of the charge resulting from the isomorphic substitution is not equal to the permanent charge of the mineral. For example a part of the lattice charge may be neutralized by specifically bound cations inside the mineral particle structure (i.e. in the interlayers), as this frequently occurs in illites (binding of potassium cations) or may be blocked by multivalent polycations adsorption (Keren, 1986). The amount of permanent charge is characteristic for the mineral and conditions of its genesis. For most frequently occurring clay minerals this charge amounts from a few (kaolin group) by few tens (mica group – illites) to hundreds (smectites, zeolites) of centimoles per kilogram of the mineral. Permanent charge minerals dominate in mineral soils of the temperate climatic zone, therefore soils of these regions are called permanent charge soils.

Variable charge of mineral surfaces can have either positive, zero or negative charge, depending on soil pH value. In relatively low pH range, surface hydroxylic groups (SURFACE-OH) of these constituents may associate protons from soil solution via hydrogen bonds thus the surface becomes positively charged. In relatively high pH range, these surface hydroxyls may also undergo acidic dissociation, resulting in formation of negative charge. At a defined pH value surface hydroxyls neither associate the protons from the solution nor dissociate their own ones and the surface has no charge. The latter value of pH is called point of zero charge (PZC). The point of zero charge for some most frequently occurring soil constituents is: 3-4 for silicon oxides, 5-8 for iron oxides, 6-10 for aluminum oxides. The PZC of edge surfaces of clay minerals is most frequently around 8,2.

Variable charged mineral constituents, mainly oxides and hydroxides of iron, aluminum and silicon and mixed aluminum-silicon oxides – allophanes and imogolites occur in large amounts in highly weathered soils of humid tropics and subtropics, therefore soils of these climatic zones are called variable charge soils.

Both permanent and variable charge sites on mineral surfaces are heterogeneous. Petit *et al.* (1999) basing on the IR spectra of  $\text{NH}_4^+$ -saturated and KBr-exchanged smectites found that the layer charge have permanent low charge density and/or variable charge sites whereas the interlayers were characterized by high permanent charge density. Different proton interacting sites were found by Janek and Lagaly (2001) on freshly H-saturated and autotransformed smectites using potentiometric titration data. Sites with pK values of  $\sim 2.8$  were assigned to protons exchanged for sodium ions and of  $\sim 11.3$  to deprotonisation of silanol groups. Hydrated aluminum ions in freshly proton-saturated dispersions were characterized by pK $\sim 6$ . This group of weakly acidic centers also included oligomeric hydroxoaluminum cations because the amount of these sites increased during autotransformation and was accompanied by a shift in pK to  $\sim 5.5$ . Autotransformation removed all strongly acidic sites with pK $\sim 2.8$ . A specific form of Al oxyhydroxide with amphoteric properties, having two constants of deprotonation  $K_1=10^{-5}$  and  $K_2=0.32\cdot 10^{-6}$  were found by Mrad *et al.* (1997) as the product of  $\text{Al}_{13}$  polycation transformation in aluminium intercalated montmorillonite. Inhomogeneity of an illite charge indicating the existence of a multiplicity of energetically distinct surface types was found by Sinitsyn *et al.* (2000) basing on potentiometric titration. These surface sites included amphoteric silanol and aluminol groups, basal planar surfaces, and "frayed edges". The frayed edges were observed only in low ionic strength solutions.

## **ORGANIC SOIL CONSTITUENTS**

Acidic functional groups of soil organic matter (aliphatic and aromatic carboxyls, sulfoxyls, phenolic, enolic etc.) have very different acidic strength, depending not only on the kind of the group, but also on its locality. An increase of the pH of the soil solution leads to the neutralization of these groups thus they become negatively charged. Surface groups of stronger acidic character (similarly as stronger acids) are neutralized at lower pH values. The weaker acidic is the group, its neutralization requires higher pH value. Therefore the higher is the soil pH, the larger surface charge occurs on organic matter surfaces. These acidic surface groups, which are located closely to each other, create common electric field surrounding these groups and within this field their protons become delocalized (proximity effect). The delocalized protons behave as strong acids and so the neighboring groups are strongly acidic and the soil organic matter has some negative charge even at very low pH values. The negative charge at pH around 8.2 of fulvic acids reaches a few hundreds centimoles per kg and for fulvic acids up to one thousand.

## **PLANT ROOTS**

On surfaces of plant roots, variable charge of carboxylic groups dominate. The charge of plant roots was found to be closely correlated to uronic acid, present as polymerized galacturonic acid in pectic substances (Knight et al. 1961). The magnitude of root charge (CEC) was used for an explanation how various plant species survive environments with low level of cations availability (Gray et al. 1953), why plants uptake different proportion of mono and divalent cations (Huffaker and Wallace 1958), how plants compete in nutrient deficient mixed populations (Woodward et al. 1983), what are the mechanisms of aluminum toxicity (Keltjens 1995). This may be connected also with the surface charge density. The higher the SCD, the higher the surface potential and the higher relative adsorption of multivalent cations. Significant positive correlation between CEC of cell walls and Al sorption was found by Schmol and Horst (2001), who postulated that Al binding by pectin matrix is an important step in the expression of Al toxicity. The roots charge is higher for Al sensitive plants than for Al resistant plants.

## **REFERENCES**

1. Chi Ma and Eggleton, R.A. Cation exchange capacity of kaolinite. *Clays and Clay Minerals* 47, 174–180.
2. Gray B, Drake M and Colby W G 1953 Potassium competition in grass-legume associations as a function of root cation exchange capacity. *Soil Sci. Soc. Am. Proc.* 17, 235-239.

3. Huffaker RC and Wallace A 1958 Possible relationships of cation-exchange capacity of plant roots to cation uptake. *Soil Sci Soc. Am. Proc.* 22, 392,394.
4. Janek, M. and Lagaly, G. (2001) Proton saturation and rheological properties of smectite dispersions. *Appl. Clay Sci.*, 19, 121-130.
5. Keltjens W G 1995 Magnesium uptake by Al-stressed maize with special emphasis on cation interactions at root exchange sites. *Plant and Soil* 171, 141-146.
6. Keren, R. (1986) Reduction of the cation-exchange capacity of montmorillonite by take-up of hydroxy Al polymers. *Clays and Clay Minerals*, 22, 41-47.
7. Knight A H, Crooke W M and Inkson R H E 1961 Cation-exchange capacities of tissues of higher and lower plants and their related uronic acid contents. *Nature* 192, 142-143.
8. Mrad, I., Ghorbel, A., Tichit, D. and Lambert J.F. (1997) Optimisation of the preparation of an Al-pillared clay: thermal stability and surface acidity. *Appl. Clay Sci.* 12, 349-364.
9. Parks, G.A. (1965) The isoelectric points of solid oxides, solid hydroxides and aqueous hydroxo complex systems. *Chemical Review*, 65, 177-198.
10. Petit, S.; Righi, D.; Madejova, J. and Decarreau, A. (1999) Interpretation of the infrared NH<sub>4</sub><sup>+</sup> spectrum of the NH<sub>4</sub><sup>+</sup>-clays: application to the evaluation of the layer charge. *Clay Minerals* 34, 543-549.
11. Rampazzo, N. and Blum, W.E.H. (1991) Decrease of layer charge in 2:1 clay minerals through soil acidification. In: *Proceedings of 7th Euroclay Conference*, Dresden, M. Storr, K.H. Henning and P. Adolphi, eds., 863-864.
12. Sinitsyn, V.A., Aja, S.U., Kulik, D.A. and Wood, S.A. (2000) Acid-base surface chemistry and sorption of some lanthanides on K<sup>+</sup>-saturated marblehead illite: I. Results of an experimental investigation. *Geochim. Cosmochim. Acta*, 64, 185-194.
13. Van Olphen, H. *An Introduction to Clay Colloid Chemistry*, Wiley Interscience Publishers, New York, (1963)
14. Ward, D.B. and Brady, P.V. (1998) Effect of Al and organic acids on the surface chemistry of kaolinite. *Clays and Clay Minerals* 46, 453-465.
15. Woodward R A, Harper K T and Tiedemann A R 1984 An ecological consideration of the significance of cation-exchange capacity of roots of some Utah range plants. *Plant and Soil* 78, 169-180

## DESCRIPTION OF VARIABLE CHARGE FROM BACK TITRATION DATA

*Józefaciuk G., Matyka-Sarzyńska D.*

Back titration procedure (Duquette and Hendershot 1993, Józefaciuk and Shin 1996a, Nederlof *et al.*, 1991, 1993) has been widely used for characterizing variable surface charge of minerals, soils and plant roots. The titration is performed separately for the suspension and for its equilibrium solution (supernatant), starting from low pH upwards. The idea of this method is based on the assumption that the hydroxylic ions of the base added to the suspension are consumed by acids present in the equilibrium solution and by acidic functional groups present on the surface of the suspended solid. Therefore after subtraction of the titration curve of the equilibrium solution from this of the whole suspension, one obtains the titration curve of the solid.

### THEORY

The solid phase titration curve i.e. an amount (mole) of base consumed by the suspension,  $N_{susp}$ , minus the amount consumed by the supernatant,  $N_{sol}$ , is treated as an increase of the variable surface charge of the solid phase,  $\Delta Q_V(\text{pH})$ , during the titration:

$$\Delta Q_V(\text{pH}) = N_{susp} - N_{sol} \quad (1)$$

The  $\Delta Q_V(\text{pH})$  accounts for an increase of negative charge and a decrease of positive charge.

The variable charge vs. pH dependence can be interpreted in terms of proton dissociation/association of surface functional groups using site-heterogeneity theory (De Wit *et al.*, 1990; Jozefaciuk and Shin, 1996b; Koopal *et al.*, 1987), that is briefly outlined below.

Assuming that the variable charge origins from dissociation of surface acidic groups of kind  $i$ :  $\text{SOH}_i = \text{SO}^-_i + \text{H}_s^+$ , ( $\text{H}_s$  denotes a proton in a plane of dissociation) and the (intrinsic) dissociation constants  $K_i$ :

$$K_i = [\text{SO}^-_i][\text{H}_s^+]/[\text{SOH}_i], \quad (2)$$

where the brackets denote surface activities, the variable charge at a given pH is:

$$Q_V(\text{pH}) = \sum_{i=1}^n [\text{SO}^-_i](\text{pH}) = \sum_{i=1}^n N_i \alpha_i(K_i, \text{pH}_s), \quad (3)$$

where  $\alpha_i(K_i, \text{pH}_s) = [\text{SO}^-_i]/[\text{SOH}_i]$  is the degree of ionization of groups kind  $i$  and  $N_i = [\text{SOH}_i]$  is their amount. For any pH during the titration:

$$Q_V(\text{pH})/N_t = \alpha(\text{pH}) = \sum_{i=1}^n \alpha_i(K_i, \text{pH}_s) N_i/N_t = \sum_{i=1}^n \alpha_i(K_i, \text{pH}_s) f(K_i), \quad (4)$$

where  $N_t$  is the total amount of surface groups and  $f(K_i)=N_i/N_t$  is a fraction of  $i$ -th groups. Using condensation approximation (Nederlof *et al.* 1993) the  $f(K_i)$  values are:

$$f(K_i) = 1/N_t \Delta Q_V(\text{pH})/\Delta K_i; \quad K_i = [\text{H}_s^+], \quad (5)$$

and in logarithmic scale:

$$f(\text{p}K_i) = 1/N_t \Delta Q_V(\text{pH})/\Delta \text{p}K_i; \quad \text{p}K_i = \text{pH}_s. \quad (6)$$

The distribution function of surface dissociation constants, i.e.  $f(K_i)$  vs.  $K_i$  dependence, can be calculated knowing both surface protons activity ( $\text{pH}_s$ ) and  $N_t$  values. Soil components, as well as plant root surfaces may have different shapes and different charges thus may vary in surface potential values. For  $\text{pH}_s$  (and  $K_i$ ) calculations, basing on the diffuse double layer theory, a single potential value spread uniformly over all surfaces of the same shape is a common assumption, which seems not to be valid in the case of soils and plants. Also, there still exist much controversies on the application of the DDL theory to surface chemistry (Mc Bride, 1997). Therefore, the surface proton activity is replaced by the solution activity and  $N_t$  is taken as  $N_{max}$  = maximal value of  $(N_{susp}-N_{sol})$  measured within the experimental window and, instead of the intrinsic, the distribution functions of apparent surface dissociation constants,  $K_{app}$ , are determined:

$$f(\text{p}K_{app,i}) = 1/N_{max} \Delta Q_V(\text{pH})/\Delta \text{p}K_{app}; \quad \text{p}K_{app} = \text{pH}. \quad (7)$$

The average value of  $\text{p}K_{app}$ ,  $\text{p}K_{app,av}$ , is calculated as:

$$\text{p}K_{app,av} = \sum_{i=1}^n \text{p}K_{i,app} f_i(\text{p}K_{app}), \quad (8)$$

which is direct measure of the average energy of the proton binding.

Having the variable charge vs. pH dependence one can find the relation of actual surface charge,  $Q_A$ , vs. pH. To do this the  $Q_V(\text{pH})$  curves are shifted against y-axis to meet the actual charge value at any pH e.g. a cation exchange capacity of the studied solid, estimated at the same ionic strength, at which the titration is performed. One should select a higher pH value to diminish eventual occurrence of positive surface charge that is not determined during the CEC measurements.

## PRACTICAL REMARKS

The titration curve of a solid, and especially of the soil, may include free acidic ions adsorbed on the surface (exchange acidity), which are not surface acidic groups. Therefore there exist a danger of interpretation of exchange acidity in terms of variable charge. To avoid the latter prior to the titration, the soil suspensions should be exchange acidity depleted. This can be done by standard neutral salt washing. We use fivefold centrifuging with excess of  $1 \text{ mole dm}^{-3}$  NaCl solution of pH=3 that provides the lack of Al (ICP AES) in the supernatants. The washed sample can be directly used for the titration, provided its mass is known.

Next  $1 \text{ mole dm}^{-3}$  NaCl suspension containing around 1.00g (dry mass) of the sodium homoionic form of the solid is kept at pH $\approx$ 2.9 by additions of small increments of  $1 \text{ mole dm}^{-3}$  HCl for half an hour of mixing. During additional 3 min. mixing the pH is controlled, and if changed by more than 0.02 unit, the suspension is centrifuged and the pretreatment repeated. From the final suspension, half of the supernatant (weighing) and the remaining suspension are titrated with  $0.100 \text{ mole dm}^{-3}$  NaOH in  $1 \text{ mole dm}^{-3}$  NaCl solution with the rate of  $30 \text{ }\mu\text{l/min}$ . The amount of the titer consumed between pH 3 to 9 is recorded with a step of 0.2 pH unit. The measurements are performed in four replicates. Usually the deviation of the titration curves is lower for the suspensions (around 5%) and higher for the supernatants (around 15%). If washing of the solid and the pretreatment for the titration are properly performed, the titration curves of the supernatants are similar to a titration curve of  $1 \text{ mole dm}^{-3}$  NaCl pH=3 solution, which indicates also that the dissolution of the solid phase under experimental conditions is negligible. This is important to note that in the above procedure the equilibrium conditions are not reached, so the titration curves can be used rather for comparative purposes. 24 hours equilibrium titration of a soil consumes up to twice as much titer as the continuous titration described here and a high dissolution of the solid phase occurs as is indicated by high deviation of the titration curves of the supernatants from the titration curve of NaCl solution (Jozefaciuk and Shin, 1996a).

Applying constant and high concentration of neutral salt during titration has a few advantages. It minimizes adsorption of exchange protons at low initial pH value and their further titration (replacing exchange protons by neutral salt cations), dilution effects (changes of variable charge with salt concentration), dissolution of solid phase, and allows for a better development of variable surface charge (surface groups dissociation is less hindered by electrostatic effects at high ionic strengths).

Some results of the application of the back-titration method in analysis of various materials are presented in Józefaciuk (2002) for minerals, Józefaciuk and Szatanik-Kloc (2002) for plant roots, Jozefaciuk et. al. (2002) for soils.

## REFERENCES

1. De Wit, J.C.M., Van Riemsdijk, W.H., Nederlof, M.M., Kinniburgh, D.G. and Koopal, L.K. 1990. Analysis of ion binding on humic substances and the determination of intrinsic affinity distributions. *Analitica Chimica Acta*, 232, 189-207.
2. Duquette, M. and Hendershot, W. (1993) Soil surface charge evaluation by back-titration: I. Theory and method development. *Soil Science Society of America Journal*, 57, 1222-1228.
3. Józefaciuk, G. and Shin, J.S. (1996a) A modified back-titration method to measure soil titration curves minimizing soil acidity and dilution effects. *Korean Journal of Soil Science and Fertilizer*, 29, 321-327.
4. Józefaciuk, G. and Shin, J.S. (1996b) Distribution of apparent surface dissociation constants of some Korean soils as determined from back titration curves. *Korean Journal of Soil Science and Fertilizer*, 29, 328-335.
5. Józefaciuk G. 2002 Effect of acid and alkali treatment on surface-charge properties of selected minerals. *Clays and Clay Minerals* 50, 646-655.
6. Józefaciuk G., Muranyi A. and Alekseeva T. 2002 Effect of extreme acid and alkali treatment on soil variable charge. *Geoderma* 109, 225-243.
7. Józefaciuk G. and Szatanik-Kloc A. 2003 Decrease in variable charge and acidity of root surface under Al treatment are correlated with Al tolerance of cereal plants *Plant and Soil* 11/13/2003 (in press).
8. Koopal, L.K., Van Riemsdijk, W.K. and Roffey, M.G. (1987) Surface ionization and complexation models: a comparison of methods for determining model parameters. *Journal of Colloid and Interface Science*, 118, 117-136.
9. Mc Bride, M. (1997) A critique of diffuse double layer models applied to colloid and surface chemistry. *Clays and Clay Minerals*, 45, 598-608.
10. Nederlof, M.M., Venema, P., Van Riemsdijk, W.H. and Koopal, L.K. (1991) Modeling variable charge behaviour of clay minerals. In: *Proceedings of 7th Euroclay Conference*, Dresden, M. Storr, K.H. Henning and P. Adolphi., eds., 795-800.
11. Nederlof, M.M., De Wit, J.C., Riemsdijk, W.H. and Koopal, L.K. (1993) Determination of proton affinity distributions for humic substances. *Environmental Science and Technology*, 27, 846-856.

## **GEOCHEMICAL FUNCTION OF SOIL IN THE ECOSYSTEM**

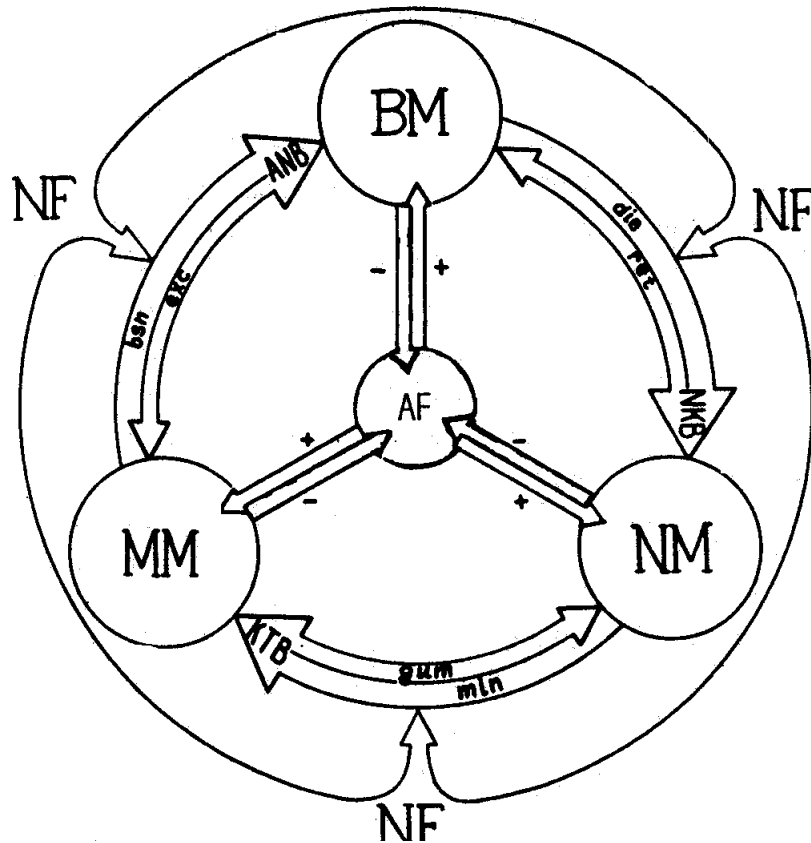
*Kerzhentsev A.S., Alekseeva T.V., Alekseev A.O., Abramichev A.Yu.*

Metabolism, the turnover of substance and energy between the vegetation (phytocenosis) and soil (pedocenosis), is the major function of natural ecosystem. Metabolism of an ecosystem is the way of manifestation and maintenance of the life by interaction of opposite processes of synthesis and decomposition of organic matter. It consists of three subprocesses: anabolism, necrobolism and catabolism (Fig. 1). Anabolism turns mineral elements into the biomass. Catabolism converts dead biomass (necromass) into the mineral elements, which enter a new cycle of metabolism. Between these strong and opposed directed processes there is a smoothing their interaction processes of necrobolism, turning the biomass used up in the life cycle into the necromass.

Natural ecosystem functions in stationary regime when the biomass synthesis is balanced with its dying and mineralization. Unbalance of metabolism makes up not more than 1% of the ecosystem mass. This allows us to consider climax ecosystem as a closed one, where the mass of mineral matter, required for biomass synthesis, equals the mass of mineral substance, released at mineralization of the dead biomass (necromass) with an accuracy of 1%. This means that in complete cycle of metabolism the ecosystem losses 1% of its mass and it is required subsequent supplement of losses due to the weathering of mountain rocks and atmospheric precipitations (liquid and solid). Migration of substances on relief and soil profile (up and down) has not been taken into consideration.

The rate of anabolism, including photosynthesis and respiration, is much higher than that one of catabolism, hence several periods of biomass synthesis correspond to a period of complete mineralization of the necromass. The time of complete mineralization of the mass of annual litter-fall is characteristic time (CT) of this soil and ecosystem within which the matter mass renews completely. In tropic soils CT does not exceed 3-5 years, in podzol soils it makes up 50-70 years, and in chernozems it reaches 300-500 years. The influence of external factors on specific soil should be considered taking into account its CT.

Long, comparable with CT, change of hydrothermal conditions in one (any) direction from the averaged or artificial change of the components of ecosystems mass: biomass, necromass, mineral mass, may disturb the dynamical equilibrium.



BM - biomass; NM - necromass; MM - mineral mass; NF - natural factors; AF - anthropogenic factors; ANB - anabolism; NKB - necrobolism; KTB - catabolism; bsn - biosynthesis; exc - excretion; die - dying off; ret - return of assimilates; min - mineralization; gum - humification.

*Fig. 1. Structural-functional scheme of an ecosystem.*

Transition of the substance from the phase of anabolism to catabolism and vice versa occurs with changing of the composition. Subsequence of consumption of mineral elements in anabolism differs from that one of their release at catabolism. The number and composition of the elements required is determined by the species composition of biocenosis and its phenology. Mineral elements during ontogenesis form different molecules, living cells, tissues, organs, physiological liquids differed by the complexity of structure and strength of chemical bonds.

As the organisms reach the generative phase, the necrobolism of turning biomass into the necromass begins. It consists of two subprocesses: the necrosis itself and return of vital substances into still functioning organs, first of all generative ones (flowers, fruits, seeds). The mature organisms provide generation of populations. Once the generative phase is completed, the biomass used up its life resource dies, turning into the necromass.

Since the “landing” of necromass, the catabolism starts: dissimilation of dead organic matter into simple mineral elements. It also comprises two subprocesses: mineralization and humification.

The sequence of dissimilation of organic matter depends upon the strength of chemical bonds, composition and activity of heterotrophic soil biota. Initially simple compounds are mineralized: sugars, proteins, amino acids, then more complicated ones and finally stable substances like lignin, chitin, and bone tissues. As a result of mineralization of simple compounds mineral gases (CO<sub>2</sub>, methane, ammonium etc.) are formed. More complicated compounds with higher ash content form except gases, mineral salts or free radicals. Gases are absorbed by the plant leaves or diffused in the atmosphere.

A great part of mineral elements is absorbed by the root system of plants. The elements not required by phytocenosis interact with free radicals, forming soil humus. The other elements migrate with water solutions on soil profile and relief incline and the ecosystem losses them. Humus, as a product of second synthesis, entering into the composition of necromass, is also the subject to mineralization, but it is mineralized more slowly and with release of much more salts than gases. Humines are the most resistant fraction of organic matter. The process of their complete mineralization lasts for decades and centuries. Mineral colloids with small amount of salts of rare elements are the products of mineralization. They completely remain in the soil, enriching the reserve of minerals and falling out from biological turnover.

In natural ecosystem the losses of substances are minimal. Usually the elements not demanded for phytocenosis and incorporated into humus are lost. The losses increase sharply at changing external conditions, which stimulate the processes of adaptation. In this connection, to endure in new conditions the organisms change their function and the ecosystem - its structure. The change of species composition disturbs the normal rhythm of substances turnover, creating the conditions for removing the chemical elements from the ecosystem. Catastrophic losses of mineral elements occurs at fires and invasion of entomological pests (locust, silkworm), when biomass is mineralized almost completely, and anabolism is blocked. The weeds become rescues of ‘gold supply’ of the mineral elements. They can increase their own mass by hundred and

thousand times at the absence of competitors and abundance of mineral food. They like biological pumps absorb mineral elements, limiting their losses from the ecosystem. Succession returns the turnover into its normal limits.

Plowing and loosening of the soil improve many times aeration, stimulating the activity of heterotrophic biota, which mineralizes soil humus, releasing mineral elements to provide high yields. However, despite many species phytoecosis, the monoculture of agroecosis is able to assimilate not more than 20% of the mineral elements released by the soil. Another 80%, as after the fire, is condemned to be removed with the run-off from the ecosystem. Minimal fresh litter-fall and the deficit of free radicals hinder active humification. The weeds try even here to play its ecological mission on protection of 'gold supply', but due to agro technical technique and means of chemical protection they are eliminated. Hence, the losses of the elements and degradation of soils in agroecosis are inevitable. By this it is possible to explain a great exceed of chemical run-off from agricultural lands over the run-off from natural landscapes.

The system of tillage free agriculture or zero treatment of soil is the most ecological, since it limits the layer of compulsory aeration of the soil with flat colter for deep planting of seeds. The soil functions in natural mode. The absence of excess of mineral elements restrains the weeds.

The system of polydominant plants, capable to absorb maximum mineral elements released by the soil, is also ecological, but its usage in practice restrains by technical difficulties of harvesting various crops grown on the same field. Ecological agriculture should be based on regulation of the capacity and the rate of metabolism in agrarian ecosystem with the account of mutual compensation of anabolism and catabolism, excluding the losses of mineral elements.

**LANDSCAPE AND GEOCHEMICAL CONDITIONS FOR GENESIS OF  
DIFFERENT KINDS OF CARBONATE ACCUMULATIONS IN  
CHERNOZEMS OF THE SOUTHERN PRE-URAL, RUSSIA**

*Khokhlova O.S., Oleynik S.A.*

Carbonate accumulations (CAs) have been studied at the topographical sequence (catena) of the Ordinary Chernozems developed on the redeposited diluvium of the Permian clays and sandstones in the Southern Pre-Ural, Russia. The study site is situated at the steppe area of this region in the floodplain of the Salmysh River (the tributary of the Sakmara River). 4 pits studied have been located on the different heights and distances from the waterlogged floodplain of the local stream (Fig. 1). The uppermost soil I occupied the automorphic position in the catena, the lowest one IV – hydromorphic position and two soils II and III in the middle part of the sequence – transit positions in the catena. The length of the catena was 200-250 m, the difference in the heights – 1,5 -2 m. CAs in the soils of catena have presented by the white soft spots, hard nodules and some intermediate forms. They have been studied morphologically (on macro-, micro and submicroscopic levels) and using instrumental techniques (X-ray diffraction pattern, thermal and isotopic analyses).

The Ordinary Chernozems of the uppermost part of catena are changed by the Meadow Chernozems in the lowest part of it. In the profile of the Meadow Chernozems there was water at the depth of 150-170 cm in summer. In the soil I of the uppermost part in catena the CAs have been presented by large brightly white soft spots, in the soils II and III of the transit positions in catena these spots become less whiteness, smaller and had a hard core, in the soil IV of the lowest part in catena there were small whity-gray hard nodules.

Internal micro- and submicrostructure of the CAs in the soils of catena were different. The white soft spots in the soil I of the uppermost part of catena is made of microcrystalline calcite, there are dissolving and recrystallizing calcite grains in voids, all mineral grains of matrix are surrounded by calcite coating. The white soft spots with hard core in the soils II and III of the middle transit part in catena have a very characteristic microstructure: on the background of homogeneous clay and carbonate plasma impregnating by microcrystalline calcite there are some packed undifferentiated cryptocrystalline sections – cores or sections of ooidsepic fabric when we can see not a single core between soft calcite accumulations but a lot of hard cryptocrystalline concretions. The hard nodules in the soil IV of the lowest part in catena have packed cryptocrystalline microstructure, the dissolving and recrystallizing calcite grains are distinctly seen in voids.

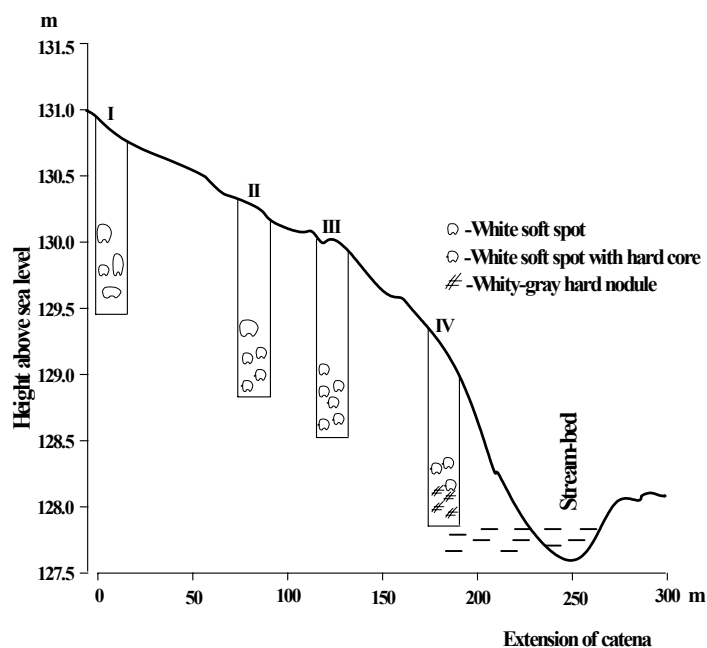


**Fig. 1.** The scheme of catena.

The differences that have been revealed in the microstructure of CAs in the soils of catena are well preserved on the submicrolevel of observation. The white soft spots is made of well crystal calcite, the hard nodules are characterized by collomorphic undifferentiated texture. In the soils of transit part in catena there is a cellular texture, the calcite grains are well crystallized mainly, the “boundary” of cell is made of cryptocrystalline calcite.

Based on the X-ray diffraction pattern and thermal analysis all the CAs are composed of pure calcite. The calcite content in CAs varies from 70 to 90% and has no differences throughout the catena (Table 1). The distribution of isotopic composition of carbon in calcite of the CAs have a catena regularity. The isotopic composition of carbon in the white soft spots and hard nodules is clear different and amounts respectively -9,6‰ and -13,2‰. The intermediate forms of CAs (the white soft spots with hard cores) have an intermediate isotopic composition of carbon as well – -10,7‰ , -12,0‰. At the same time, the isotopic composition of humus carbon in the upper humuc A1 horizon does not differentiate throughout the catena and amounts -23,4– -24,7‰ in all the soils studied. It means that calcite in the hard carbonate nodules formed in more hindered conditions of gaseous

exchange than that in the white soft spots and testifies to the hydrogenous nature of the nodules.

**Table 1.** CaCO<sub>3</sub> content in CAs, thermal characteristic, data on isotopic composition and X-ray diffraction pattern for calcite

Soil, horizon, depth, cm	Sample	Content CaCO <sub>3</sub> in CAs, %	isotopic composition of carbon in CAs, ‰	Data on			X-ray diffraction pattern  d <sub>104</sub>
				thermal analysis			
				temperature (°C) of			
				beginning	maximum	end	
				of structural decomposition			
Soil I, B2ca, 170-200	White soft spots	100	-9,6	700 810	740 860	800 890	0.037
Soil II, B1ca, 130-170	White soft spots with hard core	69	-10,7	790	880	920	0.037
Soil III, B1ca, 130-150	White soft spots with hard core	89	-12,0	770	880	920	0.037
Soil IV, B2ca, 150-170	Hard nodules	89	-13,2	800	870	920	0.037

We can conclude that the white soft spots and hard nodules in the Chernozems of the steppe area of the Southern Pre-Ural develop in distinctly different conditions, i.e., automorphic and hydromorphic ones, accordingly. If the white spots in the soil of the upper part in catena form from the true solution It can marked out the intermediate forms of CAs – the white soft spots with hard cores that develop in the transit part of catena under interchange of automorphic and hydromorphic conditions of soil formation. The complex study of CAs using hierarchical morphological approach and instrumental techniques lets us to get additional information and data that point directly to the genesis of the different kinds of CAs.

## SEASONAL VARIABILITY OF SOIL WATER RETENTION CURVES

*Korsunskaja L.P., Farkas Cs.*

### INTRODUCTION

Sustainable agricultural management requires detailed information on the effect of various management practices on soil physical properties and water regime. The complex approach of such a study should be based on both, field measurements and mathematical modelling.

The main limit on the application of soil water balance simulation models for soils under agricultural utilization is the rather strong seasonal variability of soil physical and hydrophysical properties. These properties are handled in most of the simulation models, used in practice, as constant ones. The seasonal variability of soil hydrophysical functions (soil water retention and soil hydraulic conductivity curves) under different tillage practices has not been well examined yet. This variability was found to be valuable in the low suction range for brown forest soils of Gödöllő, Hungary, developed on sandy loam (Farkas et al., 1999). The sensitivity of the SWAP simulation model to seasonal changes in soil water retention curves was proofed (Farkas et al., 2000).

Further development of soil water balance simulation models is limited because of the lack of available data. Soil surveyors face problem of sampling all the time: it is difficult to estimate, how many times and after which events soil sampling should be performed to determine the seasonal variability of soil hydrophysical functions. Such kind of monitoring is rather expensive and time confusing. Thus, finding a relationship between the water retention curve parameters and soil properties, related to soil compaction (bulk density) allows quicker and cheaper description of the effect of soil compaction on soil water regime and transport.

As several authors reported, various tillage treatments influence the shape of the pF-curve in the low suction range (Korsunskaya et al., 1995), while the form of the curve remains almost the same at low soil water content (and high soil potential) values. Based on these conclusions, a non-linear estimation method to calculate the parameters of the soil water retention curve was developed by Sobczuk and Walczak (1996), consisting of the modification of the commonly used Van-Genuchten equation (Van Genuchten, 1980). Two additional soil properties (bulk and particle densities) and a site-specific parameter were used for this purpose.

In this study the applicability of the Sobczuk's and Walczak's method was tested on an appropriate soil hydrophysical database, constructed from data of a long-term tillage treatment in Gödöllő, Hungary.

## MATERIALS AND METHODS

The research was conducted in the 4<sup>th</sup> year of a long-term field experiment of five tillage systems on the experimental field of the Institute of Crop Production at the Szent István University in Gödöllő (47°46'N, 19°21'E), Hungary. The soil is a brown forest soil formed on sandy loam, which is typical in this region and considered to be sensitive to sealing and compaction.

Tillage treatments include conventional ploughing (P- 22-25cm) and disking (D- 16-20cm), loosening-ploughing (L- 35-40cm, P- 22-25cm), loosening-disking (L- 35-40cm, D-16-20cm) and minimum tillage (direct drilling, NT) (Birkás et al., 1999). The soil was tilled in October 1996. Corn was planted in April and harvested in October.

Undisturbed soil cores of 100 cm<sup>3</sup> volume were collected 4 times (March, June, August and October) within the 1997 growing season at 5 to 10-, 15 to 20- and 40 to 45- cm depths in 3 replicates from each tillage treatment to determine soil bulk and particle densities and soil water retention curves (pF-curves). The latter were measured at pressure heads represented by the pF values of 0.0, 0.4, 1.0, 1.5, 2.0, 2.3, 2.7, 3.4 and 4.2 according to (Várallyay, 1973).

The modified Van-Genuchten parameters of the pF-curves, according to Sobczuk and Walczak (1996) were calculated, using the non-linear least square method. The following function was fit to the measured pF-curves:

$$\Theta = \left( \frac{1}{\rho} - \frac{1}{\rho_0} \right) \left[ 1 + (\alpha * \Psi)^n \right]^{1/n-1}$$

considering  $n = (\rho_0 - \rho * C) / 2$

where:

- $\theta$  - calculated water content (g/g)
- $\rho$  - bulk density of the soil sample (g/cm<sup>3</sup>)
- $\rho_0$  - density of the solid phase of the soil (g/cm<sup>3</sup>)
- $\psi$  - soil water suction (cm of H<sub>2</sub>O)
- $\alpha$  - calculated parameter (1/cm)
- $C$  - calculated parameter (cm<sup>3</sup>/g)

The mean difference (MD) and the root mean square difference (RMSD) were calculated for evaluating the accuracy of the estimated soil water retention curves and the closeness between the measured and calculated water retention curves, respectively, according to Tietje and Tapkenhinrichs (1993). The jack-knifing method was used for verification: soil water retention curves, measured at 3 sampling times were utilised to determine the parameters  $C$  and  $\alpha$ , characteristic for the tillage treatment analysed. One set of pF-curves (consisting of 9 curves: 3 depths x 3 replicates), corresponding to one measurement period was out of the fitting procedure in all of the cases to be used for the independent verification of the estimated pF-curves. Thus, 5x4 fitting procedures were performed: “5” refers to the number of the tillage treatments (NT, P, L, LP and LD), while “4” to the combination of the sampling times.

The nomination used was MM\_TT, where MM referred to the tillage treatment, whereas TT – to the number of the month, the pF-data of which was taken out of the non-linear estimation and used for the verification. In case of ploughing treatment, the estimation procedure was repeated separately for each sampled soil layer for evaluating the possibilities to reduce the estimation error. Consequently, 4x3 fitting procedures were done, where “3” refers to the number of soil layers the samples were taken from (5-10, 15-20 and 40-45 cm), while “4” to the combination of the sampling times.

## RESULTS AND DISCUSSION

The MD and RMSD values, calculated for different tillage treatments varied between  $-0.004 \div 0.038 \text{ m}^3/\text{m}^3$  and  $0.021 \div 0.048 \text{ m}^3/\text{m}^3$ , respectively (Table 1). Tietje and Tapkenhinrichs (1993) present results of soil pedotransfer function evaluation of 13 authors. They report 5 authors with 100% evident applicability. MD and RMSD values according to these authors vary between  $-0.053$  to  $0.013 \text{ m}^3/\text{m}^3$  and  $0.033$  to  $0.075 \text{ m}^3/\text{m}^3$ , respectively. Nemes (2002), comparing the soil water content dynamics, simulated with measured and estimated pF-curves concluded, that pF-curve estimations, producing RMSD up to  $0.07 \text{ m}^3/\text{m}^3$  is satisfactory for soil water content modelling. Similar Concerning these results, we can conclude, that the estimation method, proposed by Sobczuk and Walczak (1996) gave good results for the presented dataset.

The statistical evaluation of the pF-curve estimation for 3 different soil layers of the ploughing treatment is given in Table 2. In general, slight improvement of the estimation of the pF-curves was obtained, when handling soil layers separately. Estimation accuracy, however, did not increase as much as we expected, probably because ploughing homogenises the upper 20-23 cm of the soil or because more measured data is required for the calculation of the parameters ( $\alpha$  and  $C$ ).

**Table 1.** Averaged mean and root mean square differences, calculated for pF-curves of different tillage treatments

	<b>MD</b> m <sup>3</sup> /m <sup>3</sup>	<b>RMD</b> m <sup>3</sup> /m <sup>3</sup>		<b>MD</b> m <sup>3</sup> /m <sup>3</sup>	<b>RMD</b> m <sup>3</sup> /m <sup>3</sup>
<b>NT_03</b>	0.003	0.025	<b>D_03</b>	0.035	0.048
<b>NT_06</b>	0.008	0.021	<b>D_06</b>	0.038	0.044
<b>NT_08</b>	-0.004	0.029	<b>D_08</b>	0.029	0.036
<b>NT_10</b>	-0.004	0.024	<b>D_10</b>	0.012	0.025
<b>P_03</b>	0.004	<b>0.040</b>	<b>LD_03</b>	0.017	0.030
<b>P_06</b>	0.003	<b>0.026</b>	<b>LD_06</b>	0.038	0.047
<b>P_08</b>	0.002	<b>0.027</b>	<b>LD_08</b>	0.020	0.028
<b>P_10</b>	-0.002	<b>0.025</b>	<b>LD_10</b>	0.018	0.026
<b>LP_03</b>	0.000	0.028			
<b>LP_06</b>	0.021	0.034			
<b>LP_08</b>	0.034	0.037			
<b>LP_10</b>	0.012	0.024			

**Table 2.** Mean and root mean square differences, calculated for the pF-curves of each sampled soil layer of the ploughing treatment

	<b>MD</b> m <sup>3</sup> /m <sup>3</sup>	<b>RMD</b> m <sup>3</sup> /m <sup>3</sup>
<b>P_03</b>	0.005	<b>0.036</b>
<b>P_06</b>	0.003	<b>0.023</b>
<b>P_08</b>	0.005	<b>0.026</b>
<b>P_10</b>	-0.003	<b>0.031</b>

## CONCLUSIONS

The formula, proposed by Sobczuk and Walczak (1996), used in this paper allows estimation of soil water retention curves of tilled soils from bulk and particle densities, which are more easy and quick to measure. Using this method the seasonal variability of the bulk density of a previously examined soil unit can be translated into the hydraulic properties variability, avoiding time consuming measurements of the latter ones. Thus, dataset, required for the development of the soil water balance simulation models to consider the seasonal variability of the soil hydraulic properties, can be constructed.

**Acknowledgement** This paper presents results of research programs supported by the Russian and Hungarian Academies of Sciences (Bilateral Scientific Cooperation), Hungarian Ministry of Education (NKFP 3B/0057/2002) and Hungarian National Scientific Foundation (OTKA T 042996).

## REFERENCES

1. Birkás, M., Gyuricza, Cs., Gecse, M. and Percze, A. 1999. Effect of repeated shallow disc tillage on some crop production factors on brown forest soil. (in Hungarian), *Növénytermelés*, Vol. 48 (4), pp. 387-402.
2. Farkas Cs., Gyuricza Cs. és László P., 1999: Study of certain soil physical properties in long term tillage experiments on Gödöllő forest soils *Növénytermelés*, Vol. 48, pp.323-336. (in Hungarian)
3. Farkas, Cs., Gyuricza, Cs., László, P. and Birkás, M, 2000. Study of the influence of soil tillage on soil water regime. In: R. Horn, J.J.H. van den Akker and J. Arvidsson (eds.): *Subsoil compaction. Advances in Geocology 32.*, Catena Verlag, pp. 251-257.
4. Korsunskaya, L. et al. 1995. Seasonal variation of some soil structure indicators. *Int. Agrophysics* 9:37-40.
5. Nemes, A. 2002. Multi-scale hydraulic pedotransfer functions for Hungarian soils. Doctoral Thesis, Wageningen University, the Netherlands.
6. Sobczuk, H.A. and Walczak, R.T. 1996. Bulk density dependence parameterisation of water potential – moisture characteristics of soil. *Polish Journal of Soil Science*, Vol. 29. (2), pp. 81-85.
7. Tietje and Tapkenhinrichs. 1993. Evaluation of pedotransfer functions. *Soil Sci. Soc.Am. J.* 57, 1088-1095.
8. Van Genuchten, M.Th. 1980. A closed-form equation for predicting the hydraulic conductivity of unsaturated soil. *Soil Sci. Soc. Am. J.*, 44, 892-898.
9. Várallyay. Gy. 1973. A new apparatus for determination of soil moisture potential in the low suction range. *Agrokémia és Talajtan*, Vol. 22., pp. 1-22.

## CONCURRENT TRANSPORT OF REACTIVE AND NON-REACTIVE CONTAMINANTS IN UNDISTURBED SOIL COLUMNS

*Korsunskaya L. P., Shein E. V., Pachepsky Y. A.*

### ABSTRACT

Advective-dispersive contaminant transport in soils continues to be a subject of extensive studies. Transport of conservative tracers, i.e. non-reactive ions, is mostly affected by soil physical heterogeneity that causes the differences in mobility of different parts of soil solution. Transport of reactive contaminants is affected by both physical and chemical heterogeneity. The objective of this study was to observe effects of soil structure and flow velocity on transport of reactive calcium and sodium ions. Undisturbed southern chernozem and chestnut soil columns were used to monitor the concurrent chloride, calcium and sodium transport in slow-flow and fast-flow breakthrough experiments. Parameters of the advective-dispersive transport were estimated by fitting the advective-dispersive to the reduced breakthrough data. At low velocities, transport seemed to occur in pores having a wide range of effective diameters. Diffusion and slow transport in fine pores caused slow effluent concentration changes at the late stages of the transport. Creating fast flow resulted in a decrease in the proportion of pore space providing the initial breakthrough and an increase in the proportion of pore space participating in diffusion-driven mass exchange as compared with the slow flow transport. Transport of reactive ions was affected by the flow rates in the same way as the transport of the conservative tracers. Flow rate effects on transport were more pronounced in chestnut soil that had poorer structure as compared with chernozem soil.

### INTRODUCTION

Advective-dispersive transport of adsorbing chemicals in soils is the subject of extensive studies. Soil heterogeneity affects such transport. Transport of conservative tracers, i.e. non-reactive ions, is mostly affected by soil physical heterogeneity that causes the differences in mobility of different parts of soil solution. Soil solution can be provisionally divided into mobile and immobile parts (van Genuchten, 1976; Korsunskaya, 1986; Pachepsky, 2000). Because of soil chemical heterogeneity, different parts of soil pore surfaces have different affinities to the chemicals moving in soils. Soil pore surfaces are often conditionally divided into fast- and slow-adsorbing parts with different adsorbing capacities (Selim,

1992; Selim 1999). The relative importance of the two types of soil heterogeneity depends both on soil properties and on properties of the chemical.

Observing simultaneous transport of conservative tracers and reactive contaminants and examining differences in transport of the two types of chemicals should provide an insight in the relative role of the chemical heterogeneity in the transport of reactive chemicals. The objective of this work was to compare transport of the chloride ion as a conservative tracer to the transport of reactive ions of calcium and sodium in undisturbed soil columns of two major agricultural soils from Southern Russia.

## MATERIALS AND METHODS

Undisturbed southern chernozem and chestnut soil columns were used to monitor the concurrent chloride, calcium and sodium transport. The columns of 5 cm ID and 10 cm height were sampled in Stavropol region at depths from 5 to 15 cm. Selected chemical and physical properties of soils are shown in Table 1.

**Table 1.** Selected soil properties

Soil	D	BD	PP	OC	Exchangeable cations (meq 100g <sup>-1</sup> )				pH
					Ca <sup>2+</sup>	Mg <sup>2+</sup>	K <sup>+</sup>	Na <sup>+</sup>	
Southern chern.	0-30	1.38	28.7	2.10	20.9	19.0	0.97	2.35	7.30
Chestnut soil	0-30	1.61	20.6	1.70	13.8	13.4	0.90	16.8	7.65

D = Depth, cm; BD = bulk density, g cm<sup>-3</sup> PP = % of particles < 1 μm, OC = organic carbon %

The advective-dispersive transport was studied with flow rates in the range from 0.7 to 11.7 cm day<sup>-1</sup>. The slow and the fast flows were created in each column by maintaining different heights of the influent solution above soil surface. The slow rates varied from 0.7 to 1.3 m day<sup>-1</sup>, the fast ones were in the range from 5.7 to 11.7 cm day<sup>-1</sup>. At the slow rate, each column received (a) a pulse of 0.001N CaCl<sub>2</sub> solution, (b) a pulse of 0.1N CaCl<sub>2</sub> solution, (c) a pulse of 0.05N CaCl<sub>2</sub> and 0.05N NaCl solution, (d) a pulse of 0.001N CaCl<sub>2</sub>. Then this sequence was repeated with the fast flow rate. Each of the pulses was terminated when the concentration of any of the three studied ions in the effluent became equal within the 1% accuracy window to the concentration in the influent. Ion selective

electrodes (Radelkis, Hungary) were used to measure ion concentrations in the effluent.

Data on the effluent concentrations were presented as breakthrough curves, i.e. dependencies of relative concentrations  $C_{rel}$  on the relative effluent volume  $V_{rel}$ . The relative concentrations were computed as

$$C_{rel} = \frac{C_0 - C}{C_0 - C_i} \quad (1)$$

where  $C_i$  is the concentration in the influent, and  $C_0$  is the concentration in the control experiment. The relative effluent volume was computed as  $V_{rel} = V/V_{pore}$ , where  $V_{pore}$  is the pore volume of the column.

The advective-dispersive equation in the form

$$R \frac{\partial C_{rel}}{\partial V_{rel}} = \frac{D}{qL} \frac{\partial^2 C_{rel}}{\partial X^2} - \frac{\partial C_{rel}}{\partial X} \quad (2)$$

was used to simulate chloride transport in the soil columns. Here  $D$  is the dispersion coefficient,  $\text{cm}^2 \text{ day}^{-1}$ ,  $q$  is the flow rate  $\text{cm day}^{-1}$ ,  $L$  is the column length,  $\text{cm}$ ,  $R$  is the retardation coefficient,  $X$  is the relative distance from the top of the column,  $0 \leq X \leq 1$  (Korsunskaja, 2000). The software CXFIT (Toride et al., 1995) has been used to fit the semi-infinite interval solution of the equation (2) to the chloride breakthrough curves to estimate parameters. The visual inspection of shapes of breakthrough curves was used to find indications of the presence of preferential flow pathways and to assess the distribution of pore velocities (Pandey et al., 1984, Valles et al, 1994; Strock et al., 2001). The information of this type was derived mostly from the chloride breakthrough curves. Using conservative tracers for that purposes has been proposed and justified earlier (Pfannkuch, 1963; Dankwerts, 1953; Valles et al., 1990).

Preliminary tests have been done to evaluate the reproducibility of breakthrough curves measured presumably in the same conditions. Some results of such tests are shown in Fig. 1 for the southern chernozem. Breakthrough curves were compared for two pulses of 0.1N  $\text{CaCl}_2$  separated by elution with 0.001N  $\text{CaCl}_2$ . Chloride contents were measured with two ion-selective electrodes for each of the two breakthroughs. The breakthrough curves appeared to be close visually; the transport parameters were also close (Table 2).

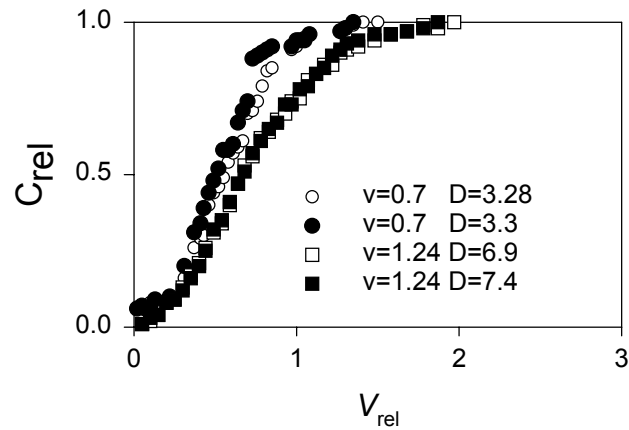


**Fig. 1.** Replicated chloride breakthrough curves;  $\circ$  and  $\bullet$  - first run,  $\square$  and  $\blacksquare$  - second run, hollow and filled symbols show measurements made with two independently calibrated ion selective electrodes.

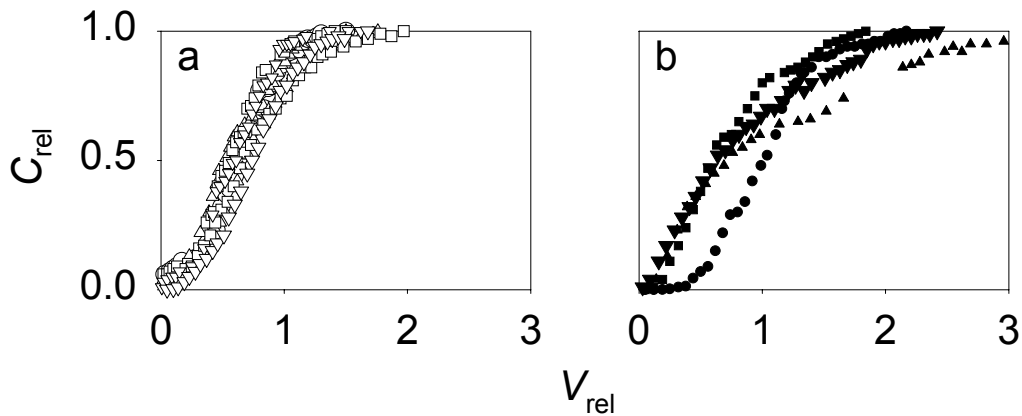
**Table 2.** Parameters of the advective-dispersive equation for data shown in figures in this paper.

Figure	Symbol	q	D	Figure	Symbol	q	D
1	$\circ$	0.70	3.28	6b	$\blacktriangle$	7.3	474
1	$\bullet$	0.70	3.30	6b	$\blacksquare$	7.3	267
1	$\square$	1.24	6.90	7a	$\circ$	0.94	29.2
1	$\blacksquare$	1.24	7.41	7a	$\triangle$	0.94	6.4
6a	$\circ$	0.8	32.8	7a	$\square$	0.94	85.3
6a	$\triangle$	0.8	518	7a	$\bullet$	5.7	248
6a	$\square$	0.8	142	7a	$\blacktriangle$	5.7	555
6a	$\bullet$	5.7	2526	7a	$\blacksquare$	5.7	40.5
6a	$\blacktriangle$	5.7	2915	7b	$\circ$	1.2	36.4
6a	$\blacksquare$	5.7	509	7b	$\triangle$	1.2	17.9
6b	$\circ$	1.06	36.4	7b	$\square$	1.2	72.1
6b	$\triangle$	1.06	17.9	7b	$\bullet$	8.1	324
6b	$\square$	1.06	72.1	7b	$\blacktriangle$	8.1	15.8
6b	$\bullet$	7.3	304	7b	$\blacksquare$	8.1	14.8

## RESULTS AND DISCUSSION

Data on  $\text{CaCl}_2$  transport of in two studied soils are shown in Fig. 2 and 3. Breakthrough curves in replications are very close for the southern chernozem at low flow rates of 0.72 to 1.4  $\text{cm day}^{-1}$  (Fig. 2a). Transport parameters are also very close (not shown). Shapes of the breakthrough curves suggest that the transport occurs in pores having a wide range of effective diameters. The inflection of breakthrough curves is caused by the dispersion in large pores. Diffusion and slow transport in fine pores cause slow effluent concentration changes at the late stages of the transport. Changes in the flow rates change shapes of the breakthrough curves from the same columns (Fig. 2b). Only one column has breakthrough curves with the inflection in the range of relative concentrations from 0 to 0.5. All other columns have breakthrough curves with an interval of the fast increase starting from the portions of the effluent. Such shape of breakthrough curves is typical for soil structures with preferential pathways including relatively small part of pore space. Such pathways carry chemicals through soil very fast because the pore water velocity in such preferential flow paths is high. The dispersion is caused by the mass exchange between preferential pathways and the bulk of soil rather than by the variations in pore water velocities within pores of large range as it has been in slow-flow experiments. Creating fast flow causes smaller part of pore space to work for the breakthrough transport and larger part of pore space to participate in diffusion-driven mass exchange as compared with the slow flow transport.

The chestnut soil demonstrates much more developed preferential flow as compared with the southern chernozem (Fig. 3a, b). The absence of inflection and the interval of the fast rise of relative concentrations are pronounced in all but one columns even at the low flow rates (Fig. 3a). High flow rates exacerbate differences in mobility of different parts of pore water (Fig. 3). Only one pore volume of effluent changes the relative concentration from 0 to 0.7. At the same time, the tail of the breakthrough curve is very long. This indicates that some parts of pore space, mostly fine pores, have a poor connection with the preferential flow pathways, and they are hardly accessible for the diffusion from/to the preferential pathways. In general, more dispersion can be seen in chestnut soil than in southern chernozem columns; the average value of the dispersion coefficient are  $25.0 \pm 14.2 \text{ cm}^2 \text{ day}^{-1}$  as compared with values of  $4.0 \pm 1.9 \text{ cm}^2 \text{ day}^{-1}$  in chernozem. The difference in dispersion coefficients in the two soils is tenfold in fast flow experiments.



**Fig. 2.** Chloride breakthrough curves in southern chernozem cores from low-flow (a) and fast-flow (b) experiments. Different symbols refer to different cores.

The differences in Cl breakthrough in the two soils can be, at least partly explained by differences in pore size distributions. Comparison of differential porosity for the two soils in this study has shown that pore size distribution in chestnut soil reflects presence of large number of fine pores with the effective diameters less than 0.01-0.06 mm. The pore size distribution for the chernozem showed the presence of much larger range of pore sizes (Korsunskaja, 2000). The chestnut soil also has been compacted as compared with the southern chernozem (Table 1). Pores less than 0.1 mm constitute more than 50% of pore space in such compacted soils (Domzhal, 1996). The domination of fine pores in chestnut soil results in larger role of such pores in convective dispersive transport in this soil as compared with chernozem.

Data on  $\text{CaCl}_2$  transport before and after the pulse of  $\text{CaCl}_2 + \text{NaCl}$  are compared in Fig. 4 and 5. Note that the actual concentrations after the pulse are decreasing as the leaching progresses. However, the relative concentrations computed with (1) increase both before and after the pulse allowing the comparison. The pulse changes the Cl breakthrough in chernozem (Fig. 4). The differences can be seen better in the slow-flow experiments. The longer tails on the after-pulse breakthrough curves imply some disaggregation and formation of additional fine pores caused by the presence of sodium ion. The fast-flow experiments show the coincidence of the initial sections on breakthrough curves before and after the pulse in three of the four columns. This can

be interpreted as a “memory” in pathways similar to the one shown in field experiments (Shein, 2000). More extensive tailing is also seen in fast flow experiments after the pulse.

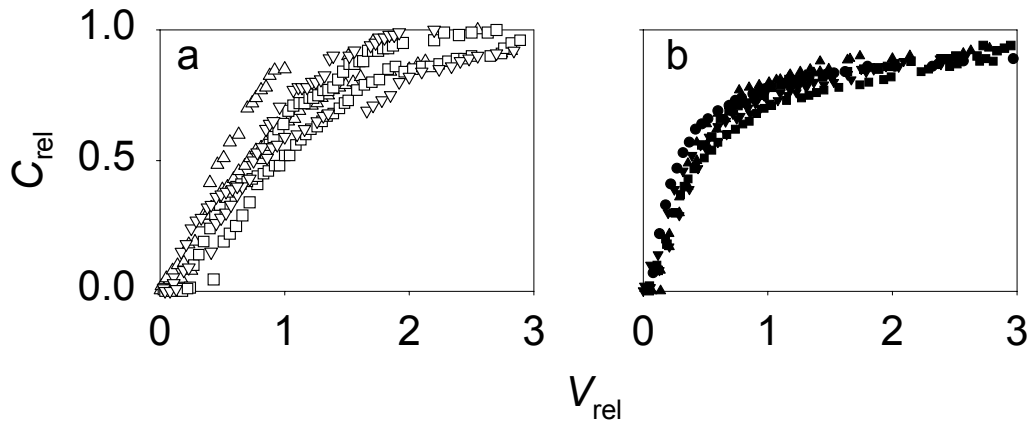


**Fig. 3.** Chloride breakthrough curves in chestnut soil cores from low-flow (a) and fast-flow (b) experiments. Different symbols refer to different cores.

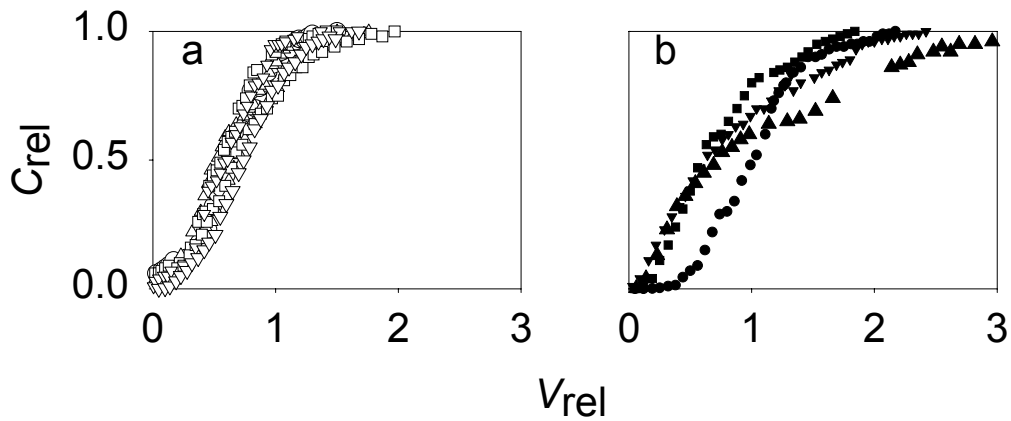


**Fig. 4.** Chloride breakthrough curves in southern chernozem cores (a) before and (b) after the pulse of  $CaCl_2 + NaCl$ .

Comparison of before- and after-pulse Cl breakthrough curves for chestnut soils (Fig. 5) reveals more extensive tailing after the pulse in slow-flow experiments. That can be attributed to the effect of sodium ion on soil structure similar to that in chernozem. The fast flow experiments resulted in breakthrough curves that were similar before and after the  $\text{CaCl}_2 + \text{NaCl}$  pulse. One possible explanation is based on the assumption that the preferential pathways occupy a small part of the pore space. The fast pulse moves predominantly through these pathways and a relatively small fraction of pore surface can be affected by the sodium solution. Another reason can be relatively short duration of the fast-flow experiments, so that the cation exchange kinetics was slow as compared with the transport time, and sodium did not have enough time enter the cation exchange complex. More time was available for cation exchange on slow-flow experiments. A similar effect was observed for uranium transport (Barnett et al., 2000).

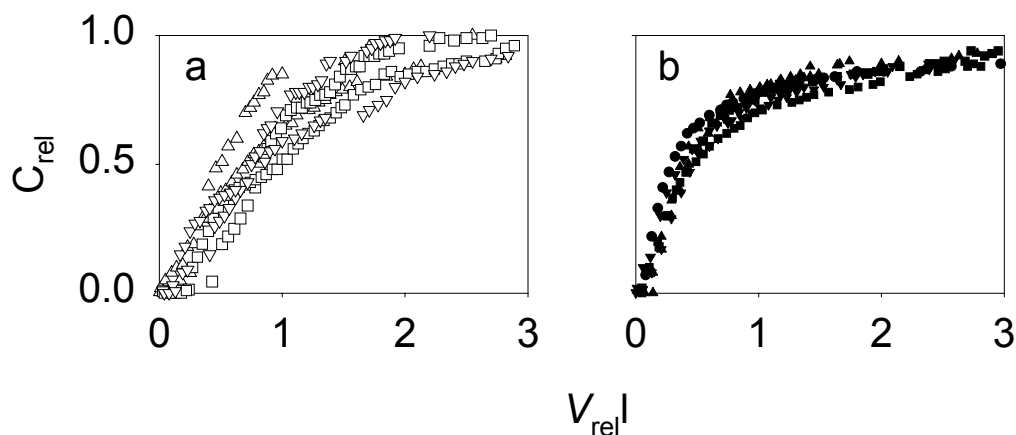


**Fig. 5.** Chloride breakthrough curves in southern chernozem cores (a) before and (b) after the pulse of  $\text{CaCl}_2 + \text{NaCl}$ .

Data on the concurrent transport of Cl, Ca and Na are shown in Fig. 6 and 7. The data come from the phase of experiments that developed after the last pulse and was monitored after about 22 and about 30 pore volumes of Ca-containing solutions for

chernozem and chestnut soils, respectively. Up to 16 pore volumes of 0.001N CaCl<sub>2</sub> solution passed the columns during this phase of the experiment. In chestnut soil, breakthrough curves of Cl, Na and Ca ions can be grouped by the flow rates rather than by the specifics of their interaction with surfaces in soils (Fig. 6). Changes in flow rates seem to cause changes in relative input of different groups of pores in the total transport in chestnut soil. The Cl ion approaches the equilibrium levels slightly slower than sodium. In chernozem samples, the differences between chloride and sodium transport are visible even better (Fig. 7). Leaching of sodium occurs as if it is available for leaching only at relatively small part of pore space. A larger part of pore space, including fine pores, is available for the chloride transport, and that causes a slower approach of the effluent concentration to the influent one. The relatively fast leaching of sodium also shows that the kinetics of ion exchange is relatively fast as compared with the ion transport.

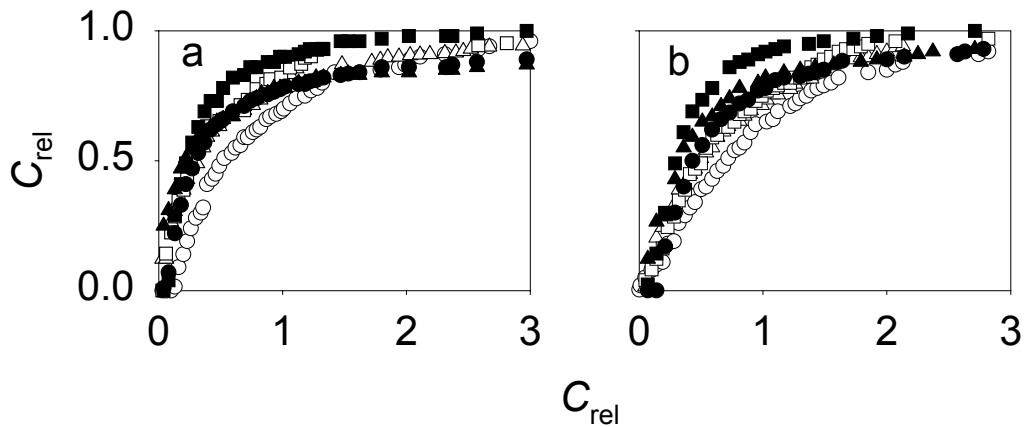


**Fig. 6.** Chloride (○, ●), calcium (△, ▲) and sodium (□, ■) breakthrough curves observed in slow-flow (hollow symbols) and fast-flow (filled symbols) experiments with two chestnut soil cores.

The physical and chemical properties in Table 1 do not explain the differences in the Cl, Ca, and Na transport in the two soils under study. The chernozem soil exhibits more aggregation and its bulk density is less than the chestnut soil. This structural differences impact transport. In the chernozem soil, the presence of large pores

provides the accessibility of cation exchange complex to moving soil solution and large mobile soil solution proportion than in chestnut soil. The over-compacted chestnut soil has a pore structure in which pore surfaces can rapidly become Ca-saturated.

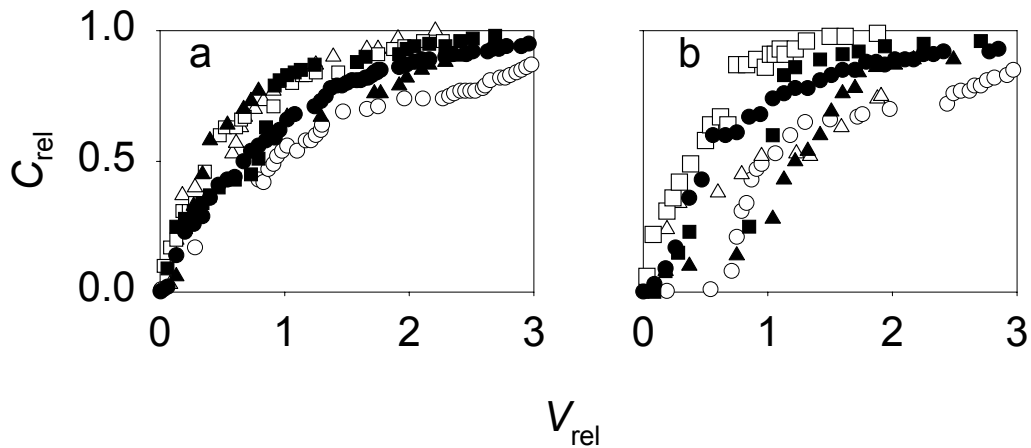


**Fig. 7.** Chloride (○, ●), calcium (△, ▲) and sodium (□, ■) breakthrough curves observed in slow-flow (hollow symbols) and fast-flow (filled symbols) experiments with two southern chernozem soil cores.

In summary, the physical heterogeneity governed transport of in ions in this work. This heterogeneity may cause fast transport of adsorbing pollutants in soil profiles, groundwater pollution, and creates a challenge incorporating the physical heterogeneity in models of pollutant transport in soils and sediments.

**ACKNOWLEDGEMENT** This work was partially supported by the Nato Science Programme, Cooperative Science & Technology Sub-Programme, Collaborative Linkage Grant # 979233.

## REFERENCES

1. Barnett M.O., P.M.Jardine, S.C.Brooks, and H.M.Selim. 2000. Adsorption and transport of Uranium(VI) in subsurface media. *Soil Science Society of America Journal*, 64: 908-917.
2. Danckwerts P.Y. 1953. Continuous flow systems. Distribution of residence times. *Chem. Eng. Sci.*, 2: 47-55.

3. Dormzhal, H, Usiarov, O. G., Zotov, K. V., Pranagal, Ya. 1990. Changes in soil pore structure caused by agricultural machinery. *Pochvovedenie*, (12): 25-37 (in Russian).
4. Gaston L.A., R.S.Mansell, and H.M.Selim. 1992. Prediction removal of major soil cations and anions during acid infiltration: model evaluation. *Soil Science Society of America Journal*, 56: 944-950
5. Kirda, C., Nielsen D.R., and Biggar J.W. 1973. Simultaneous transport of chloride and water during infiltration. *Soil Science Society of America Journal*, 37: 339-345
6. Korsunskaya, L. P., Shein E. V. 2001. Effect of bulk density and flow rate on mass transfer parameters in soils. *Moscow University soil science bulletin*, (2): 25-29.
7. Korsunskaya, L. P.D. P. Meleshko, and Ya. A. Pachepsky. 1986. Infiltration heterogeneity and convective-dispersive mass transfer in soils. *Soviet Soil Science*: 18: 78-88.
8. Pachepsky, Ya. , D. Benson and W. Rawls. 2000. Simulating Scale-Dependent Solute Transport in Soils with the Fractional Advective-Dispersive Equation. *Soil Science Society of America Journal*, 64:1234-1243
9. Pandey R.S., Gupta S. 1983. Analysis of breakthrough curves: effect of mobile and immobile pore volumes. *Australian Journal of Soil Research*, 22, 23-30
10. Pfannkuch H.O. 1963. Contribution a l'etude des desplacement fluides miscibles dans un milieu Revue de l'institut francais du petrole, 18: 25-42.
11. Selim H.M., B.Buchter, C.Hinz, and L. Ma. 1992. Modeling the transport and retention of cadmium in soils: multireaction and multicomponent approaches. *Soil Science Society of America Journal*, 56:1004-1015
12. Selim H.M., L. Ma, H. Zhu. 1999. Predicting solute transport in soils: second-order two site models. *Soil Science Society of America Journal*, 63: 885-892.
13. Shein, E.V., Marchenko, K. V. Preferential pathways of water transport in soils. *Moscow University Soil Science Bulletin*, 2: 13-17.
14. Stroock J.S., D.K.Cassel, M.L.Gumpertz. 2001. Spartial variability of water and bromide transport trough variably saturated soil blocks. *Soil Science Society of America Journal*, 65: 1607-1617.
15. Toride N., F. Leij, M.Th. van Genuchten. The CXTFIT code for estimation transport parameters from laboratory or field tracer experiments. Version 2.0. Research Rep. 137. U.S. Salinity Lab., 1995. Riverside, CA
16. Valles V., L. P. Korsunskaya, Ya. A. Pachepsky, and R. A. Shcherbakov. 1990. Interrelations between static and dynamic characteristics of soil structure. *Soviet Soil Science*, 23:87 – 92.
17. Van Genuchten M.Th., Wierenga P.J. 1976. Mass transport studies in sorbing porous media. *Analytical solutions*. *Soil Science Society of America Journal*, 40: 473-480.

## MODEL RESEARCH ON FORMATION OF SYNTHETIC ORGANIC-MINERAL BINDINGS AT VARIOUS pH AND AT PRESENCE OF ALUMINUM IONS

*Księżopolska A.*

Humus compounds in soils occur most of all in the form of bindings with the mineral part of soil. However, investigating those bindings in natural conditions, extracted directly from the soil is too complicated due to the destructive influence of extractants.

This paper aims at determining the degree of reaction of humic acids with minerals at various pH (3-7) and at the presence of aluminum ions on the basis of electrolytic conductivity and specific surface area. In order to prepare the organic-mineral preparations, humic acids from chernozem using the Schnitzer and Stevenson method [Schnitzer and Schluppli 1989; Stevenson 1994] and Namontmorillonite, mica, kaolinite and aluminum chloride were used. Suspensions of minerals with 0.1 M NaOH solution in the 1:10 ratio were formed. Then the preparations of humic acids were added to those suspensions in the amount of 0.4 g humic acid and 0.4 g AlCl<sub>3</sub>. The suspensions obtained were occasionally shaken by stirring and left for 24 hours to react. Then they were brought to the scheduled pH (3-7) values using the solution of hydrochloric acid and sodium base, gradually for three weeks in order to obtain a relatively constant desired pH value.

The aim of this research was to elaborate the optimum reaction of the suspension for the synthesis of organic-mineral bindings, as well as the role of aluminum. Electrolytic conductivity turned out to be a good parameter determining the degree of reaction between the humic acids and minerals because the mobility of ions decreased as the result of the complexing reaction. The lower the value of electrolytic conductivity was, the higher the degree of complexation was stated. EC was determined using a micro-computer conductivity meter CC311 (Elmetron, Poland) at 20°C +/-5°C. The measuring chamber of the conductivity meter was calibrated using standard KCl solutions of different concentrations. The organic-mineral complexes were resuspended in distilled water with an electrolytic conductivity of 5.8\*10<sup>-6</sup>Ω<sup>-1</sup> cm<sup>-1</sup>. Prior to the measurement, the suspensions were allowed to stand for 24 h with occasional mixing [Kalra and Maynard 1991].

Electrolytic conductivity, i.e., the ability of a solution to conduct electric current as a function of the number of ions in the solution and the electric charge is believed to be a reliable indicator for the characterization of organo-clay complexes [Cyganski 1991; Podsiadło 1990].

Electrolytic conductivity of preparations with Na-montmorillonite without aluminum is (8.9-36.3 mS), with aluminum (8.1-15.7 mS), of preparations with mica without aluminum (8.7-10.7 mS), with aluminum (8.8-39.4 mS), and of the preparations with kaolinite without aluminum (9.6-18 mS), with aluminum (9-26.7 mS). An important influence of the pH value of the suspension was stated on the value of electrolytic conductivity. The greatest correlation was found in the organic-mineral preparations with kaolinite and with aluminum ( $r=0.93^{***}$ ) and in the preparations with mica without aluminum ( $r=0.75^{***}$ ). It was proved that the greatest degree of reaction of the humic acids with Na-montmorillonite and with mica took place at pH 5, and with kaolinite at pH 7 (in the above mentioned combinations with aluminum). Aluminum clearly stimulated the increase in the degree of complexity of humic acids with minerals.

Specific surface area is a very good parameter that characterizes the structure of the organic-mineral adsorbent. Specific surface area was determined using the initial part of the water vapour adsorption isotherm at 20°C within an adsorbate relative pressure range of  $0, P/P_0, 0.35$  in accordance with the Brunauer, Emmet and Teller (BET) equation [Brunauer et al. 1938]. Water vapour adsorption were determined at 20°C gravimetrically (by weight), using a vacuum dryer in a temperature-controlled room according to Stawiński et al. (1999). The results of the specific surface area were statistically analyzed, including analysis of variance using the Statgraf software, and regression analysis using the Excel software. The calculated relations were then described with a linear equation, logarithm and power equation. The description of the relation analysis was made using the most fitted function.

The variability of surface phenomena during the formation of synthetic organic-mineral bindings is proved by different values of the specific surface area. The specific surface area of the bindings with Na-montmorillonite without aluminum ranges between 87 and 150.4 m<sup>2</sup>/g; with aluminum 145.6 to 152.8 m<sup>2</sup>/g; for bindings with mica without aluminum 83.2 to 150.4 m<sup>2</sup>/g; with aluminum 145.6 to 152.8 m<sup>2</sup>/g; for bindings with kaolinite without aluminum 14.1 to 43 m<sup>2</sup>/g; with aluminum 15.9 to 38.5 m<sup>2</sup>/g. A significant influence of the pH value of the suspension on the size of the specific surface area was stated. The highest correlation was observed in the bindings with kaolinite ( $r=0.93^{***}$ ). It was proven that the addition of aluminum to the bindings with Na-montmorillonite significantly influenced the growth of the specific surface area at pH 5, in bindings with mica-at pH 7, and in bindings with kaolinite- at pH 3 and 4. At pH 3 there was a significant decrease in that value and there was an increase at pH 4. The greatest degree of reaction was stated in bindings with Na-montmorillonite (without Al) at pH 5, with mica (without Al) at pH 7, and with kaolinite at pH 5,6 and 7.

The analysis of the specific surface area of the investigated preparations proved that the addition of humic acids to the minerals caused an increase in their specific surface area at all pH values both with and without aluminum. Observing the impact of pH on the specific surface area there was noticed growing tendencies with decreasing pH value from 7 to 3, which might have been caused by the transformation of the crystal lattice of the used clay minerals during the elaboration leading to formation of the synthetic bindings of minerals, humic acids and aluminum ions. That gradual increase of the specific surface area might also be related to the formation of amorphous silica of a great area in the processes of acid mineral destruction [Drees et al.1989]. Therefore, at pH 3, the specific surface area has the greatest value. The changes in the suspension of the organic-mineral bindings may cause the destruction of the crystal lattice of clay minerals. Those processes occur at the presence of hydrogen ions adsorbed exchangeably on the mineral surface. The attack of protons in the case of montmorillonite takes place on the face side, while in kaolinite – on the side of mineral plate, which has a great impact on the specific surface area of the investigated minerals [Motowicka-Terelak 1979; Milene et al. 1995; Józefaciuk 1995; Józefaciuk 1998].

Generally it can be stated that the degree of reaction of humic acids with minerals depends most of all on the type of mineral, pH value, and the presence of aluminum.

## REFERENCES

1. Brunauer S., Emmet P.H, Teller E., 1938. Adsorption of gases in multi-molecular layers. *Journal of the American Chemical Society*, 60, 309-319.
2. Cygański, A., (1991). *Electrical-analytical methods.*, (in Polish). Wydawnictwo Naukowo-Techniczne, Warsaw.
3. Drief, A., Nieto, F. And Sanchez-Nevas A. 2001. Experimental Clay-mineral formation from a subvolcanic rock by interaction with 1M NaOH solution at room temperature.
4. Józefaciuk, G. (1998). Changes of surface properties of soils and clay minerals in acidification and alkalization processes. (in Polish). *Acta Agrophysica*, 15, Monograph.
5. Józefaciuk, G., Hajnos, M., Sokołowska, Z., Renger, M. (1995). Influence of surface coverage by humic acids on surface free energy and wettability of quartz and kaolin. *Polish Journal of Soil Science*, 28 ,30-35.
6. Kalra, Y.P., Maynard, D.G. (1991). *Methods manual for forest soil and plant analysis*. Information Report Nor-X-319, Canada, 35-37 pp.
7. Milne, C. J. Kinnburgh, D. G., de Wit, J.C.M., van Riemsdijk, W. H. & Koopal, L.K. (1995). Analysis of proton binding by a peat humic acid using a simple electrostatic model. *Geochemica et Cosmochimica Acta*, 59, 1101-1112.

8. Mortland, M.M. (1970). Clay-organic complexes and interactions, *Advanced in Agronomy*, 22, 75-117.
9. Motowicka-Terlak, T., (1980). Response of some crops to the presence of active aluminum fractions in the soil in a pot experiment. *Pamiętnik Puławski*, 73, 151-165.
10. Podsiadło, H. (1990). *Laboratory practice book of physical chemistry*. (in Polish). Oskar Lange Academy of Economics, Wrocław.
11. Schnitzer, M., Schloppli, P. (1989). Method for the Sequential extraction of organic matter for soils and soil fractions. *Soil Science Society of America Journal*, 53, 1418-1424.
12. Stawiński, J., Józefaciuk, G., Wierzchoś, J., Rodriguez, Pascual, C. (1989). Influence of the pH on the content of Al, Fe and Si in equilibrium soil solution of constant ionic strength. *Polish Journal of Soil Science*, 23, 59-65.
13. Stawiński, J., Józefaciuk, G., Wierzchoś, J. (1987). Methodological aspects of soil acidity measurements. *Zeszyty Problemowe Postępów Nauk Rolniczych*, 344, 127-135.
14. Stevenson, F.J. (1994). *Humus Chemistry: Genesis, composition, Reactions*. John Wiley & Sons, New York.

## PHOSPHATE-INDUCED CHANGES IN THE SPECTRAL AND CHEMICAL PROPERTIES OF SOIL HUMUS SUBSTANCES

*Kudeyarova A. Yu.*

### INTRODUCTION

The capability of soil to bind phosphate-anions is determined by the coordination reactions that occur at the solid-liquid interfaces. Soil metal – containing solids as sorbents for phosphate (P) are usually covered with humus molecules and thus exhibit the properties of metal-humus complexes. Little is known about the P-induced changes in the metal-humus sorbing surfaces. Much attention should be given to high P additions simulating soil conditions in the immediate vicinity of P fertilizer granules.

The aim of this study is to examine spectral and chemical properties of the alkali-soluble humus substances (HS), the humic acid (HA) and fulvic acid (FA) fractions at different stages of their transformation in the P-enriched soil.

### MATERIALS AND METHODS

A soil sample was taken from the humus horizon of an arable grey forest soil (humic luvisols). The main chemical properties of the initial soil were as follows:  $\text{pH}_{\text{KCl}}$  – 5.15; total and exchangeable acidity – 2.7 and 0.7 meq/100 g soil, respectively; exchange capacity – 16.5 meq/100 g soil; and base saturation – 83.1%. The total content of  $\text{C}_{\text{org}}$  constituted 1.2% (according to the Tyurin method); the content of  $\text{C}_{\text{org}}$  in 0.1 N NaOH extract – 627 mg/100 g soil; the contents of total phosphorus and organic – bound phosphorus in 0.1 N NaOH extract – 15.0 and 10.3 mg/100 g soil, respectively. Soil with added  $\text{NH}_4\text{H}_2\text{PO}_4$  (in amounts corresponding to  $\frac{1}{2}$  of the total P-binding capacity, 102 mg  $\text{P}_2\text{O}_5$ /100 g soil) or  $\text{NH}_4\text{NO}_3$  (in amounts corresponding to the content of N in the added phosphate salt, 28 mg N/100 g soil) was incubated for 7 days, 1 year, and 3 years at a temperature of  $20 \pm 2^\circ$  and the moisture content of 55% of the WHC. Soil samples after the incubation were air-dried, ground (1 mm), and then used for analyses. The soil HS were extracted with 0.1 N NaOH (the soil-to-solution ratio of 1:50) without preliminary decalcification. Soil suspensions in flasks were shaken for 2 h and then left for a night, after which they were filtrated.

In the extracts obtained, the contents of carbon (C), Fe and Al (metals, M) were determined. The C content was determined by the bichromate oxidation method. To determine the contents of M, aliquots of alkaline extracts were treated with a mixture (3:1) of concentrated  $\text{H}_2\text{SO}_4$  and 57%  $\text{HClO}_4$  on heating. Then,

metal concentrations were determined using the atomic absorption method. To obtain the HA and FA fractions, the 0.1 *N* NaOH extracts were acidified to pH 1.5 with 1 *N* H<sub>2</sub>SO<sub>4</sub>. After the separation of precipitated HA from acid FA solution, the P content in two fractions was determined by the Murphy-Riley method. The contents of C, Fe, and Al were determined as noted above.

Difference electronic spectra of the alkaline extracts, HA and FA were obtained using the solvent (0.1 *N* NaOH for soil extracts and HA, a mixture of 0.1 *N* NaOH and 1 *N* H<sub>2</sub>SO<sub>4</sub> for FA) as a reference.

The HA obtained from initial soil was used to prepare Fe-HA complex. The treatment of HA with FeCl<sub>3</sub> provided C:Fe ratio of 1:6. The Fe-HA complex prepared was treated for five weeks with KH<sub>2</sub>PO<sub>4</sub> solution added to have a C:P ratio of 1:17. The pH value for systems was 4.1. Control complex and its P-modified organic product were used for the IR examination (KBr – technique). IR spectra of HA and FA from initial soil were also obtained.

## RESULTS AND DISCUSSION

Table 1 shows that extractability of C and M by 0.1 *N* NaOH tended to increase with increase in incubation period of P-enriched soil. Under these conditions, the difference in distribution of alkali-soluble C and M between the HA and FA fractions became more and more obvious. The amount of C associated with HA was greater, the greater was the incubation period of P-enriched soil. On the contrary, the amount of M associated with HA decreased sharply after one-year incubation of soil enriched in P.

**Table 1.** The contents of C<sub>org</sub>, metals (Fe+Al), and P, mg/100 g soil

Soil treatment	0.1 <i>N</i> NaOH extract		HA			FA		
	C <sub>org</sub>	M	C <sub>org</sub>	M	P	C <sub>org</sub>	M	P
1 year incubation without P	628	170	369	87	10	259	83	10
with added P	570	210	365	114	24	205	96	29
3 years incubation without P	657	190	403	107	4	254	83	11
with added P	745	250	552	73	3	193	177	58

According to the data of Table 1, the chemical composition of HA and FA varied considerably in the course of incubation. It is however seen that there is a relationship between the contents of M and P in HA and FA. After incubation of P-enriched soil for 3 years, the contents of M and P decreased considerably in HA but increased in FA. Consequently, the P incorporation in humus molecules resulted in the change of their reactivity in an acid medium. The P promoted reactions of M elimination.

The reactivity of organic compounds is a function of the distribution of electron density in their molecules. The UV-VIS absorption spectrum reveals the excitability degree of molecular electron system. The variation of excitation state from ground state may characterize energetic state of electrons belonging to functional groups having double bonds.

The difference electronic spectra (Fig. 1) show the pronounced effect of P on the electron energy state in the extractable HS. This fact suggests the P-induced structural changes in humus molecules. Bathochromic band shift observed in the region of 210-230 nm can be indicative of the appearance of additional C=C bonds in the side chains of the P-modified molecules of HS. Another P-induced spectral change is observed in the region of 250-350 nm (Fig. 1). This absorption band is

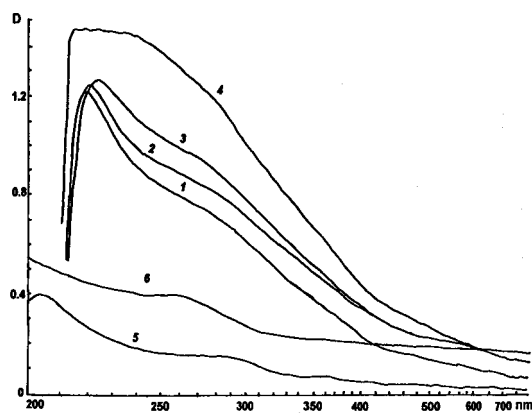


**Fig. 1.** Electronic spectra of alkali-soluble HS and FA: 1 - initial soil; 2 - P-treated soil, incubation for 7 days; 3 - incubation for 1 year; 4 - incubation for 3 years; 5 - FA from initial soil; 6 - FA from P-treated soil, incubation for 3 years.

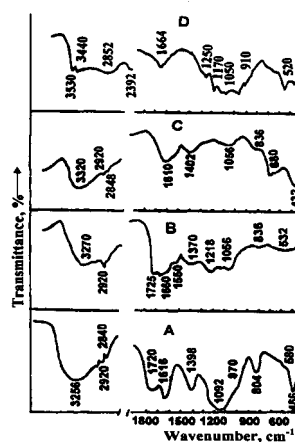


**Fig. 2.** IR spectra: A - FA; B - HA; C - Fe-HA-complex; D - P-treated complex.

attributed to the transition of free electronic pairs belonging to the nucleophilic atoms (mainly oxygen, for one, in the C=O group and its heteroanalogs). Hypsochromic shift of this absorption band increasing with the increase of incubation period of the P-treated soil could probably be due to the appearance of new polar P=O groups in the P-modified HS.

To gain insight into the mechanism of reactions resulting in the formation of new bonds in humic ligand, the prepared Fe-HA complex was tested as the metal-humus sorbent for P anions. Figure 2 shows that control and P-modified complexes differed structurally. There are the absorption bands at 1610 and 1402  $\text{cm}^{-1}$  in the control IR spectrum which can be attributed to the coordinated C=O groups. The P treatment resulted in the disappearance of these frequencies. At the same time, some new absorption bands arose in the spectrum. Among them are the bands at 1250 and 1170  $\text{cm}^{-1}$  which can be attributed to the vibration frequencies of the P=O groups having the dissimilar surroundings.

The data obtained prove the possibility of intra-complex formation of P=O bonds in humic macroligand through the substitution of prior C=O groups. It is known that compounds with P=O group are more capable of binding metal ions in the forms of very inert soluble complexes than compounds with C=O group. This fact allows to explain the increased elimination of metals from the P-modified humus molecules and their accumulation in FA (Table 1). According to the IR spectra of HA and FA (Fig. 2), the O-containing functional groups tended to accumulate in FA whereas C=C bonds tended to accumulate in HA. As evident from Fig. 1, in the spectrum of the P-modified FA there is a hypsochromic shift of the absorption band concerned with the transition of electrons belonging to oxygen atoms. This shift can be attributed to the P=O groups passing to FA fraction of HS.

## CONCLUSION

Consecutive changes in spectral and chemical properties of alkali-extractable humus substances have been revealed in the soil incubated with orthophosphate salt. The most considerable changes were observed at the end of the incubation period (3 years). The P-modified humus molecules were characterized by the accumulation of C=C bonds and P-containing polar groups. Structural changes corresponded to the observed changes in chemical properties of humus substances. It is shown that chemical composition of humic and fulvic acids varied significantly in the course of incubation of the P-enriched soil. The longer was incubation period, the lower were contents of metals and phosphorus in humic acid. The P incorporation in humus molecules promoted elimination of metals in the forms of soluble P-containing complexes and their discovery in fulvic acid fraction.

## MINERAL-ORGANIC COMPOUND OF SOILS: FORMATION MECHANISMS, PROPERTIES, FUNCTIONS

*Kurochkina G. N., Pinsky D.L.*

### INTRODUCTION

The adsorption of organic substances on an aluminosilicate matrix with high energy is an essential problem of pedogenesis, primarily, of the formation of highly dispersed mineraloorganic (MO) derivatives of the soil adsorbing complex (SAC) [Gorb, Orł]. Greenland believes that 50 to 80% of soil organic matter is bound to clay mineral [Greenland]. The composition, degree of accumulation, and migration of mineraloorganic derivatives determine the adsorbing capacity, the type and fertility of soils and their resistance to anthropogenic impact [Malin Orł]. Many authors revealed that adsorbed MO form no continuous film on the surface of a mineral; they are immobilized on a minor part of its surface, on so-called adsorption sites [Mal Theng]. The energy of interaction between these sites and organic molecules affects the conformation of adsorbed molecules, the strength of surface adsorption compounds, and finally, the degree of humus immobilization and its resistance.

The aim of this work was to study the mechanism of adsorption interaction between organic molecules and soil's aluminosilicate in controlled conditions.

### EXPERIMENTAL

The experimental subjects were synthetic gels with various contents of silica and alumina, which were used as analogs of soil's aluminosilicate (Table 1).

**Table 1.** Basic physicochemical characteristics of the adsorbents

Sample	SiO <sub>2</sub> /Al <sub>2</sub> O <sub>3</sub>	S, m <sup>2</sup> /g	V, cm <sup>3</sup> /g	Surface Charge
S	100% SiO <sub>2</sub>	750	1.01	—
AS-1	4/1	167	1.71	—
AS-2	2/1	248	0.75	+
AS-5	1/2	194	0.53	+
A	100% Al <sub>2</sub> O <sub>3</sub>	244	0.51	+

Note: S, silica gel; AS, aluminosilicate gel; A, alumina gel; s, the specific surface area as measured with argon; and v, total pore volume.

The sorptives were high-molecular-weight aliphatic polyelectrolytes (PE) containing various polar groups. These compounds are surfactants; their physico-chemical characteristics are summarized in Table 2.

**Table 2.** Composition of the functional groups and molecular mass of the polyelectrolytes

Polyelectrolyte	Functional groups, %	$M \times 10^{-5}$ , g/mol
PVA	OH (100)	0.22
PAA	COOH (100)	18.8
PAAM	CONH <sub>2</sub> (100)	5.0
PAA-1	CONH <sub>2</sub> (25-30), OC-NH-CO (13.3), COOH (50-60)	52.7
K-4	COOH, COONa, CONH <sub>2</sub>	2.4

Note: PVA, polyvinyl alcohol; PAA, polyacrylic acid; PAAM, polyacrilamide; PAA-1, a copolymer of the derivatives of acrylic acid; K-4, an incompletely hydrolyzed polyacrylonitrile; and M, molecular mass.

The adsorption of the PE from dilute aqueous solutions on the aluminosilicates was measured by viscosimetry as a function of the time and temperature over a concentration range from  $1 \times 10^{-5}$  to  $1 \times 10^{-1}$  wt %. The kinetics of the adsorption of the PE in 1% suspensions at  $\sim 20$  °C was studied by adding a weighted portion of an adsorbent to a polymer solution of desired composition. The suspension was stirred in a closed vessel with a mixer for 1 to 2 min and allowed to stand for 15, 30 or 60 and so min, after which it was separated on a centrifuge into liquid and solid part. The centrifugates were extracted and kept at 20 °C for 15 min, after which the concentration of the PE was measured.

The effect of temperature on the kinetics and equilibrium of adsorption were studied in a thermostat at 25, 50, and 90 °C for 15, 30, 60 and so min, and then centrifuged them. After kept in a thermostat at 20 °C for 30 min the physicochemical characteristics of the PE (viscosity, refractive index, etc) were measured. The adsorption was calculated by the formula

$$G \text{ (mg/g)} = (C_0 - C_t) V \times 10 / m \quad \text{and} \quad G_1 \text{ (mg/g)} = (C_0 - C_t) V \times 10 / (mS),$$

where G and G<sub>1</sub> are the adsorption values (mg/g), C<sub>0</sub> and C<sub>t</sub> are the initial and current concentrations of PE in solution at time t, g/100ml; m is the weight of the adsorption sample, g; and S is the specific surface area, m<sup>2</sup>/g.

## RESULTS AND DISCUSSION

An analysis of the results obtained shows that the adsorption of the PE by aluminosilicate occurs at different rates. For example for the adsorption PAAM, PAA-1, and k-4 at 20 °C on AS-2 and AS-3, the time of attainment of adsorption equilibrium was ~10 h; the analogous value for AS-1 was found to vary from ~70 to 80 h. By contrast, the kinetics of adsorption of PAA on the A, AS-2, and AS-3 with positive overall charge of the surface exhibited the shortest time of attainment of adsorption equilibrium (10-12 h) and the highest adsorption values. The adsorption of PAA on adsorbent S and AS-1 was first negative (for 2 h for S and 50 h for AS-1), where upon it positive.

These phenomena are controlled by mechanism of the interaction of PAA with the surface of adsorbents. PAA, a weak acid (pK 4.8), exist under our experimental conditions in two forms: as an anion and a natural molecule. Positively charged surfaces adsorb the anionic form of PAA due to the action of electrostatic forces and, in part, ion-dipole interactions of positively charged sites with nondissociated polymer molecules. At the same time, the adsorption of PAA anions on the negatively charged area of surface is negative. In experiments we observe a superposition of these processes.

The observation that negative PAA adsorption, which occurs at the beginning of the process, gives way to positive adsorption can be interpreted in a different manner. According (17-21), the negative adsorption of polymers on hydrophilic adsorbents is normally due to the adsorption water (solvent), which competes with nondissociated PAA molecules. At the same time, water adsorption causes no change in the sign of the surface charge. This signifies that the positive adsorption of PAA cannot neutralize the surface. The time it takes for the surface charge to change sign from negative to positive suggests that the reaction is an activated process.

The adsorption rate was found to increase with the temperature; for example, the time taken for the system to attain the state of equilibrium at 90 °C varied from 2 to 4 h. The apparent rate of physical adsorption decreases with temperature due to an increase in the desorption rate (Timofeev, 1962). When the adsorption rate increases with the temperature, one can conclude that the PE forms stronger bonds with the surface, with the different states of adsorption being separated by barriers.

To calculate the thermodynamic parameters of adsorption of the PE on gel with different ratios of the positive and negative surface charges, we plotted adsorption isotherms for temperatures 25, 50, and 90 °C. All the isotherms were closely described by the Langmuir equation. The parameters of this equation and layer thickness were estimated.

For all the systems under study, the heat of adsorption is negative; i.e., the process is endothermic. This conclusion is supported by the fact that, in all cases, the

adsorption value increased with the temperature. Negative heats of adsorption were obtained for other (mostly unionized) polymer, which can be explained by the influence of the entropy factor.

For all systems studied, the absolute values of the heats of adsorption decreased with the coverage of the surface with polymer molecules. There are two characteristic regions of coverages that substantially differ in the value of  $|\Delta H|$ : at small coverage (below 10%), the heat of adsorption varies from 10 to 40 kcal/mol, whereas, at higher coverage, it varies from 10 to 1 kcal/mol.

At all coverages, the adsorption value for gel with positive surface charge is higher than that for gel with negative surface charge. For example, for the positively charged gel (AS-2, AS-3, and A), the heat of adsorption at small coverages varies from 20 to 40 kcal/mol, decreasing to 3-4 kcal/mol at high coverages. For the negatively charged gels, the heat of adsorption is below 20 kcal/mol in the entire range of coverages.

Thus, the character of the adsorbent surface plays an extremely important role in adsorption of organic macromolecules and in the formation of organic films at the surface of aluminosilicates. Estimating of the all experimental results it is possible to propose that the modified by adsorption soil aluminosilicates surface has clusters structure.

## REFERENCES

1. Gorbunov, N.I., and Orlov, D.S. The nature of bonds between organic substances and soil mineral // *Pochvovedenie*. 1977. N 7. pp. 117-128.
2. Greenland D. Interactions between clays and organic compounds in soil // *Soil and Fertilizers*. 1965. V. 28. N 5-6. P. 521-532.
3. Greenland D. Interaction between humic acids and fulvic acids by clays. *Soil Science*, 1971. V. 111, No. 1., P. 34-41.
4. Malinovskii, T.Yu., Shein E.V., and Stepanov, A.A. Liophobic-liophilic properties of organic matter and soil structure // *Pochvovedenie*. 1993. N 6. pp. 122-126.
5. Orlov, D.S. *Khimiya pochv (Soil Chemistry)*. M.: Moscow Gos. Univ. 1995.
6. Theng, B.R.G. *Formation and properties of Clay-Polymer complexes*. Amsterdam: Elsevier. 1979.
7. Timofeev D.P. *Kinetika adsorbtsii (Adsorption Kinetics)*. M.: Akad. Nauk SSSR. 1962.

## CHEMICAL DEGRADATION OF MUCKS - EFFECT OF pH ON DISSOLVED ORGANIC MATTER RELEASE

*Matyka-Sarzyńska D., Sokołowska Z.*

### INTRODUCTION

In nature some of organic matter substances (humus) are sorbed by soil solid particles and some are transported through unsaturated zone into the saturated zone, where they can remain dissolved in, and move with the groundwater. So, DOM is an important component of not only soil but also aquatic environments. The nature and the amount of DOM in soil solution can influence the quality of groundwater and surface waters. Furthermore, DOM is involved in a number of biogeochemical processes, including pH buffering, nutrient cycling, ionic balance, mineral weathering, metal leaching, pollutant toxicity, mobility and bioavailability (Kononowa M.M., 1966; Schnitzer M. and Khan S. U., 1978; Sposito G., 1989; Wershaw R., 1994)

Peatlands are large sources of dissolved organic matter. In Poland most of the peatlands have been drained and subjected to agricultural use. While water conditions change soil mass loses its sorption abilities and gains more hydrophobic character. The mechanism of the above changes is called secondary transformation. As the consequence of the secondary transformation, soil degradation and lost of fertility occurs. One of important factor of these phenomena can be release of organic matter.

The availability of organic matter and its mobility in the soil is a consequence of many factors, including properties of the soil, as well as changes in climate, especially temperature and rainfall patterns. Chemical composition of aqueous phase, and particularly the pH, are very important for both adsorption of organic matter on soil particles and its release into soil solution (McDowell W.H. and Wood T., 1984).

The present study was carried out to look for effects of the degree of the secondary transformation on the DOM release at various pH's in peat-moorsh soils.

### MATERIALS AND METHODS

Fourteen samples of upper layers of weakly moorshed MtI, medium moorshed MtII and strongly moorshed MtIII peats were studied (Okruszko H., 1976). The degree of transformation of the peat was characterized by the value of water holding capacity index  $W_1$ . This index, being the ratio of the moisture of the sample predried at 105°C, rewetted by one week and centrifuged at 1000 g to that

of the fresh sample, segregated all the samples into four classes of secondary transformation state. The first class of  $W_1$  value ranging from 0,36 to 0,45 comprises moorsh formations of initial state of secondary transformations, the fifth class of  $W_1 > 0,90$  holds for totally degraded moorshes (Gawlik J., 1992; Gawlik J. and Harkot W. 2000).

Homoionic hydrogen forms of fresh moorsh materials containing exactly 0,4 g of dry organic matter were treated by NaOH solutions at pH = 5, 6, 7, and 8 at 1:100 w/w solid to liquid ratio. Concentrations of the DOM in the extracts (0.45  $\mu\text{m}$  filtrates) were determined spectrophotometrically at 470 nm using Jasco V-500 apparatus (MacCarthy P. and Rice J.A., 1985). A calibration curve was based on sodium humate solutions (Aldrich H1, 675-2).

## RESULTS AND DISCUSSION

The amounts of DOM which was released in the process of alkalization are shown in Figure 1.

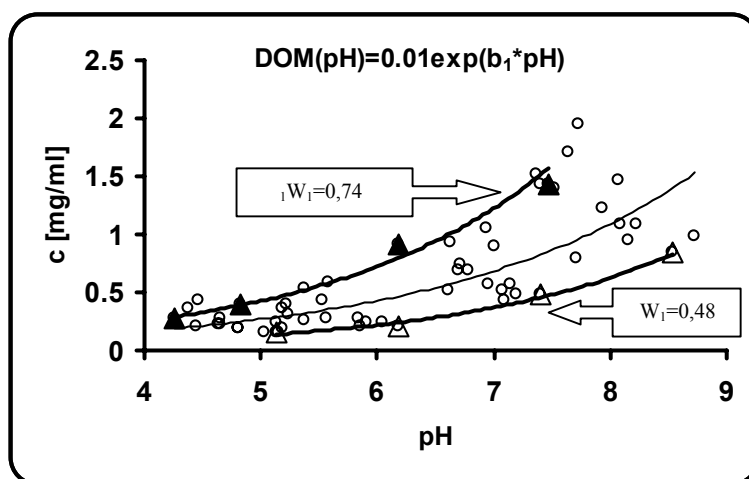


**Fig. 1.** Concentration of organic matter released at various pH's.

The dissolution of soil organic matter was significantly affected by pH. At low, initial pH values, the dissolved organic matter concentration was small. Changes in pH affect the electrostatic charge that induces repulsion-attraction of negatively charged surfaces of humic acids to other soil components. Generally the increase in pH resulted in the increase in dissolution of organic due to negative charge increase

of organic particles and their electrostatic repulsion from solid phase to the solution.

The concentration of the DOM increased exponentially with the pH of the extraction. An equation  $DOM(pH)=0,01\exp(b_1*pH)$  provided high correlation between the experimental data ( $R^2>0.94$  in most cases). The highest concentration of released OM was obtained for the strongly secondary transformed sample ( $W_1=0,74$ ). The opposite result was obtained for the weakly secondary transformed sample ( $W_1=0,48$ ).

## CONCLUSION

The  $b_1$  index could be satisfactorily used to quantify the DOM release process in relation to the increase in soil pH. The release of the DOM depended on the degree of the secondary transformation of the studied peat-moorsh soils.

## REFERENCES

1. Gawlik J.: Water holding capacity of peat formations as an index of the state of their secondary transformation, *Polish J. of Soil Sci.*, 2, 121-126, 1992.
2. Gawlik J., Harkot W.: Influence of the kind of moorsh and the state of its transformation on germination and growth of *Lolium perenne* in the pot plant experiment during spring-summer cycle, *Acta Agrophysica*, 26, 25-40, 2000.
3. Kononowa M.M.: *Soil organic matter*, Pergamon, Elmsford, N.Y., 1966
4. McDowell W.H., Wood T.: Podzolization: soil processes control dissolved organic carbon concentrations in stream water, *Soil Sci.*, 137, 23-32, 1984.
5. MacCarthy P., Rice J.A.: Spectroscopic methods for determining functionality in humic substances. In G.R. Aiken et al. (ed.) *Humic substances in soil, sediment and water*. John Wiley and Sons, New York. 1985.
6. Okruszko H.: The principles of identifications and division of hydrogenic soils for amelioration purposes (in Polish), *Bibl. Wiad. IMUZ*, 52, 7-54, 1976.
7. Schnitzer M., Khan S. U., *Soil organic matter*, Elsevier. Sci. Pub.Comp., N.Y., 1978.
8. Sposito G.: *The Chemistry of Soils*, N.Y., Oxford, Oxford University Press, 1989.
9. Wershaw R.: Membrane – Micelle model for humus in soils and its relation to humification. U.S. Geological Survey Water Supply, 2410, 1994.

## VALIDATION OF TRANSFER FUNCTIONS FOR CD AND PB USING DATA FOR CONTAMINATED AND BACKGROUND SOILS IN KOLA PENINSULA

*Pampura T., Rutgers M., Lukina N., Nikonov V., Koptsik G.*

Transfer functions link reactive (total) metal content in soil with metal concentration (activity) in soil solution and the main soil characteristics as pH, soil organic matter and clay content (Groeneberg et al, 2003). Transfer functions allow estimating of metal concentration in soil solution if data for soil solid phase are available. However there are a number of methods to obtain soil solution and to determine so called reactive and total metal pools in soil. This creates big variability in existing TF. For example Dutch (Römken et al, 2002) and UK (Tipping et al., 2002) datasets are based on 0.43 HNO<sub>3</sub> extractions, whereas German datasets (Pampura et al, 2002, Liebe, 1999, DIN V 19735) are based on weaker 1M NH<sub>4</sub>NO<sub>3</sub> extraction for reactive metals. To approximate soil solution 0.002M CaCl<sub>2</sub> extraction, sampling with Rhizon samplers, and soil saturation extracts (BSE) were used in Dutch, UK, and German datasets correspondingly.

In this paper different methods for both soil solution and reactive metal extraction are compared. Validation of TF derived for German soils (Pampura et al., 2002) with the new field data for contaminated and background Russian Podzols (Kola Peninsula) is also presented. Partitioning of Cd and Pb in Podzols (O and B horizons) along pollution gradient created by Monchegorsk Cu - Ni smelter, Kola Peninsula, Russia was investigated. Although the main polluting metals in this area are Cu and Ni, contamination of soil with Cd and Pb also takes place.

**Solid phase of soil.** “Reactive” metals (Q) were extracted with 0.43M HNO<sub>3</sub> and 1M NH<sub>4</sub>NO<sub>3</sub> (DIN 19730), “pseudo total pool” was extracted with aqua regia (AR). Comparison of different extraction methods is presented at Fig. 1. Results demonstrated that for both Cd and Pb NH<sub>4</sub>NO<sub>3</sub> extraction is much weaker than HNO<sub>3</sub> extraction. For Pb the difference is much more pronounced than for Cd. Probably 1M NH<sub>4</sub>NO<sub>3</sub> extracts mainly exchangeable weakly bound cations, whereas nitric acid destroys also strong complexes with OM and is able to release metals occluded in Fe-(hydro)oxides. Table 1 demonstrates the range of reactive metal fraction with respect to “pseudo total” along pollution gradient (200 km). Figures for background soil are shown in brackets. Fraction of “reactive pool” significantly decreased with increasing depth and decreasing level of contamination, fraction of NH<sub>4</sub>NO<sub>3</sub> -extractable metal seems more sensitive to contamination in comparison with that of HNO<sub>3</sub>. For O horizon metal content in

HNO<sub>3</sub> –extractable form is very close to “pseudo total” one, especially in contaminated soils.

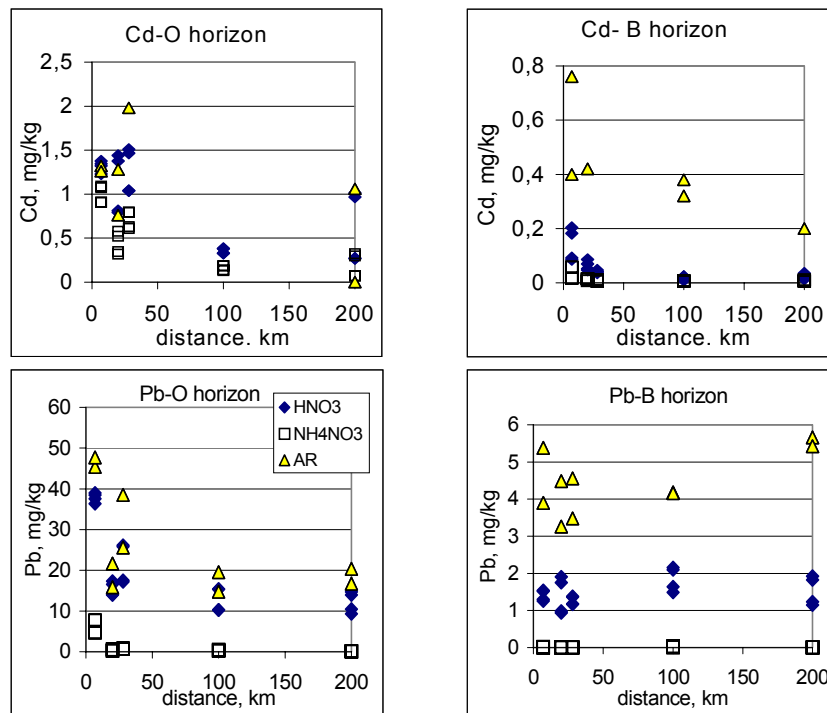


**Fig.1** Relation between HNO<sub>3</sub>, NH<sub>4</sub>NO<sub>3</sub>, and Aqua Regia extractable pools of Pb and Cd.

**Table 1.** Portion of HNO<sub>3</sub> and NH<sub>4</sub>NO<sub>3</sub> extractable pool with respect to AR in highly contaminated (7 km of smelter) and background (100-200 km) soils.

Metal	Horizon	HNO <sub>3</sub> / AR (%)	NH <sub>4</sub> NO <sub>3</sub> /AR(%)
Pb	O	86-(56)	17-(0.4)
	B	39-(20)	0.5-(0.1)
Cd	O	104-(74)	82-(28)
	B	27-(2)	8-(1.7)
Cu	O	89-(29)	16-(0.9)
	B	64-(6)	2-(0.20)

**Soil Solution.** Soil solution was approximated by 0,002 M CaCl<sub>2</sub> extraction (CaCl<sub>2</sub>) (soil: solution ratio was 1:2 for B horizon and 1:4 for O horizon), and soil saturation extracts (BSE, at moisture content equal to 100% of water holding capacity). For organic horizon (O) soil solution approximated with CaCl<sub>2</sub> had lower pH and higher values of dissolved organic carbon DOC in contaminated soils, which resulted in higher Pb and Cd concentrations. For B horizon values of pH and Pb concentrations were similar for both methods, whereas DOC and Cd concentrations were higher in the case of CaCl<sub>2</sub> extraction.

Results demonstrated that terms “reactive pool” and “soil solution” are operationally defined and values of metal concentrations depend on extraction method used. It means that for “soil solution” concentration prediction metal concentration in test soil should be determined using the same type of extract as for TF database.

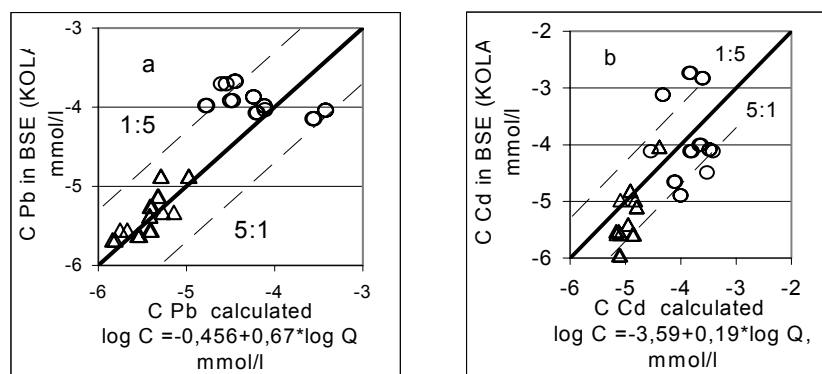


**Fig. 2.** Agreement between metal concentration measured in BSE (Kola field data) and those predicted with TF. TF based on field partitioning data for German soils, a – Pb, b- Cd (Pampura et al., 2002).

**Transfer functions validation.** Applicability of TF linking concentration in BSE and reactive metal pool in soil (extracted with 1M NH<sub>4</sub>NO<sub>3</sub>) was checked by comparison of Kola field data (metal concentration in BSE) with values predicted with TF (Fig. 2). Transfer functions are based on metal field partitioning data (German soils, Pampura et al., 2002). In this case the simplest form of TF function was used without considering any soil characteristics (Fig. 2). Lines designated as 1:5 correspond to the ratio 1:5 between observed and calculated values of metal concentrations in soil solution.

Results demonstrated that Pb and Cd concentration in Kola soil solutions were predicted with accuracy within one order of magnitude; however observed trends within horizons could be different from those predicted with TF. Concentration of Pb in BSE in O horizon was nearly constant for different levels of contamination perhaps because of strong buffering effect of soil organic layer.

**Acknowledgements** Our work was supported by INTAS project N 01- 2213 and NWO project N 047.014.002.

## REFERENCES.

1. Groeneberg, J. E, Römken, P., Tipping, E., Schütze, G, Throl, Ch., 2000. Transfer functions for Pb, Cd, Hg. Ad Hoc International Expert Group on Effect-based Critical Limits for Heavy Metals. Bratislava, Slovak Republic, 11-13<sup>th</sup> October 2000. Proceedings, p 142-145.
2. Pampura, T., de Vries, W., Schuetze, G. Transfer functions for the calculation of critical loads for lead and cadmium. Background Document for the Expert Meeting on Critical Limits for Heavy Metals and Methods for Their Application, Berlin, 2-4 December 2002, Umweltbundesamt, texte 47/03, Berlin Juli 2003, p 79-102.
3. Liebe, F., 1999 in : Schütze, G, Throl, Ch., 2000. Transfer functions for Pb, Cd, Hg. Ad Hoc International Expert Group on Effect-based Critical Limits for Heavy Metals. Bratislava, Slovak Republic, 11-13<sup>th</sup> October 2000. Proceedings, p 142-145.
4. Pampura, T., H.-D. Gregor, Hofmann, R., Pecher, W., Sauter, W., Schinz, V., Schleyer R., Utesch, E. Nagel, H.-D, Schütze, G. Nagel, H.-D, Schütze, Terytze, K. G. Groeneberg , J. E. Report Transfer Functions for cadmium and lead based on field and laboratory data. In: Zwischenbericht zum UBA F/E-Vorhaben FKZ 201 63 210, Gesellschaft für Oekosystemanalyse und Umweltdatenmanagement mbH (OEKO-DATA), Strausberg, November 2002, im Auftrag des Umweltbundesamtes, Berlin.
5. Römken, P.F.A.M., J. E. Groeneberg, J.Brill, and W. de Vries, 2002. Derivation of partition relationships to calculate Cd, Cu, Pb, Ni and Zn solubility and activity in soil solutions: an overview of experimental results. Alterra Green World Research, Report no. 305.
6. Tipping, E., J. Rieuwerts, G. Pan, M.R. Ashmore, S. Lofts, M.T.R. Hill, M. E. Farrago and I. Thornton. (2002) The solid solution partitioning of heavy metals (Cu, Zn, Cd, Pb) in upland soils of England and Wales. Environ.Pollut. 125, p.213-225.

## **EFFECTS OF THE FULVIC ACID ON THE BEHAVIOR OF Cu (II), Zn (II), Pb (II) AND Cd (II) IN THE SYSTEM SOLUTION – NATURAL ADSORBENTS.**

*Pinsky D.L., Zolotareva B.N.*

### **INTRODUCTION**

The condition and functions of heavy metals (HM) in soil are affected by the following major processes: interaction of HM with soil adsorbing complex (SAC), creation of difficultly soluble compounds of various composition and complexing with the solution components. Fulvic acids are known to be specific components of soil solutions actively interacting with HM. This study investigates the effects of fulvic acid both on the state of  $\text{Cu}^{2+}$ ,  $\text{Zn}^{2+}$ ,  $\text{Pb}^{2+}$  and  $\text{Cd}^{2+}$  in the solution and adsorption of cations by natural adsorbents with different physical-chemical characteristics, namely kaolin, bentonite, madder loam, loess-like loam and Chernozem.

### **MATERIALS AND METHOD**

The samples of humus horizon of leaching chernozem and were collected in the Voronezh region, the samples of madder loam were collected in the Tver' region, the samples of kaolin and bentonite were obtained at the Mineralogy Museum of the Russian Academy of Sciences (RAS). In the experiment, the adsorbents were used in their natural ion-form. The major physical and chemical characteristics of the employed adsorbents are listed in Table 1.

The fulvic acids (FA) were isolated from the water of Lake Velikoe in the Meschera lowland. The isolation, accumulation and purification of FA were carried out according to the methods described by Orlov (1995). The dry sample of HA has 1.36% of ash content and 12 m-eqv/g of acidic groups including 8.1 m-eqv/g of carboxylic groups. The constant of dissociation of the acidic groups amounted to 4.0. The weighted average of the FA molecular mass at pH 3,4,5, was 500, 1500, 2000 respectively.

The initial solutions were prepared from the exact weight of dry FA and  $\text{Cu}^{2+}$ ,  $\text{Zn}^{2+}$ ,  $\text{Pb}^{2+}$  and  $\text{Cd}^{2+}$  nitrates. The initial solutions served as a basis for a series of working solutions varying in HM and FA concentration, ranging from  $2 \cdot 10^{-5}$  to  $32 \cdot 10^{-5}$  mol/l at pH 3; from  $0.67 \cdot 10^{-5}$  to  $10.6 \cdot 10^{-5}$  mol/l at pH 4; and from  $0.5 \cdot 10^{-5}$  to  $8.0 \cdot 10^{-5}$  mol/l at pH 5. The ratio of solid faze:solution remained invariable 1:250 in all the experiments on adsorption. At the end of the one-hour shaking period, suspended matter were left intact for 24 hours in order to restore their balance and then filtered through a membrane filter. Equilibrium concentrations of Cu, Zn, Pb and Cd were measured using the atomic-absorption method; the FA concentra-

tion was measured using the Tjurina micro-method. The standard deviation (SD) for HM did not exceed 10% and SD for FA did not exceed 5%.

**Table 1.** Physical and chemical characteristics of adsorbents

Indexes	Subjects				
	Bentonite	Kaolin	Loess-like loam	Madder loam	Chernozom
S m <sup>2</sup> /g	400	22	60	39	58
pH (H <sub>2</sub> O)	8,2	6,2	7,9	6,3	6,8
SEC, m-equiv/100g	73	9	21	11	31
Ca+Mg, m-equiv/100g	43	3	14	6	26
C org., %	—	—	—	—	—
CO <sub>2</sub> carb., %	1,69	0,72	3,62	0,89	4,77
Type of mineral	2:1	1:1	2:1	2:1	—

## RESULTS AND DISCUSSION

The data obtained show that at pH 3, nearly 100% of Cd and Zn are present in the solution in the form of free cations. The concentration of metal-fulvic complexes (MeFA<sup>+</sup>) reaches 70% for Cd at pH 8 and 95% for Zn at pH 6.5. The sum of the concentrations of Cd<sup>2+</sup> and CdFA<sup>+</sup> remains constant throughout the entire series of the solutions employed in the experiment and stretches to 100%. These findings allow hypothesizing the possibility of sorption of Cd in the form of charged metal-fulvic complex. The concentration of Pb<sup>2+</sup> at pH 3 amounts to 70%, and concentration of Cu<sup>2+</sup> does not exceed 50%. The highest concentration of PbFA<sup>+</sup> reaching 100% is observed in solutions with pH ranging from 4.5 to 7. The highest concentration of CuFA<sup>+</sup> is observed in solutions with pH 5.5. The sum of the concentrations of Cu<sup>2+</sup> and CuFA<sup>+</sup> is about 70% at pH >6. At pH 8 the most Cu is associated with OH<sup>-</sup> and CO<sub>3</sub><sup>2-</sup>.

In sum, the investigated cations of HM interact differently with components of the employed solutions and fulvic acids. It has also been shown that HM cations assume different forms depending on the solution pH and therefore are subjects to various degrees of adsorption by adsorbents. During the interaction of adsorbents and HM solutions, partial acidification of equilibrium solutions occurs.

Two types of pH change regularly accompany the acidification process. The first type of pH change can be characterized as uneven, depending on the acidic-alkali buffering ability of the adsorbents. The second type of pH change is constant and connected with the transition of the protons from their bound, absorbed form into the solution during the process of HM adsorption.

The coefficients of the HM distribution in the investigated systems were assessed. Finally, a bivariate prediction model was constructed, with the amount of adsorbed cations as an independent variable and the amount of desorbed cations as a dependent variable. The regression relation was significant at  $p < 0.005$ . The following relationships were observed between the amount of desorbed cations and the amount of adsorbed cations at various pH levels:

Cu desorbed =  $6.51 + 0.539$  Cu adsorb.  $R=0.786$

Zn desorbed =  $10.51 + 0.538$  Zn adsorb.  $R=0.879$

Cd desorbed =  $10.31 + 0.541$  Cd adsorb.  $R=0.829$

Lead behaves differently, which can be explained by its more complex chemical properties in the investigated systems.

***Acknowledgment*** This research was supported by grants from the Russian Fund of Basic Research, to whom the authors would like to express their gratitude.

## OUTPUT FLUXES OF LEAD IN FOREST ECOSYSTEMS: SOME APPROACHES TO CALCULATING AND MAPPING

*Priputina I., Mikhailov A., Abramychev A.*

The input of heavy metals (HM) to terrestrial ecosystems is well known to be a large scale environmental problem. Aerial deposition because of industrial emissions is the dominant input of metals to forest ecosystems that can be resulted in increasing of HM concentrations in the soils as well as in plants and ground waters. Indications of adverse effects on biota dealt with high levels of metal accumulation in forest soils are found in many areas in Europe (Curlik et al., 2000). The methods of calculating of permissible levels of metal inputs to ecosystems have been continuously developed since the mid of the 1990's in the framework of UN/ECE Convention on Long-range Transboundary Air Pollution (De Vries, Bakker, 1998; UBA, 2003). Critical load approach is widely used under CLRTAP to be based on steady-state mass balance equation of HM in soil layer. If internal ecosystem fluxes of HM have been excluded from mass balance equation than critical load can be accounted as a sum of the harmless metal outputs from the ecosystem minus natural replenishment through weathering. The main outputs of HM in forest soils are metal leaching with percolation waters and metal removal because of growth biomass uptake (only wood biomass is considered). This paper describes some approaches to calculating and mapping critical loads of Pb in regional scale on the example of forest ecosystems located in the Centre of the European Russia.

**Leaching estimation.** In accordance with (De Vries et al., 2002), metal output flux from the soils with infiltration water regime can be calculated on the base of following equation:

$$M_{le} = 10 * Q_{le} * [M]_{ss} \quad (1)$$

where:  $M_{le}$  – metal leaching from considered soil layer (usually, mineral topsoil), [g/ha.yr];  $Q_{le}$  – flux of drainage water leaching from soil layer, [m/yr];  $[M]_{ss}$  – metal concentration in soil solution, [mg/m<sup>3</sup>]. The factor 10 is needed to convert the unit from mg/m<sup>2</sup>.yr to g/ha.yr.

**Metal concentration in soil solution** ( $[M]_{ss}$ ) which depends on main soil properties ( $pH$ ,  $h$  and  $clay$ ) and metal concentration in solid phase are accounted using special transfer functions (UBA, 2003). The results of calculating for the main soil types from the background sites in the central Russia are presented in Table 1.

**Table 1.** Data on Pb concentration in soil solutions of different soil types

Soil	Soil characteristics			Concentration of Pb	
	pH	humus, %	clay, %	in solid phase, mg/kg	in solution, mg/m3
<i>Podzols il-Fe</i>	4.15	1.7	2.5	11.5	11.6
<i>Podzoluvisols</i>	5.05	5.57	8.2	14	1.5
<i>Luvisols</i>	5.95	4.8	8.5	28.5	3.25
<i>Grayzems</i>	5.45	3.1	12.9	10	0.9
<i>Chernozems</i>	7.7	4.7	17.8	29	0.6
<i>Fluvisols</i>	7.6	4.1	19.8	30	0.8

Depending on data available, there are some methods to account the water percolation flux. So, **water balance** equation can be calculated using the data on precipitation, both soil and interception evaporation as well as plant transpiration. If these data are in deficiency, simplified method of calculating based on approximation of total evapotranspiration as a linear function of mean air temperature can be applied accordingly to (Michalzik et al., 2001):

$$Q_{le} = P - (1 + T/10^0) * 0.25 \quad (2)$$

where:  $P$  - precipitation, [m/yr];  $T$  - mean air temperature, [°C].

Both parameters are available through the regional or international climate database (for example, <http://www.iwmi.org>). Also, runoff data can be applied for this kind of calculating, especially for the areas with negative water balance when water leaching is during short period (mostly in the spring). Analysis of different calculations carried out using climate data (Medvedeva et al., 1983) have shown that if average data on precipitation and evapotranspiration have been used the value of water leaching equal to 190-200 mm/yr. On the other hand,  $Q_{le}$  accounted using Eq.2 are in two times higher (about 400 mm) that are too high since total runoff values for the same area had been estimated in 115-125 mm (Zaslavskaja et al., 1983). So, metal leaching in forest ecosystems for area under investigation have been estimated in average from 1.0 up to 10 mg/m<sup>2</sup>.yr and higher depending on soil parameters. The main uncertainties have water percolation data.

**Removal by wood biomass growth.** The following equation can be used to estimate metal outputs with biomass uptake:

$$M_{up} = f_{ru} * Y * M_{hpp} \quad (3)$$

where:  $f_{ru}$  – root uptake factor, to scale the net uptake in the root zone to the depth considered, [-];  $Y$  – annual biomass growth, [kg/ha.yr];  $M_{hpp}$  – metal content in the harvested parts (wood in the forest ecosystems), [mg/kg].

Regional data on ***Pb concentrations in wood biomass*** have been obtained on the base of special wood sampling in background area. As can see from Table 2, Pb concentrations in stem wood are lower for all tree types in comparison with the values obtained for branches and bark. The differences equal 4-6 times. As can be mentioned in (Remezov et al., 1959), concentrations of the element in different tree parts are maintained during all vegetation period if environmental conditions are not changed. So, the same data can be used for estimations of metal removing with biomass for trees of either age.

**Table 2.** Data on Pb accumulation in wood biomass of the main tree types in the central Russia (based on: Zolotareva et al., 1983; Pripulina et al., 2003)

<b>Tree Type</b>	<b>Compartments</b>	<b>Samples number</b>	<b>Pb, mg/kg</b>
<i>Spruce</i>	<i>stem</i>	16	0.51
	<i>branches</i>	14	3.00
	<i>bark</i>	6	2.00
<i>Pine</i>	<i>stem</i>	11	0.38
	<i>branches</i>	10	1.75
	<i>bark</i>	7	1.70
<i>Oak</i>	<i>stem</i>	10	0.43
	<i>branches</i>	10	2.70
	<i>bark</i>	4	5.00
<i>Birch</i>	<i>stem</i>	10	0.68
	<i>branches</i>	15	2.54
	<i>bark</i>	10	1.45

As known, there are differences in the ***rates of annual biomass growth*** for the trees of different ages (as well as tree compartments) that can be taken into consideration in regional estimations (Fig.1). The results of wood productivity simulations (based on EFIMOD) show that average rates of annual biomass growth at age of 50-80(100) years are higher in 1.5-2 times in comparison with average data calculated for 10-100(150) years period. Taking into account the differences of Pb concentrations in the wood of stem/branches the fluxes of metal removal with biomass uptake have been calculated for pure stands of the main tree types: Spruce, Pine, Oak, Birch (Tab.3).

Data presented in this paper had been used for preliminary calculating and mapping of critical loads of Pb for forest ecosystems in the basin of the Upper Oka.

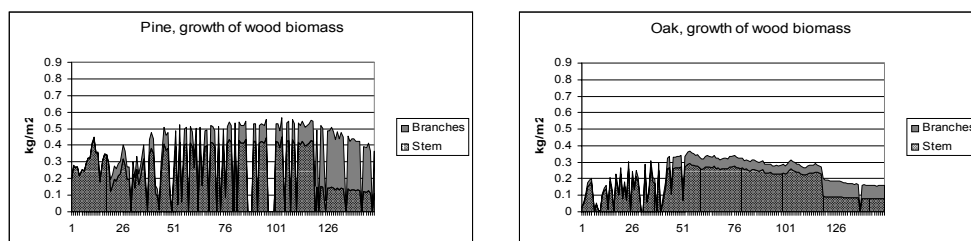


*Fig. 1. Data of simulating of wood biomass growth in the pure stands*

**Table 3.** Data on Pb removal with wood biomass uptake

<u>Type</u>	Period, yrs	Pb removal, kg/m <sup>2</sup>		
		Stem	Branches	Sum
<i>Spruce</i>	10-160	0.12	0.31	0.43
	<b>50-100</b>	<b>0.26</b>	<b>0.31</b>	<b>0.57</b>
<i>Pine</i>	10-160	0.08	0.16	0.24
	<b>50-100</b>	<b>0.15</b>	<b>0.16</b>	<b>0.31</b>
<i>Oak</i>	10-150	0.10	0.15	0.25
	<b>50-100</b>	<b>0.11</b>	<b>0.16</b>	<b>0.28</b>
<i>Birch</i>	10-90	0.23	0.06	0.29
	<b>50-100</b>	<b>0.24</b>	<b>0.07</b>	<b>0.31</b>

**REFERENCES:**

1. Curlik, J. (Ed.) (2000) AD HOC International expert group on effects-based critical limits for heavy metals. Proceedings of work-shop in Bratislava, 11-13 Oct. 2000.
2. De Vries, W., D.J.Bakker (1998) Manual for calculating critical loads of heavy metals for terrestrial ecosystems. Guidelines for critical limits, calculation methods and input data. Wageningen, the Netherlands, DLO Winand Staring Centre, Report 166. 144 P.
3. Medvedeva, I.F., S.Bykhovets, E.Nesmelova, N.Fadeev (1983) Climatic characteristics of the Prioksko-Terrasny biosphere reserve // Ecological monitoring of Prioksko-Terrasny biosphere reserve. Pushchino. ONTI. 224 p.(in Russian)
4. Michalzik, B., K.Kalbitz, J.H.Park (2001) Fluxes and concentrations of dissolved organic C and N – a synthesis for temperate forests. Biogeochemistry 52: 173-205.
5. UBA (2003) Proceedings Expert Meeting on Critical Limits for Heavy Metals and Methods for their Application. Berlin, 2-4 December 2002.
6. Zaslavskaya, M.B., V.Sorokovikov, S.Shashkov (1983) Formation of the water and chemical runoff in the basin of the Upper Oka // Regional ecological monitoring. Moscow. Nauka. P.130-145. (in Russian)

## DEVICE FOR EVALUATION OF THE RAPE PODS CRACKING SUSCEPTIBILITY

*Rudko T., Piekarz J., Lamorski K.*

Both wild and cultivated plants are characterized by natural tendency to preserve the species, to maintain old and expand to new areas. Therefore, ripe fruits (e.g. siliques or pods) tend to crack and shatter (sow) seeds. Among the cultivated plants, this phenomenon is specially observed and industrially important in case of rape because it is the reason of losses of seed yield, ranging from 3 to 20%.

Cracking susceptibility of rape has been evaluated with the use of various methods. This phenomenon has been characterized on the base of the number of seeds shattered on the soil surface, by the number of cracked pods or by the number of seeds shattered into containers, placed between the rows of plants [1,4]. Another method incorporated counting the plants that grew up from shattered seeds or the number of cracked pods after provocative keeping the plants in the field after reaching the full ripeness [2]. A different group has been created by direct methods, which were originally based on determination of the force, causing the cracking of pods. These include the simplest evaluation, consisting in squeezing the pod in hand [10] or applying a constant force for the plants fastened in a special threshing device [1]. The mechanism of pods cracking has been explained through the analysis of morphological and mechanical structure of pods susceptible and unsusceptible to cracking. The intensity of internal stresses in the pod depends on its anatomical structure. Irregular lignification and various depths of cell walls of internal parenchyma cause irregular drying of cells during ripening. The result of this is the differences in tension, causing the cracking of pods. To investigate the microstructure of pods for determination of causes of cracking, the mercury porosimetry has been applied. The basic research work has been done with the use of the testing machine, which was applied to disrupt the joints of pod's valves at dissepiment. The force causing the cracking has been determined by bending the whole pod [3]. The valve of the pod, stuck to the basis, was ripped off [5]. The strength parameters can be described in detail when using a method consisting in torsion of the pod by a constant angle in a testing machine [6,9]. In the methods using the testing machine, the measurement is made difficult due to irregular shapes of pods, different lengths, sickle-shaped bending occurring at various frequencies and very low values of the force (about 1-2 N) causing the cracking of the pod. A method has been elaborated, using the bending test of the pod stalk and eliminating the above measuring difficulties and enabling to determine the value of the force, causing the cracking of a pod [7].

Basing on this simplified bending test, the apparatus has been constructed for evaluation of pod cracking susceptibility, presented here. The measuring procedure consists in pressing the pod (at a characteristic ring-shaped swelling of the stalk) at the measuring holder of the sensor of force. A person performing the measurement keeps the pod in hand in a precisely defined way. As a result of the force interaction, a cracking takes place of the valves with the linking septum. This way the cracking and opening of pods in natural (field) conditions is imitated. For registration of the bending course, determination of the force values and saving the results, a program has been elaborated. A portable instrument collaborates with commonly used PC computers. It weighs 1,2 kg and has dimensions of 20x20x7 cm. A series of measurements with the instrument has given the results comparable with the results obtained by other method (torsion of pods). The usefulness of the instrument has been stated, for simple and fast evaluation of rape pods cracking susceptibility in the conditions of an indifferently equipped laboratory.

#### REFERENCES

1. Jakubiec J., Grochowski L.: 1963, Polowa i laboratoryjna ocena odporności dwóch odmian rzepaku jarego na pęknięcie łuszczyń. Zesz. Nauk SGGW – Rolnictwo, 7, 49-65.
2. Josefsson E.: 1968, Investigations on shattering resistance of cruciferous oil crops. Zeitschrift für Pflanzenzucht 59/4, 384 - 395. Communic from Swedish Seed Association No.306.
3. Kadkol G. P., Mac Millan R. H., Burrow R. P., Halloran G. M.: 1984, Evaluation of brassica genotypes for resistance to shatter. I. Development of a laboratory test. EUPHYTIA. Netherlands J. of plant breeding. Vol 33: 63 - 73.
4. Loof B.: 1961, Platzfestigkeit als zuchtproblem bei oilpflanzen der familie Cruciferae. Zeitschrift für Pflanzen - zuchtung, 46, 405 - 416.
5. Morgan C.L., Bruce D.M., Child R., Ladbroke Z.L., Arthur A.E.: 1998, Genetic variation for pod shatter resistance among lines of oilseed rape developed from synthetic *B. Napus*. Field Crops Research 58, 153-165.
6. Reznicek R. 1973 Vysterovani Agrofizikalnych vlasnosti repky. Zem. Tech. 2, 87 - 92.
7. Rudko T.: 2000, Próba zastosowania testu zginania do oceny podatności łuszczyń rzepaku jarego na pęknięcie. Acta Agrophysica, 37, 193-198.
8. Rudko T., Sokołowska Z., Hajnos M.: 2003, Zastosowanie metody porozymetrii ręciovowej do badania mikrostruktury łuszczyń rzepaku. Konferencja Naukowa. Olsztyn. Właściwości geometryczne, mechaniczne i strukturalne surowców i produktów spożywczych. Referaty i doniesienia, 64.
9. Szot B., Tys J.: 1987, Metodyka badań mechanicznych właściwości łuszczyń i łodyg rzepaku. Zeszyty Problemowe Postępów Nauk Rolniczych. 321, 193-202.
10. Tomaszewska Z.: 1964, Badania morfologiczne i anatomiczne łuszczyń kilku odmian rzepaku i rzepiku ozimego oraz przyczyny i mechanizm ich pęknięcia. Hodowla Roślin, Aklimatyzacja i Nasiennictwo. tom 8, z. 2, 147 - 180.

## **SPECTROSCOPIC COMPARISON OF HUMIC ACID FRACTIONS ISOLATED FROM SOIL WITH DIFFERENT EXTRACTION TECHNIQUES.**

*Shirshova L.T., Ghabbour E.A., Davies G.*

### **INTRODUCTION**

Isolation of humic substances (HSs) from soil has been always a challenging task for researchers. The classical acid-alkali isolation procedure gives the maximal yield but alkaline extractants promote HSs alteration.<sup>1</sup> The sequential extraction procedure with cation exchange resins and aqueous alkaline solution yields near the same amount of HSs as classical procedure from different sources under much milder conditions.<sup>2</sup> However, the ash content of resin isolated HSs is rather high that obscures natural properties of these humic fractions.<sup>3</sup> In this study we report the results of spectroscopic investigation of humic acids (HAs) of low ash content isolated from soil using resin and alkali-extraction procedures.

### **MATERIALS AND METHODS**

HAs were obtained from a bog soil in New Hampshire (NH), USA with three protocols (Table 1). Protocol 1 included soil pre-treatments with 2:1 benzene:methanol and 0.1M HCl followed by conventional extraction with aqueous 0.1M NaOH.<sup>4</sup> Protocol 2 included exhausted extraction with Na<sup>+</sup>-saturated RSO<sub>3</sub>Na-resin followed by Na<sup>+</sup>-saturated RCOONa-resin in deionized water and extraction with aqueous 0.1M NaOH.<sup>2</sup> Protocol 3 included pre-washing with benzene:methanol followed by resin-alkali sequential extraction procedure applied in protocol 2. Humic acids were precipitated at pH 1-2, de-ashed using HCl/HF, and freeze-dried.<sup>4</sup>

The carbon, hydrogen and, nitrogen content of solid HA samples were measured by Oneida Research Services, INC. The ash contents were determined by combustion of 50.0 mg of HA samples in air at 850° C for 2 h. FTIR spectra were recorded on a Satellite FTIR Mattson spectrometer on pellets made from 1:200 mixture of HAs/KBr.<sup>5</sup> Absorbances in the ultra violet (UV) and visible ranges were measured with a Perkin Elmer Lambda 20 spectrophotometer on 0.05M NaHCO<sub>3</sub> solutions of HAs (from 200 to 12.5 mg/L). Fluorescence emission and synchronous spectra were measured with a Hitachi 850 fluorescence spectrometer on 0.05M NaHCO<sub>3</sub> solution of HAs (spectral absorbances of 0.3 at 337 nm) using recommendation.<sup>6</sup>

## RESULTS AND DISCUSSION

The highest HAs yields were obtained by extraction with 0.1M NaOH (Table 1) while solid HS fractions extracted from NH with RSO<sub>3</sub>Na (Protocols 2 and 3) were yellow and did not contain HA residues. Five HA fractions isolated with RCOONa resin (C2 and C3) and 0.1M NaOH (A1, A2 and A3) have low ash content and similar elemental composition (not shown).

**Table 1.** Steps of humic acids extraction procedures and some HAs characteristics.

<i>Protocol No</i>	<i>Soil pre-treatments</i>	<i>Extractant used</i>	<i>HAs fraction</i>	<i>Yield,<sup>a</sup> %</i>	<i>Ash<sup>b</sup> %</i>
1	Benz.:meth., 2:1; 0.1M HCl	0.1M NaOH,	A1	8.3	0.66
2	RSO <sub>3</sub> Na-H <sub>2</sub> O	RCOONa-H <sub>2</sub> O	C2	2.2	0.46
	RSO <sub>3</sub> Na-H <sub>2</sub> O; RCOONa-H <sub>2</sub> O	0.1M NaOH	A2	4.3	0.54
3	Benz.:meth, 2:1; RSO <sub>3</sub> Na-H <sub>2</sub> O	RCOONa-H <sub>2</sub> O	C3	2.7	0.22
	Benz.:meth., 2:1; RSO <sub>3</sub> Na-H <sub>2</sub> O; RCOONa-H <sub>2</sub> O	0.1M NaOH	A3	5.0	0.52

<sup>a,b</sup> All data were averaged from two/three replications, <sup>a</sup> on a dry source weight basis, <sup>b</sup> on a dry HAs weight.

Based on UV-visible characteristics (Table 2) resin-extracted HAs absorb more UV light compared to alkali-extracted HAs. The latter (except A3) absorb more strongly at  $\lambda = 665$  nm, and have lower values of A<sub>254</sub>/A<sub>436</sub> and E<sub>4</sub>/E<sub>6</sub> ratios, suggesting<sup>7</sup> a higher aromaticity and/or higher particle size of alkali-extracted material.

The fluorescence emission spectra (Figure 1) of all HA fractions are characterized by a broad band centered around 465 nm for resin extracted HAs and between 450 and 460 nm for alkali-extracted ones. Alkali-extracted HAs exhibit lower fluorescence intensities across the entire emission and synchronous spectra (not shown) in respect to resin-extracted HAs, suggesting<sup>6,7</sup> that alkali-extracted material contains higher amount of conjugated aromatic  $\pi$ -electron systems. The fact that benzene:methanol pre-washing of soil has no effect on fluorescence

behavior of sequentially extracted HA fractions (spectra C2 and C3, A2 and A3, Figure 1) indicates that the fluorescence observed is mainly associated with fluorescence structures incorporated to the humic materials.

**Table 2.** The specific spectral absorbances ( $A_{nm} / \text{DOC}, \text{dm}^3 \text{g}^{-1} \text{cm}^{-1}$ ), and ratios between spectral absorbances of HA fractions (Table 1).

HAs fraction	$A_{254}$	$A_{436}$	$A_{465}$	$A_{665}$	$A_{254}/A_{436}$	$E_4/E_6$
C2	16.75	2.80	2.08	0.27	5.99	7.72
A2	14.95	2.81	2.15	0.37	5.24	5.76
C3	18.95	3.25	2.41	0.32	5.83	7.65
A3	10.81	2.08	1.64	0.29	5.19	5.59
A1	14.53	2.67	2.13	0.38	5.45	5.58

Relative standard deviations associated with estimation of all spectral parameters were no more than 0.3%.

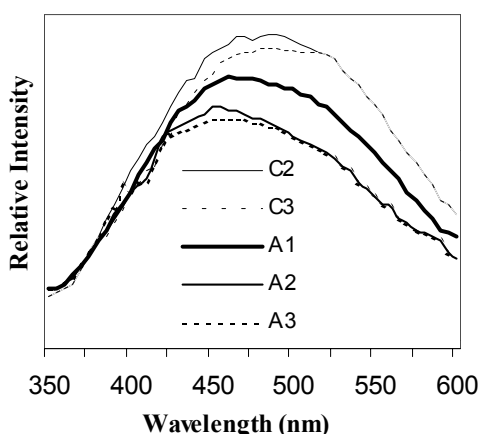


**Fig. 1.** Fluorescence emission spectra of HA fractions (Table 1) with excitation in 337 nm.

Some information concerning structural features of HAs was apparent from the FTIR difference spectra illustrated in Figure 2. Close inspection of occurrence and relative intensity of bands observed in the difference spectra recorded for resin and alkali-extracted HAs shows that alkali-extracted HAs contain more aliphatics (bands in 2927-2850, and 1470-1389  $\text{cm}^{-1}$  regions), polysaccharides (bands at 1088-1065  $\text{cm}^{-1}$ ), and aromatic C=C bonds (bands at 1514-1506  $\text{cm}^{-1}$ ) in respect to resin-extracted material that is relatively enriched in carboxylic and phenolic groups (bands in 2592, 1728-1657, 1435 and 1257  $\text{cm}^{-1}$  regions).<sup>5</sup>

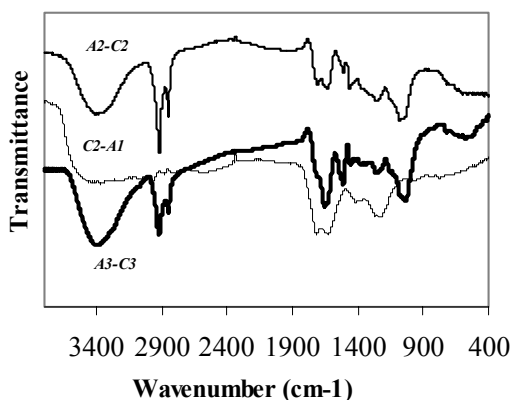


**Fig. 2.** FTIR difference spectra recorded for HA fractions (Tab.1).

We conclude that sequential resin-alkali extraction procedure provides some separation of humic acids in respect to their association with specific compounds (such as aliphatics, carbohydrates, lignin-derived structures), coextracted/incorporated mostly to alkali-isolated material. The photophysical parameters of alkali-extracted humic acids may differ significantly from those of resin-extracted sub-fraction. Therefore resin-alkali technique offer advantages over the classical acid-alkali isolation procedure in studying of humic acids.

This work was supported by USA Fulbright Foundation.

## REFERENCES

1. Hayes, M.H.B., Graham, C.L. 2000. In 'HumicSubstances: Versatile Components of Plants, Soil and Water' Royal Soc. of Chem., Cambridge, 91.
2. Shirshova, L.T.1991. *Finnish Humus News*, 3, 339.
3. Rosell, R.A., Sochtig, H., Salfeld, J., Flaig, W. 1981. *Agrochemica*, 25, 286.
4. Davies, G., Fataftah, A.K., Cherkassky, A., Ghabbour, E.A., Radwan, A., Jansen, S.A., Kolla, S., Paciolla, M.D., Sein, L.T., Buermann, W., Balasubramanian, M., Budnick, J., Xing, B.J. 1997. *Chem. Soc. Dalton*, 4047.
5. Bufo, S.A., Latrofa, A., Brunetti, G. 1994. In 'Humic Substances in the Global Environment and Implications on Human Health'. Elsevier, Amsterdam, 245.
6. Senesi, N., Miano, T.M., Provenzano, M.R., Brunetti, G. 1991. *Soil Sci.*, 152, 259.
7. Hayes, M.H.B., MacCarthy, P., Malcolm, R.L., Swift, R.S. 1989. 'Humic substances II - in search of structure'. Wiley, Chichester.

## MODERN MONITORING SYSTEMS FOR THE MEASUREMENT OF SOIL PHYSICAL PARAMETERS

*Skierucha W., Wilczek A., Walczak R. T.*

### INTRODUCTION

Selective measurements, without destructive interference to the measurement process and measured medium from unpredictable reasons are easy for interpretation but practically hard to accomplish. The unwanted sources of error when identified can be eliminated by application of a physically good model of the observed process or by empirical corrections based on reference measurements. A lot of measurement errors happen during the wire-transmission of an analog signal from the sensor equipped by an appropriate transducer, converting the usually non-electrical signal to its electrical representation, to the measuring unit. To avoid wire-transmission errors modern measurement systems combine the measuring unit with the sensor-transducer element in the form of a smart transducer or smart sensor. Smart sensors are equipped with unique identifiers and microcontrollers or digital signal processors capable to convert the measured signal to the digital form, performing individual calibrations and necessary corrections. Thus most of the data processing is completed at the sensor and the command and data communication with it usually performed in digital, preferably wireless way.

The development of mobile telephony enabled to finance the development of other fields in electronics, particularly new, low power consumption converters of non-electrical signals to electrical ones, efficient microcontrollers integrated with signal converters and the systems of wireless data communication on short and medium distances. Since the transducer market is very diverse, transducer manufacturers are seeking ways to build low-cost, networked smart transducers. Currently, it is too costly for transducer manufacturers to make unique smart transducers for each network on the market (Ethernet, CAN, Profibus, USB, proprietary and many others). Therefore a universally accepted transducer interface standard - IEEE P1451 is proposed to be developed to address these issues [1]. This standard is to make it easier for transducer manufacturers to develop smart devices and to interface those devices to networks, systems, and instruments by incorporating existing and emerging sensor and networking technologies. There are four working groups incorporated in IEEE 1451 [1] dealing with different aspect of the standard, one of which IEEE 1451.2 has a goal to make the sensor “plug and play” compatible independently of the network it is connected to [2]. The presented below application tries to implement some ideas of the IEEE 1451 standard for

connecting smart-transducers into a easily accessible network, with the special focus on the connection to the network in the wireless way.

## DESIGN OF THE WIRELESS COMMUNICATION SYSTEM

The application of wireless transmission in the license-free frequency bands for communication in short distances is very popular in environmental monitoring systems as well as in the control of industrial processes. Very attractive are frequency ranges 433 MHz and 868 MHz called ISM (Industrial, Scientific and Medical) frequency bands. There are many electronic devices available dedicated for ISM bands, particularly modern tranceivers integrating radio receivers and transmitters in the same integrated circuits [3,4]. The ready to apply radio modules are available for electronic engineers in the form of mounted and tested tiny electronic boards for the price of only about 10 Euro. The hardware and software of the radio communication systems should be designed with the following criteria in mind: (i) minimize the transmission errors, (ii) maximize the radio link range, (iii) minimize the current consumption (the systems are usually battery operated).

The presented prototype system allows to control the measurement process and transmission of the soil profile temperature. The software communication protocol as well as MASTER and SLAVE hardware devices carried out the point-to-point radio link. The communication protocol can be enhanced to point-multipoint connection for radio network system.

The functional diagram of the prototype communication system, serving as an implementation IEEE1451 standard NCAP – Network Capable Application Processor, is presented in Fig. 1.

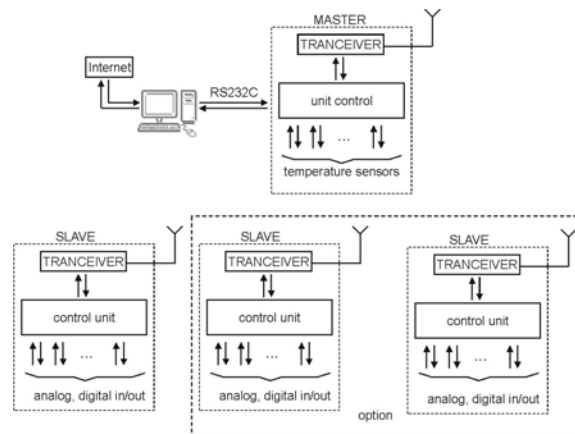


**Fig. 1.** Functional diagram of the prototype soil physical parameters monitoring system with the wireless communication link

The control of the measurement system is accomplished by application software running on a PC computer. There exists a possibility to connect PC computer to Internet and to move the priority control of the measurement process higher. The PC application software written in Borland C++ sends commands and receives data from a MASTER unit by serial asynchronous link and stores the measured data in the text file. MASTER and SLAVE units have embedded microcontrollers well equipped with analog and digital input/output functions including analog-to-digital and digital-to-analog converters.

The internal circuitry of MASTER and SLAVE units is the same, the differences are in the program inscribed in the microprocessor program memory of the units. The MASTER unit decodes the PC commands and controls the radio link with the SLAVE units and when the required data from the addressed SLAVE is received, the MASTER unit sends the data to PC.

## EXPERIMENTAL RESULTS

The presented system of wireless communication was tested by connecting seven temperature sensors to the SLAVE unit, one of which measured the ambient temperature, the others were placed in the soil at the depths: 5, 10, 15, 20, 30 and 40 cm below the ground level. The SLAVE unit was placed in metal enclosure, protecting the electronics from rain, in a field plot at the distance about 70 m from the building with the PC computer controlling the MASTER unit.

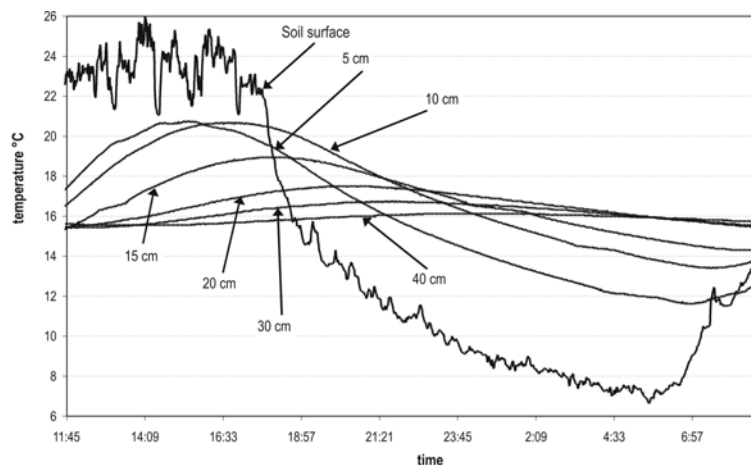


*Fig. 2. Example readout of temperature sensors located on different depths of soil profile*

The described setup worked several days measuring and transmitting the temperature data by the radio link. Totally there were 2772 radio connections with 97% performed in the first attempt. Only 3% connections were repeated; 11 1-time, 74 2-times and 1-time the attempt of radio connection had to be repeated 3 times to succeed. The readouts from the temperature sensors placed on various depths in the soil profile are presented in Fig. 2. As expected, the sensor that measured the ambient temperature had the shortest response time to the temperature change.

The deeper the sensor was located, the slowest reaction on temperature change was observed. Additionally, reaction of sensors to the temperature change were shifted in time because of limited speed of temperature change in soil profile [5].

## **SUMMARY**

The project of a modern monitoring system for the measurement of soil physical parameters is presented that is intended to be equipped with smart sensors and wireless communication in the ISM (Industrial, Scientific, Medical) frequency band 433 MHz. The system is designed on the base of advanced electronic circuits and its partial implementation in the form of two-point communication for the temperature measurement in a soil profile is presented. The study proves that the availability of advanced technology enables to enhance the existing measurement systems and sometimes only the sensors with functional and not expensive radio communication system for the remote control of measurement devices in the distance of several hundred meters. The developed hardware and software can be adapted to more complex monitoring systems working in compliance with IEEE 1451 standard and covering larger areas including air-borne or satellite remote sensing and serve as a source for ground reference measurements.

## **REFERENCES**

1. IEEE 1451 Web Site at <http://ieee1451.nist.gov>
2. IEEE Std. 1451.2-1997, "IEEE Standard for Smart Transducer Interface for Sensors and Actuators – Transducer to Microprocessor Communication Protocols and Transducer Electronic Data Sheet (TEDS) Formats", IEEE IMS, TC-9 Committee on Sensors Technology, IEEE, New York, N.Y., Sept.1998.
3. nRF401-Single Chip RF Transceiver 433MHz, Revision: 1.6, Nordic VLSI ASA, [www.nvlsi.no](http://www.nvlsi.no), February 2002.
4. CC1000 Single Chip Very Low Power RF Transceiver, Chipcon, PRELIMINARY Datasheet (rev. 2.1), 2002-04-19.
5. Walczak R.: Basic problems of mass and energy transfer in the soil-plant-atmosphere system. Zesz. Probl. Post. Nauk Roln., vol. 346, 12-22, 1987.

## ADSORPTION AND SURFACE AREA OF SOILS

*Sokolowska Z.*

Two factors, surface area and porosity are recognised to play complementary parts in adsorption phenomena for a vast range of solids. To understand the way, in which measurements of the adsorption of gases or vapours can be used to obtain information about surface area and porosity, it is necessary to deal briefly the concept of the adsorption isotherm.

### ADSORPTION OF GASES OR VAPOURS ON SOLIDS

The term *adsorption* appears to have been introduced by Kayser in 1881 to connote the condensation of gases on free surfaces, in contradistinction to gaseous *absorption* where the gas molecules penetrate into the mass of the absorbing solid. The term *sorption* proposed by McBain in 1909, embraces both types of phenomena, adsorption and absorption. When a solid is exposed in a closed space to a gas or vapour at some definite pressure, the solid begins to adsorb the gas or vapour. The amount of gas adsorbed can be then calculated from the fall in pressure (by application of the gas law if the volumes of vessel and of the solid are known), or it can be determined directly as the increase in weight of the solid. The adsorption is a consequence of the field force at the surface of the solid (*the adsorbent*), which attracts the molecules of the gas or vapour (*the adsorbate*). The forces of attraction emanating from a solid may be of two main kinds, physical and chemical, and they give rise to physical adsorption and chemisorption, respectively. The physical adsorption is also called as van der Waals adsorption. In the present paper we are concerned with physical adsorption.

### THE ADSORPTION ISOTHERM OF A GAS OR A VAPOUR

At the boundaries between solids and gases an accumulation of the particles occurs. The amount adsorbed per gram of a solid depends on the equilibrium pressure  $p$ , the temperature  $T$ , and also on the nature of the gas and the solid:  $N=f(p, T, \text{gas, solid})$ . This function at a constant  $T$  is called the *adsorption isotherm* if  $p$  increases, and *desorption isotherm* - if  $p$  decreases. For a given gas adsorbed on a given solid, maintained at a fixed temperature, this equation simplifies to:  $N=f(p)_{T, \text{gas, solid}}$ , and if the gas is below its critical temperature the alternative isotherm equation is:  $N=f(p/p_0)_{T, \text{gas, solid}}$ , where  $p_0$  is the saturated vapour pressure of the gas. The adsorption,  $N$ , may be measured in any suitable units i.e. grams or milligrams, moles or millimoles, and  $\text{cm}^3$  (N.T.P.).

The adsorption isotherm is the most popular expression of adsorption data. A complete adsorption isotherm covers the whole range of equilibrium pressures from very low pressures to the neighbourhood of the saturation pressure. Complete adsorption isotherms are common pointing by plotting along the abscissa the relative vapour pressure  $p/p_0$ . The isotherm naturally start at the origin of the coordinates and they end is at a nearly of the saturated vapour. No simple interpretation can be given to the main part of the curve. It is often supposed that at the higher relative pressures (at which adsorption hysteresis occurs) the adsorbed substance is capillary condensed, while at the lower  $p/p_0$  the surface of adsorbent is covered with a thin layer of gas molecules. The beginning part of the isotherm is used to obtain the surface area, and the end part to evaluate the pore structure in a solid body. The volume of liquid which is adsorbed at nearly saturated vapour by 1 gram of adsorbent is called the pore volume of the adsorbent.

#### ***Theory and equation of the adsorption isotherm***

In many instances an algebraic expression of the adsorption isotherm is more convenient than its graphic presentation. A few equations have been found to reproduce a large number of experimental isotherms.

The older one, commonly know as Freundlich isotherm:  $N = kp^{1/n}$ , where N is the amount of adsorbed of gas,  $p$  is the pressure,  $k$  and  $1/n$  are constants. Many gases and vapours have  $1/n$  values between 0,3 and 0,5.

The other equation is knows as Langmuir isotherm:  $N = (N_m kp)/(1 + kp)$ , where  $k$  is the constant. Langmuir regarded the surface of the solid as array of adsorption sites, each site being capable of adsorbing one molecule, and all sites were characterised by the same adsorption energy, and the attractive interactions between adsorbed molecules could be ignored. The Langmuir equation described localised monolayer adsorption on the homogeneous surface of adsorbent.

Brunauer, Emmett and Teller approach the problem of adsorption kinetically. In 1938, they explicitly extended the Langmuir evaporation-condensation mechanism to second and higher molecular layers. The state of affairs when equilibrium is reached at any given pressure may be represented formally as varying numbers of molecules being condensed on any one site. The BET model assumes that the surface is energetic uniform i.e. that all adsorption sites are exactly equivalent. The model neglects horizontal interactions between the molecules within the adsorption layer, and takes into account only the vertical interactions, and postulate that the heat of adsorption in the higher layers is equal to the latent heat of condensation. The BET equation described localised multilayer adsorption on the homogeneous surface of adsorbent:

$$N = \frac{N_m x C_{BET}}{(1-x)[1 + (C_{BET} - 1)x]}$$

where  $x = p/p_0$  relative pressure of water vapour,  $N$  amount of adsorbed water vapour, and  $C_{BET}$  constant.

The range of validity of BET equation does not always extend to relative pressure as high as 0.30 or 0.5. Many additional equations for the polymolecular adsorption isotherm have been published in the literature, for example the Dubinin-Radushkevich (DR), the Huttig, the Frenkel-Hasley-Hill (FHH) or the Aranovich equation

## SURFACE AREA

### *Kind of the surface area*

Solid phase of a soil is a mixture of different inorganic constituents as nonporous materials of different size and shape, porous materials with microcapillares or pores and phyllosilicates with the interlayer structure, as well as organic species, mainly organic matter.

Different kind of the surface area may be found in soils. The *geometric* surface area is calculated, knowing shapes and dimensions of representative soil particles. *The internal surface area* is the surface inter walls of the microcapillares (the term "internal surface" is usually restricted in its application to those cavities, which have an opening to exterior of the grains). *The external surface area* is defined as the sum of geometric and internal surface area. *The interlayer surface area* - the surface of interlayer walls of minerals type as montmorillonite. *The total surface area* is the sum of the external, internal and the surface area of organic matter.

The specific surface area of a soil sample is combined surface area of all the particles in the sample as determined by some experimental technique and expressed per unit mass of the sample. As its definition implies, term *specific surface area* is an operational concept.

The numerical value found for a given soil depends which experimental method has been used. There are two principal reasons for this very important characteristic. First, the properties of the solid surfaces in soil can often be altered during preparation of the sample for a surface measurement. Secondly, if a surface reaction is involved in the measurement of the specific surface area, the data obtained reflect only the characteristics of the surface functional groups that participate in the reaction, and provides only information about the solid surfaces that were reactive under the condition of the measurement.

### ***Methods of measure of surface area***

The principal physical methods for measuring specific surface areas of soils are electron microscopy and X-ray diffraction. The most of methods are based on measurement of adsorption of polar and nonpolar gases or vaporous. The adsorbable compounds used to determine specific surface area are chosen on the basis of their molecular properties. Nitrogen is commonly used as the adsorbate because it interacts weakly with a broad array of surface functional groups and therefore permits for the determination of exposed area of soil. The limitation on the use of this adsorbate is stereochemical. Relatively large radius of N<sub>2</sub> molecule prevents it from interacting with the surface functional groups occluded in very small void spaces. Polar adsorbates are water vapour, ethylene glycol or ethylene glycol monoethyl. Typical non polar adsorbates are nitrogen, argon, krypton.

Here we shall consider the application of physical adsorption of gases for the estimation of the specific surface area of soils. The starting point is the adsorption isotherm, and the problem reduces to determination of the specific surface area, or the *monolayer capacity*,  $N_m$ , of the adsorbent from the isotherm by mathematical analysis. The monolayer capacity is defined as the quantity of an adsorbate which can be accommodated in a completely filled, single layer of molecules on the solid surface. The surface area,  $S$ , is directly proportional to the  $N_m$ , and the relationship between these two quantities is given by the equation:  $S = N_m \times \omega$ , where  $\omega$  is the area occupied per molecule of the adsorbate in a completely filled monolayer. To find the value of  $N_m$  from an isotherm it is necessary to interpret the isotherm in a quantitative manner. A number of different theories have been proposed for the interpretation of adsorption data. The best known and probably the most frequently used theory, is that proposed by Brunauer, Emmett and Teller (BET). It leads to the equation called *the BET equation*, which has proved remarkably successful in the calculation of specific surface from the isotherms of the type II.

### ***Calculation the specific surface area from adsorption data***

Surface area of soils was evaluated from adsorption-desorption isotherms in the BET range of relative water vapour pressure, using the Brunauer-Emmett-Teller (BET) method. The first step in the application of this method is to obtain the monolayer capacity ( $N_m$ ) from the BET plot in the range of relative pressures  $0 < p/p_0 < 0,35$ :

$$\frac{x}{N(1-x)} = \frac{1}{C_{BET} N_m} + \frac{(C_{BET} - 1)}{C_{BET} N_m} x$$

where are  $x = p/p_0$  relative pressure of water vapour,  $N$  amount of adsorbed water vapour, and  $C_{BET}$  constant.

According to this, when  $x/N(1-x)$  is plotted against  $p/p_0$  a straight line should result with slope  $s=(C_{BET}-1)/N_m C_{BET}$  and intercept  $i = 1/ N_m C_{BET}$ . Solution of the two simultaneous equations gives  $N_m$  and  $C_{BET} - N_m=1/(s+i)$  and  $C_{BET}=(s/i)+1$ .

The second step is to calculate the surface area from the dependence:

$$S=N_m \times M^1 \times L \times \omega,$$

where  $L$  is the Avogadro number ( $6.02 \times 10^{23}$  molecules mole),  $M$  is the molecular weight of water (gram/mole) and  $\omega$  is the molecule cross-sectional area ( $10.8 \times 10^{-20}$  m<sup>2</sup> for water). If  $N_m$  is expressed in grams of adsorbate per gram of solid the surface area  $S$  (m<sup>2</sup>g<sup>-1</sup>) is estimated from the monolayer capacity as  $S=3612 \times N_m$ .

In order to use of any of these formulae, it is necessary to know the value of the molecule cross-sectional area,  $\omega$ . Emmett and Brunauer proposed that  $\omega$  be calculated from the density  $\rho$  of the adsorbate in the ordinary liquid or solid form. This leads to the formula:

$$\omega = f(M/\rho N)^{2/3} \times 10^{16}$$

Here  $M$  is the molecular weight of adsorbate,  $N$  is Avogadro's constant,  $f$  is a packing factor and  $\rho$  is the mass density of the bulk liquid. With the hexagonal close packing at the density of bulk liquid phase the value of  $f$  is 1.091 and if  $\rho$  is expressed in kilograms per cubic meter  $\omega$  is expressed in square nanometers. For nitrogen as adsorbate at -195° the value  $\omega=0.162$  nm<sup>2</sup> (16.2 Å<sup>2</sup>). The adsorption of water vapour is complicated in that it is highly specific and it appears that the application of the BET equation to water isotherms, in many cases, has no real validity. Early work indicated that the value of the molecule cross-sectional area is 10.6 Å<sup>2</sup> (0106 nm<sup>2</sup>). Harkins and Jura showed that it was 14.8 Å<sup>2</sup>.

## MEASUREMENT OF SURFACE AREA

According to Polish Standard PN-Z-19010-1 the surface area is estimated as described further. Before the adsorption measurement the soil samples are dried in a vacuum chamber with the concentrated sulphuric acid until the weight of samples reached constant values. The soil sample of the weight equal approximately to 3g is put into the glass vessel and placed over sulphuric acid solution. The sample is equilibrated with water vapour during two days. The amount of adsorbed water vapour is computed as the difference between the weight of the sample with water and the dry sample (dried in an oven at 105°C). The relative water pressures are obtained from the density of sulphuric acid solutions. Five levels of relative pressure are selected in range of 0.034 to 0.352. The adsorption measurements are replicated three times keeping the temperature constant, T=20°C ± 0.5. The specific surface area is calculated from adsorption data as described above.

## SURFACE AREA AND OTHER SOIL PROPERTIES

Surface area is highly sensitive indicator of various processes occurring in soils: organic matter accumulation, leaching and oxidation, soil acidification, alkalization, silica accumulation, wetting-drying cycles and many others. Surface area is well correlated with many soil properties, as this is shown in Table 1.

**Table 1.** Correlation coefficients of linear regression between the specific surface area, obtained from water vapour and nitrogen, and selected properties of mineral soils (482 soil samples)

	Fraction		OM	CEC	Exchangeable cations				
	<0.02	<0.002			H hydr.	Ca	Mg	K	Na
soils formed from loess									
S(N <sub>2</sub> )	0.419	<b>0.705</b>	<b>-0.550</b>	<b>0.589</b>	<b>-0.555</b>	<b>0.570</b>	<b>0.646</b>	-0.197	0.263
S(H <sub>2</sub> O)	<b>0.701</b>	<b>0.976</b>	0.395	<b>0.936</b>	-0.309	<b>0.906</b>	<b>0.920</b>	0.098	<b>0.738</b>
soils formed from clay									
S(N <sub>2</sub> )	<b>0.720</b>	<b>0.656</b>	<b>-0.503</b>	<b>0.542</b>	0.062	0.400	<b>0.641</b>	0.312	<b>0.553</b>
S(H <sub>2</sub> O)	<b>0.627</b>	<b>0.832</b>	-0.068	<b>0.579</b>	-0.178	0.357	<b>0.891</b>	<b>0.666</b>	0.480
soils formed from silt									
S(N <sub>2</sub> )	<b>0.547</b>	<b>0.679</b>	-0.251	0.067	0.268	0.007	<b>0.612</b>	0.030	-0.125
S(H <sub>2</sub> O)	<b>0.696</b>	<b>0.875</b>	<b>0.865</b>	<b>0.535</b>	0.084	0.478	<b>0.901</b>	0.303	0.270
soils formed from loam									
S(N <sub>2</sub> )	<b>0.805</b>	<b>0.792</b>	-0.332	<b>0.666</b>	-0.011	<b>0.606</b>	<b>0.712</b>	0.019	0.479
S(H <sub>2</sub> O)	<b>0.936</b>	<b>0.902</b>	0.018	<b>0.667</b>	0.203	<b>0.568</b>	<b>0.838</b>	0.171	<b>0.559</b>
soils formed from sand									
S(N <sub>2</sub> )	<b>0.561</b>	<b>0.641</b>	0.491	0.425	0.278	0.404	<b>0.521</b>	0.191	0.049
S(H <sub>2</sub> O)	<b>0.589</b>	<b>0.770</b>	<b>0.607</b>	<b>0.700</b>	0.358	<b>0.655</b>	<b>0.751</b>	0.252	0.146
brown soils formed from loam									
S(N <sub>2</sub> )	<b>0.732</b>	<b>0.677</b>	-0.422	0.430	<b>0.538</b>	<b>0.653</b>	0.153	0.464	<b>0.615</b>
S(H <sub>2</sub> O)	<b>0.937</b>	<b>0.824</b>	-0.168	<b>0.579</b>	<b>0.537</b>	<b>0.829</b>	0.357	<b>0.637</b>	<b>0.667</b>
podzolic soils formed from loam									
S(N <sub>2</sub> )	<b>0.827</b>	<b>0.872</b>	-0.255	<b>0.727</b>	-0.116	<b>0.687</b>	<b>0.790</b>	-0.216	<b>0.528</b>
S(H <sub>2</sub> O)	<b>0.931</b>	<b>0.954</b>	0.078	<b>0.624</b>	0.238	<b>0.548</b>	<b>0.902</b>	-0.048	<b>0.535</b>
black earth formed from loam									
S(N <sub>2</sub> )	<b>0.940</b>	<b>0.949</b>	<b>-0.530</b>	<b>0.826</b>	-0.147	<b>0.710</b>	<b>0.947</b>	0.319	0.395
S(H <sub>2</sub> O)	<b>0.943</b>	<b>0.973</b>	-0.399	<b>0.669</b>	0.088	0.491	<b>0.925</b>	0.388	0.267
brown soils formed from sand									
S(H <sub>2</sub> O)	<b>0.591</b>	<b>0.769</b>	<b>0.594</b>	0.461	0.160	0.452	<b>0.517</b>	0.163	0.151
podzolic soils formed from									
S(H <sub>2</sub> O)	<b>0.542</b>	<b>0.876</b>	<b>0.777</b>	<b>0.620</b>	<b>0.879</b>	0.398	<b>0.940</b>	0.263	-0.055

Fraction = particle fraction of defined size, OM = organic matter content, CEC = cation exchange capacity.

## POTENTIAL OF *AZOLLA CAROLINIANA* TO REMOVE PB AND CD FROM WASTEWATERS

*Stepniewska Z., Bennicelli R.P., Balakhnina T.I., Szajnocha K., Banach A., Wolińska A.*

### INTRODUCTION

Heavy metals are common in human activity and constitute a serious health risk because they easily accumulate in soils, water and organisms. Lead (Pb) and cadmium (Cd) are such metals. They are quite widespread (Evanko and Dzombak, 1997) and expose people to high toxicity. Cadmium has a mutagenic effect on live organisms (Watanabe and Endo, 1997). Also lead is a very dangerous metal, which easily accumulates in tissues, especially in bones and liver (Krieger, 1990).

One of the methods of lowering the content of heavy metals in the environment is to use plants to remove them from the substratum; this is called phytoremediation. There are many plants which can absorb extremely high amounts of heavy metals. They are called hyperaccumulators and they are exploited to clean up the environment (Evanko and Dzombak, 1997).

The aquatic fern *Azolla caroliniana* Willd. (*Azollaceae*) is a small plant, common in many parts of the world, especially in tropical environments (Watanabe et al., 1992). A specific feature of this fern is its symbiosis with the cyanobacterium *Anabaena azollae* Strasb. (*Nostocaceae*) which can bind atmospheric nitrogen. Due to this *Azolla* sp. is used as a green manure, especially in rice fields in Asia (Carrapiço, 2001). The fern has other applications (Bennicelli et al., 2004) and one of them is the bioaccumulation of heavy metals.

The aim of the present paper was to study the effect of Pb and Cd concentration in nutrient solution on biomass growth of *A. caroliniana* and the accumulation of these metals.

### METHODS

The fern was put into aquariums containing a 3 dm<sup>3</sup> liquid nutrient medium prepared according to International Rice Research Institute (IRRI) recommendation (Watanabe et al., 1992). The metals examined were introduced into each aquarium in their salt form (PbCl<sub>2</sub> and CdCl<sub>2</sub>·2½H<sub>2</sub>O) in 3 concentrations: 0.1, 0.5 and 1.0 mg dm<sup>-3</sup>. These did not contain nitrates so that the *A. caroliniana* could use the nitrogen provided by the *A. azollae*. In this way 9 treatments (3 per metal) were

obtained. A 10<sup>th</sup> aquarium was used as a control which contained only a nutrient medium. The initial *A. caroliniana* biomass was 20 g.

The experiment was carried out at photoperiod 18/6, air temperature 25°C and the air humidity about 70%. The *A. caroliniana* was cultured for 2 weeks with 6 control points during this period. The following observations were performed: temperature and humidity of air, the fern and concentration of Pb(II) and Cd(II) in the solution. At the end of the experiment, the biomass of *A. caroliniana* was collected, washed and weighed to determine its fresh mass. After that the dry mass of the plants was determined after drying at 80°C and used to determine the metals content in the biomass. These measurements after mineralizing by acid digestion (HNO<sub>3</sub>) in a microwave closed system were conducted by FAAS (flame atomic absorption spectrometry) method in liquid samples and ICP-AES (inductively coupled plasma atomic emission spectrometry) method.

## RESULTS

In the control treatment there occurred about a 4.5-fold increase of biomass up to 89.9 g during two weeks of experiment. In the remaining treatments the growth rate was lower; in the case of Pb, an addition 0.5 mg dm<sup>-3</sup> of lead ions caused the strongest inhibition *A. caroliniana* growth (36.8%). For the 0.1 and 1.0 mg dm<sup>-3</sup> Pb(II) treatments this inhibition amounted to 29.5 and 31.6%, respectively. The lowest dose of cadmium (0.1 mg dm<sup>-3</sup>) caused the smallest decrease in biomass equal to 23.6%. Higher Cd doses limited the increase of biomass by more than 40% (40.8% for 0.5 Cd(II) treatment and 46,5% for 1.0 mg dm<sup>-3</sup> Cd(II) treatment). This suggests that Cd is more toxic metal to *A. caroliniana* than lead in higher doses.

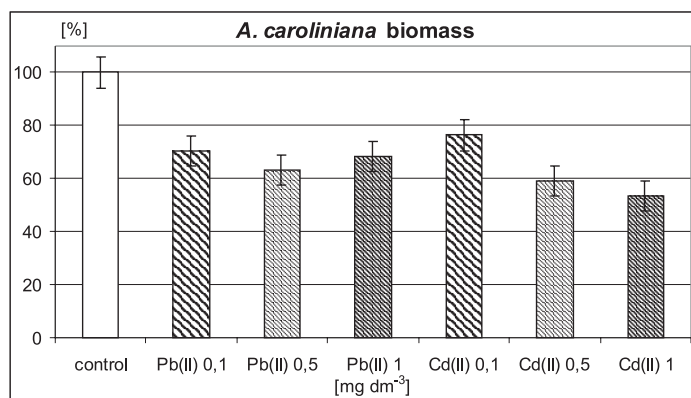


**Fig. 1.** The fresh biomass of *A. caroliniana* after 12 days of culturing compared to the control.

The decrease of Pb(II) and of Cd(II) in solution medium amounted to 90% and 22%. Respectively. In the *A. caroliniana* tissues content of tested metals were up to 416 mg Pb per kg d.w. and up to 259 mg Cd per kg d.w.

Changes in concentration of lead and cadmium ions in all the treatments are shown in Fig 2. Concentrations of Cd(II) in all the tested treatments underwent small changes during the experiment. Decrease of the metal concentration on the level of 10, 18 and 22% for 0.1, 0.5 and 1.0 mg Cd(II) dm<sup>-3</sup> treatments was found. Positive correlation between Pb(II) and Cd(II) concentration in water solution and biomass content was noted ( $R^2 = 0,999$  and  $R^2 = 0,992$  respectively).

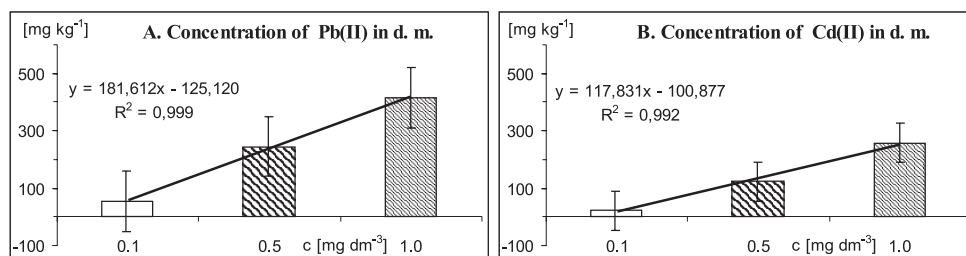


**Fig. 2.** Concentration of lead (A) and cadmium (B) in *A. caroliniana* biomass in all treatments.

The experiment performed shows that *A. caroliniana* is a good bioaccumulator of tested metals and can take up to 53-416 mg·kg<sup>-1</sup> d.m. of Pb and up to 23-259 mg·kg<sup>-1</sup> d.m. of Cd, depending to metal concentration in water solution during 12 days of growth and can be very effective in bioremediation as compared to other plants.

In many experiments conducted on live and dried plants at different pH values. *M. sativa* bound 7.1 mg Cd, 7.7 mg Cr(III), 43 mg Pb(II), 4.9 mg Zn(II) but no Cr(VI). The recovery of bound metals from biomass amounted to 90% for Pb, Zn, Cr and 70% for Cd (Gardea-Torresdey et al., 1996). Another hyperaccumulator, *T. caerulea*, bound 62800 mg Cd(II) in 1 kg of d.w. (Nedelkoska and Doran, 2000). However in the *H. lupulus* the leaves contained 72400 mg Pb(II) in 1 kg of biomass (Gardea-Torresdey et al., 2002). Willows accumulated 40-80% of Cd introduced into the soil (Klang-Westin and Perttunen, 2002). *Agrostemma githago* L. (*Caryophyllaceae*) roots contained 1800 mg Pb per kg and in *T. officinale* there was 15.4 mg Cd per kg (Pichtel et al., 2000). Of legumes, *P. vulgaris* had in its roots the largest amount of accumulated Pb equal 75 mg per g d.w. (Piechalak et al., 2002). The common aquatic plant *L. minor* can remove up to 90% of soluble Pb from water (Rahmani and Sternberg, 1999).

Sorption of lead ions by dried *Azolla filiculoides* L. depended on pH values. When it was higher (3.5 and 4.5) the sorption was the highest – 95%. At lower pH values (1.5) the accumulation decreased to 30%. This plant removed up to 93000 mg Pb per kg of d.w. (Sanyahumbi et al., 1998). However *Azolla pinnata* Brown takes up to 90% of Cd from medium (Gaur and Noraho, 1995). Experiments using *Azolla* sp. until now were performed mostly on dried plant which was packed into columns.

## REFERENCES

1. Bennicelli, R., Stępniewska, Z., Banach, M., Szajnocha, K., Ostrowski, J. (2004) The ability of *Azolla caroliniana* to remove heavy metals (Hg(II), Cr(III), Cr(VI)) from municipal waste water. *Chemosphere* 55 (1),141-146.
2. Carrapiço, F. (2001) The *Azolla-Anabaena*-Bacteria System as a Natural Micro-cosm. *Proceedings of SPIE* 4495, 261-265.
3. Evanko, C.R., Dzombak, D.A. (1997) Remediation of Metal-Contaminated Soils and Groundwater. *Technology Evaluation Report*, GWRTAC Series, TE-97-01.
4. Gardea-Torresdey, J.L., Gonzalez, J.H., Tiemann, K.J., Rodriguez, O. (1996) Biosorption of Cadmium, Chromium, Lead, and Zinc by Biomass of *Medicago Sativa* (Alfalfa). *Proceedings of the Eleventh Annual EPA Conf. on Hazardous Waste Research*, (HSRC/WERC Joint Conference on the Environment), Edited by L.R. Erickson, D.L. Tillison, S.C. Grant, and J.P. McDonald, Albuquerque, NM, pp. 11-20.
5. Gardea-Torresdey, J., Hejazi, M., Tiemann, K., Parsons, J.G., Duarte-Gardea, M., Henning, J. (2002) Use of hop (*Humulus lupulus*) agricultural by-products for the reduction of aqueous lead (II) environmental health hazards. *Journal Hazard Materials* 91 (1-3), 95-112.
6. Gaur, J.P., Noraho, N.(1995) Adsorption and uptake of cadmium by *Azolla pinnata*: kinetics of inhibition by cations. *Biomed Environ Sci* 8 (2), 149-57.
7. Gleba, D., Borisjuk, N.V., Borisjuk, L.G., Kneer, R., Poulev, A., Skarzhinskaya, M., Dushenkov, S., Logendra, S., Gleba, Y.Y., Raskin, I. (1999) Use of plant roots for phytoremediation and molecular farming. *Proc. Natl. Acad. Sci.* 96 (11), 5973-5977.
8. Klang-Westin, E., Pertub, K. (2002) Effects of nutrient supply and soil cadmium concentration on cadmium removal by willow. *Biomass and Bioenergy* 23 (6), 415-426.
9. Krieger, R.I. (1990) Toxicity and bio-availability studies of lead and other elements in the lower Coeur D'Alene River. Idaho Bureau of Land Management, *Technical Bulletin* 90-3.
10. Nedelkoska, T.V., Doran, P.M. (2000) Hyperaccumulation of cadmium by hairy roots of *Thlaspi caerulescens*. *Biotechnol Bioeng* 67 (5), 607-615.
11. Pichtel, J., Kuroiwa, K., Sawyerr, H.T. (2000) Distribution of Pb, Cd and Ba in soils and plants of two contaminated sites. *Environmental Pollution* 110 (1), 171-178.

12. Piechalak, A., Tomaszewska, B., Baralkiewicz, D., Malecka, A. (2002) Accumulation and detoxification of lead ions in legumes. *Phytochemistry* 60 (2), 153-162.
13. Rahmani G.N.H., Sternberg, S.P.K. (1999) Bio-removal of lead from water using *Lemna minor*. *Bioresource Technology* 70 (3), 225-230.
14. Sanyahumbi, D., Duncan, J.R., Zhao, M., van Hille, R. (1998) Removal of lead from solution by the non-viable biomass of the water fern *Azolla filiculoides*. *Biotechnology Letters* 20 (8), 745-747.
15. Watanabe, T., Endo, A. (1997) Cytogenetic effects of cadmium on unfertilized oocytes in short-term zinc deficiency in hamsters. *Mutation Research* 395, 113-118.
16. Watanabe, I., Roger, P.A., Ladha, J.K., Van Hove, C. (1992) Biofertilizer Germplasm Collections at IRRI. *IRRI*, 8.

## **SURFACE AREA OF PLANT ROOTS FROM WATER VAPOR AND NITROGEN ADSORPTION AS AFFECTED BY pH AND ALUMINUM**

*Szatanik- Kloc A.*

### **INTRODUCTION**

Surface area of plant root system is a key parameter for description of absorption of water and nutrients by plants (Nye 1973, Silberbrush and Barber 1983). Usually the surface area of plant root of a few square centimeters per gram, measured by immersion of the roots in water or in electrolyte solutions, is reported (Carley and Watson 1966, Ansari et al. 1995). In these methods a very thick layer of water (solution) adhered to the surface and shading real surface details is taken as a measure of the surface area. Certainly the finest roots do not contribute to this value and the external geometrical surface of root is measured. Very high root surface areas result from direct calculation of the geometric field of root + root hair (from length and diameter). In this way Dittmer estimated the surface area of one rye plant roots of 765 square meters (Vilee 1978). Close to the latter value, the specific surface area of roots can be estimated from water vapor adsorption isotherm. Low-temperature nitrogen adsorption, although widely used in surface area determination of great number of adsorbents has not yet been used for plant root material.

The purpose of the present studies was to compare surface areas of plant roots using both adsorbates and to estimate changes of these surface areas under low pH and aluminum stress of different concentrations. This is known that aluminum ions severely alter plant roots cell structures.

### **MATERIALS AND METHODS**

Tillering and shooting stage plant roots of two wheat (*Triticum L.*) varieties: acid resistant (*Inia 66/16*) and acid sensitive (*Henika*), and a very sensitive barley (*Ars*) were studied. The plants were grown in a nutrient solution prepared according to Marshner and Romheld (1983), at pH=7 with 16 h (23oC) / 8 h (18oC) day/night regime. After the plants reached the requested growth stage, the pH was adjusted to the value of 4.0 and aluminum chloride was added to reach an Al level of 20 mg dm<sup>3</sup> that induced a strong toxicity. After one week, all roots were harvested, rinsed 3 times in 0.01 mol dm<sup>-3</sup> HCl, 5 times in distilled water, air dried and collected for further analyses.

Water vapor adsorption isotherms were measured using a vacuum chamber method (Polish Standard PN-Z19010-1) at 298±0.1 K. (Jozefaciuk and Szatanik-

Kloc, 2001]. Nitrogen adsorption isotherms were measured instrumentally at liquid nitrogen temperature using Sorptomatic 1990 made by Fisons (Petersen et.al.1996).

The surface area of solids were calculated from adsorption data using the Brunauer-Emmet-Teller (BET) equation (Brunauer et al. 1938):

$$y/a = 1/(a_m C) + x(C-1)/(a_m C), \quad (1)$$

where  $y=x/(1-x)$ ,  $x=p/p_0$ ,  $p_0$  (Pa) is the saturated vapor pressure at the temperature of the measurements  $T(K)$ ,  $a_m(kg\ kg^{-1})$  is the statistical monolayer capacity,  $C=\exp(-(E_a-E_c)/RT)$  is the constant related to the adsorption energy,  $E_a(J\ mol^{-1})$ , and condensation energy of water,  $E_c(J\ mol^{-1})$  and  $R(J\ mol^{-1}\ K^{-1})$  is universal gas constant. Having calculated  $a_m$  values from the slope and the intercept of Eq (1), the surface area of the solid,  $S(m^2\ kg^{-1})$  can be calculated using:

$$S = N\omega a_m / M_r, \quad (2)$$

where  $N(mol^{-1})$  is the Avogadro number,  $M_r(kg)$  is molecular weight of the adsorbate and  $\omega (m^2)$  is the area occupied by a single adsorbate molecule, assumed to be  $1.08 \times 10^{-19} m^2$  for water and  $1.08 \times 10^{-19} m^2$  for nitrogen.

## RESULTS AND DISCUSSION

The surface areas of plant roots measured from water vapor adsorption were around 10 times higher than these derived from nitrogen adsorption that is presented in Table 1.

**Table 1.** Surface areas of the studied plant roots

Surface area	Shooting stage			Tillering stage		
	<i>Ars</i>	<i>Inia</i>	<i>Henika</i>	<i>Ars</i>	<i>Inia</i>	<i>Henika</i>
H <sub>2</sub> O (m <sup>2</sup> g <sup>-1</sup> )	147	164	156	150	172	164
N <sub>2</sub> (m <sup>2</sup> g <sup>-1</sup> )	27.4	22.25	35.33	29.1	24.92	24.03

Such large differences may arise from differences in water and nitrogen molecules polarities: water is adsorbed on polar surfaces while nitrogen on nonpolar ones. Possibly in the roots polar surfaces dominate. However, principles of physical adsorption state that surface areas (at least of flat homogeneous adsorbents should be similar. In this respect one should look for the reason of the differences mentioned either in complicated geometry of root surfaces or in their heterogeneous energetic character. Also, the nitrogen adsorption method requires prior evacuation and heating of the sample, which thins water films and brings the root tissues closer. The quasi-contact of the root material (e.g cell walls) can extend

over a significant portion of the surface that becomes inaccessible for nonpolar (nitrogen) molecules. If the root contains expansible or swelling material it can collapse on evacuation, giving the same effect. Also the molecular sieving effect is believed to differentiate the entrance of various size gas molecules into narrow spaces (Volzone *et al.*, 1999) leading to differences in surface areas measured with various size adsorbates. The kinetic effects may diminish the adsorption of nitrogen to a great extent when entrances to larger spaces are of nitrogen molecule dimensions. To easily pass such narrow entrance, the thermal energy of the molecule should be similar to the energy barrier of the adsorption field among the entrance walls. At liquid nitrogen temperature the thermal energy is low and therefore the adsorption equilibrium may not be reached within a standard time of the measurement. Many restrictions hold also for interpretation of surface area measured from water vapor adsorption, among which is different hydration of different surface cations, strong lateral interaction of polar water particles in adsorbed layer and/or dependence of water layer thickness at a point of the statistical monolayer coverage on surface charge density. Comprehensive discussions on nitrogen and water adsorption interpretation are presented by Gregg and Sing (1967).

An important observation is that both water and nitrogen root surface areas follow the same trends due to low pH and aluminum stress, suggesting that both methods detect similar root tissue damage after the stress that is shown in Fig. 1. showing relative changes in root surface areas. On the Y axis one can see the ratio of the surface area of the stressed roots to this of the control ones.

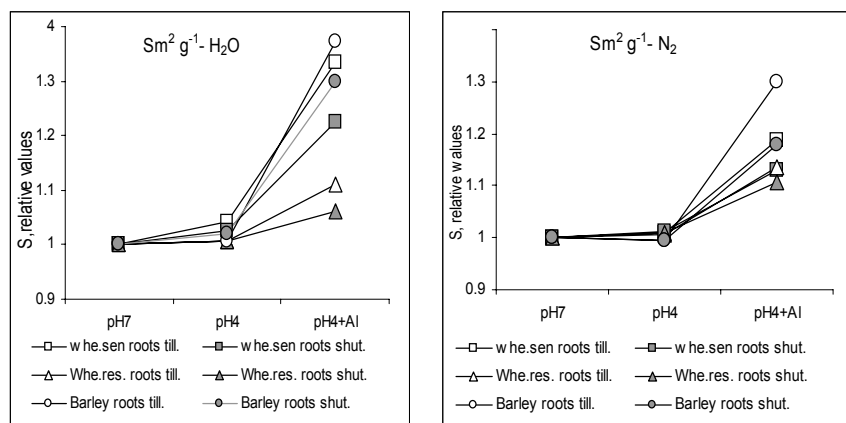


**Fig.1.** Relative values A- water vapor surface area, B-nitrogen surface area

This is worth noting that the lowering of the growing solution pH without Al addition causes insignificant changes in surface areas indicating that the root material survives low pH intact. The intensity of the changes in root surface areas is higher for the Al sensitive plants as this is the highest for barley and the lowest for Al-resistant wheat *Inia*. The younger, tillering stage plant roots were more susceptible for the Al stress, as their surface areas increased to a larger extent.

## REFERENCES

1. Ansari S A, Kumar P, Gupta B N 1995 Root surface area measurements based on adsorption and desorption of nitrite. *Plant Soil* 175, 133-137.
2. Brunauer S, Emmet P H, Teller E 1938 Adsorption of gases in multimolecular layers. *J. Am. Chem. Soc.* 60, 309-314.
3. Carley H E, Watson R D 1996 A new gravimetric method for estimating root-surface areas. *Soil Sci.* 102, 289-291.
4. Gregg S J, Sing K S W 1967 Adsorption, Surface Area and Porosity. Academic Press London and New York, 35-223.
5. Józefaciuk G., Szatanik-Kloc A. 2001: Aluminium-induced changes in the surface and micropore properties of wheat roots: a study using the water vapor adsorption-desorption technique. *Plant and Soil*, 233, (1), 95-108
6. María Luz Pérez-Rea, Fernando Rojas, Victor M. Castano. 2003. Nitrogen adsorption method for determining the mesopore slit-like size distribution of expansive soils, *Materials Research Innovations*, Vol. 7, 6.
7. Marschner H, Romheld V 1983 In vivo measurement of root-induced pH changes at the soil-root interface: effect of plant species and nitrogen source. *Z. Pflanzenphysiol.* 111, 249-254.
8. Nye P H 1973 The relation between the radius of a root and its nutrient-adsorbing power. *J. Exp. Bot.* 24, 783-786.
9. Petersen L.W., Moldrup P., Jacobsen O.H., Rolston D.E. 1996. Relation between specific surface area and soil physical and chemical properties. *Soil Sci.*, 161, s.9-21.
10. Siberbrush M, Barber S A 1983 Sensitivity of simulated phosphorus uptake to parameters used by a mechanistic-mathematical model. *Plant and Soil* 74, 93-100.
11. Stawinski J., Gliński J. Ostrowski J., Stępniewska Z., Sokołowska Z., Bowanko G., Józefaciuk G., Księżopolska A., Matyka-Sarzyńska D., 2000. Przestrzenna charakterystyka powierzchni właściwej gleb Polski. *Acta Agrophysica*, Monografia.
12. Szatanik-Kloc A., Józefaciuk G. 1997. Effect of pH and aluminum on surface properties of barley roots as determined from water vapor adsorption. *Acta Physiologiae Plantarum.* 19, 3, 327-332.
13. Vilee C A 1978 *Biology*. PWRIL Warsaw. p 228.
14. Volzone, C., Thompson, J.G., Melnitchenko, A., Ortiga, J. and Palethorpe, S.R. (1999) Selective gas adsorption by amorphous clay-mineral derivatives. *Clays and Clay Minerals*, 5, 647-657.

## SPATIAL DISTRIBUTION OF SELECTED SOIL PHYSICAL AND CHEMICAL PROPERTIES

*Usowicz B, Hajnos M., Sokółowska Z., Józefaciuk G.,  
Bowanko G., Kossowski J.*

Basic soil properties are documented on maps of different scales and degree of generalization, and in databanks. From these one can see different variability of soil properties on a given area. Despite the heterogeneity of soil on a field scale may be high, this is frequently neglected not only by farmers, but also by scientists. As a rule the soil in a single field is considered to be homogeneous so one-point measurements are used for determination of its properties and uniform agricultural practices are applied, as well. In general, least knowledge on soil spatial variability has been collected in respect of its mathematical-physical description, and in respect of its natural and anthropogenic components.

In this work spatial variability of selected soil physicochemical properties was studied on an area of a whole commune (Trzebieszów, Lublin voivodship) and on a single field. The statistic and geostatistic analysis including estimation of spatial distribution and estimation error of soil granulometric composition and pH are presented.

### MATERIALS AND METHODS

Trzebieszów commune is located on a flat landscape of denivelations rarely exceeding 10 m, with a few shallow valleys of flooding rivers. The lowland is mostly built from outwash material, with loose sands to low clayey sandy soils [4]. The mean annual temperature is 7,3 °C; the mean temperature of the warmest month (July) is 17,7 °C, and of the coldest one (January) is –3,5 °C. The annual rainfall is 537 mm, 64% of which comes during vegetation period (IV-IX).

The soils were sampled in summer from randomly located points (commune) and regular network points (field), that is shown in Fig. 1. Analysis of granulometric composition was performed using areometrical-sedimentation method and of the pH (H<sub>2</sub>O and KCl) potentiometrically.

Both for the commune and the field areas the basic statistical parameters were estimated: mean value, standard deviation, coefficient of variability (CV), skewness and kurtosis. Spatial characteristics of the studied soil features was performed using geostatistical methods. Exspermental semivariogram –  $\gamma(h)$  for the distance  $h$  was calculated from the equation [4, 5]:

$$\gamma(h) = \frac{1}{2N(h)} \sum_{i=1}^{N(h)} [z(x_i) - z(x_i + h)]^2$$

where:  $N(h)$  is number of pairs of points located at a distance  $h$ .

For each semivariogram three characteristic parameters were distinguished: nugget, sill and range. Known mathematical functions (exponential, spherical linear, etc.) were fitted to the experimentally derived semivariogram that was used further for spatial analysis and its visualization by space estimation of a given physical property applying standard kriging method [1, 2].

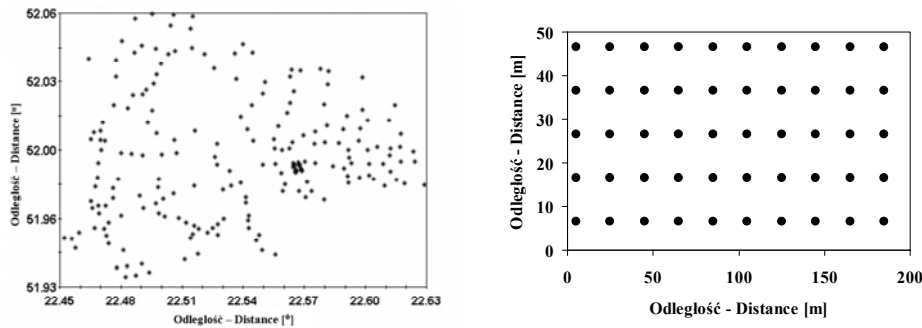


**Fig. 1.** Location of sampling points on the Trzebieszów commune area (left) and selected individual cultivated field (right).

## RESULTS AND DISCUSSION

The studied soils were rich in sand (60% in average), twice as less was silt fraction and six times less clay, that is shown in Table 1. These proportions were similar in both commune and field areas. Values of pH indicated high soil acidity, somewhat lower for the commune (4,7 in average) that for the field (4,2). Generally, the variations in the analyzed soil properties were high within both areas. The highest dispersion of the measured values was observed for sand fraction and the lowest for clay, and the highest differences between the commune and the field were noted for sand content. Dispersion in pH values was two times higher for the commune that for the field. The coefficient of variability for defined granulometric fractions content was the highest for clay (over 40%), and the lowest for sand (14-18%) that was in reverse order that the respective average values. The coefficient of pH variability was two times lower for the field that for the commune area. The statistical distributions of all but silt-in-commune granulometric fractions were asymmetric (slightly right-hand skewed) and values of kurtosis were close to

normal distribution (with the exception of clay fraction in commune scale). The distribution of pH values was also right-hand skewed and the kurtosis for commune was close to the normal. Field pH distribution was smoother than in commune.

**Table 1.** Statistical parameters for granulometric fraction content and pH in 0-10 cm soil layer within commune and field areas.

Parameter	Commune				Field			
	% of fractions, mm			pH	% of fractions, mm			pH
	1-0,1	0,1-0,02	<0,02	KCl	1-0,1	0,1-0,02	<0,02	KCl
Points nr	214	214	214	214	50	50	50	50
Mean	59,6	29,0	11,4	4,7	54,7	34,5	10,8	4,18
Std. Dev.	10,9	7,9	4,9	0,82	7,6	6,7	4,8	0,38
CV	18,1	27,4	42,8	17,7	13,8	19,5	44,4	9,0
Skewness	0,614	-0,53	0,564	0,972	0,005	0,273	1,377	1,688
Kurtosis	2,954	3,03	3,37	2,98	2,618	2,213	5,1	6,616

Spatial dependences of the studied soil properties in both areas were found. Higher semivariance values were noted for the commune than for the field (Fig. 2).

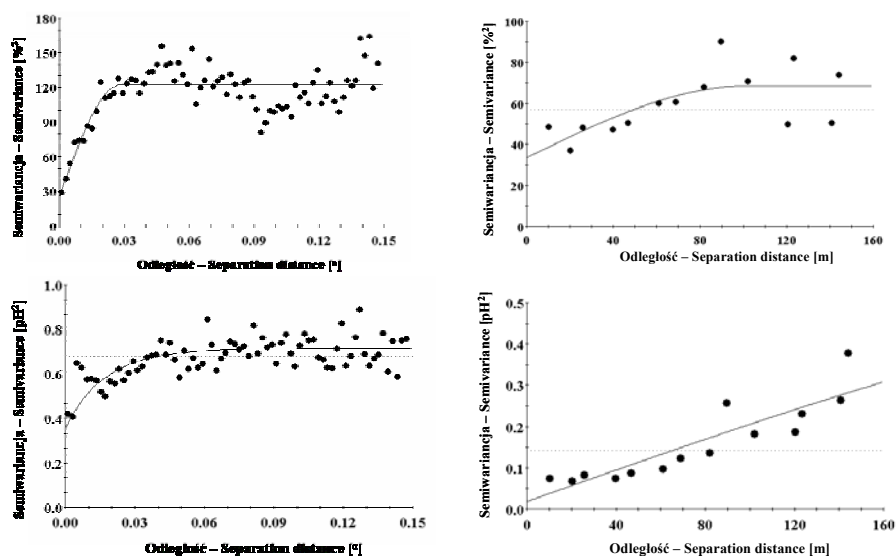


**Fig. 2.** Semivariograms and estimated mathematical models of sand content (upper graphs) and pH (lower graphs) for commune (left) and field (right).

Exemplary spatial distributions (sand content and pH) estimated by kriging method on the base of experimental semivariograms are presented in Fig. 3 (commune) and in Fig. 4 (field).

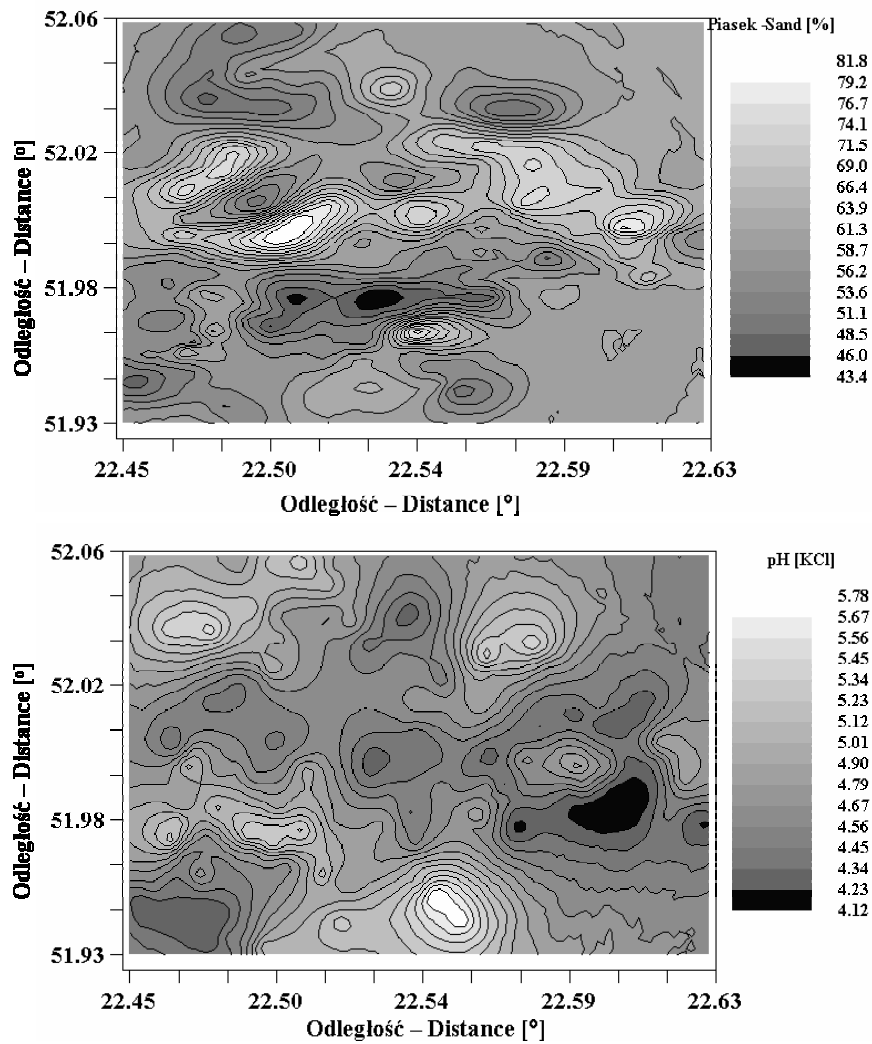


*Fig. 3. Estimated distributions of sand content and pH values in top layer of soil on commune area (in geographical coordinates).*

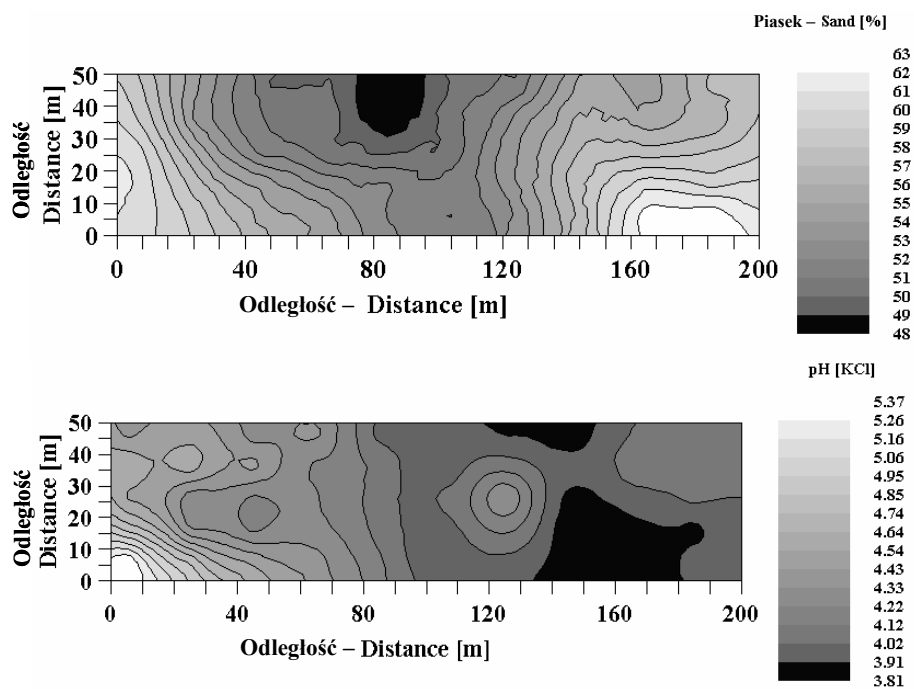


*Fig. 4. Estimated distributions of sand content and pH values in top layer of soil on cultivated field*

Values of semivariances, similarly to the standard deviations for defined granulometric fractions were the highest for sand and the lowest for clay. The range of spatial dependence (spherical model) of all granulometric fractions for the commune was similar (around  $0,03^\circ$ ). In the field this range was from 80 m (sand) to 15 m (clay). The range of spatial dependence for pH values in commune area was around  $0,03^\circ$  (exponential model), and this was not determinable in the field due to the linear character of the semivariance.

The interrelation between spatial distributions of granulometric fractions was observed for both the commune and the field. Moreover their latitudinal changes occur in the commune area. The sand content was highest in the central part of the commune while silt and clay prevailed in its northern and southern parts. Similar spatial distribution of pH was noted. One should mention that the estimation error for all soil properties on the whole sampling area was lower than 10% and this was around 2% in the vicinity of the sampling points.

This is worth noting that significant differentiation in spatial distribution of soil granulometric fractions and pH were observed in a field having the area of only 1 ha, where one usually expects homogenic soil properties. This indicates a need of taking more samples for estimation of soil properties in a field scale, as well as a need of estimation their spatial distribution.

## **CONCLUSIONS**

Geostatistic analysis of spatial distribution of soil granulometric fractions content and pH showed their significant differentiation and occurrence of spatial dependence in commune and field scales. Ranges of the spatial dependences were generally conjugated with the scale of the studied object.

The maps of the spatial distributions of the studied soil properties may be used for projecting proper soil management (tillage, fertilization, liming) in the studied areas.

## **REFERENCES**

1. Englund E., Sparks A. 1988: Geostatistical Environmental Assessment Software. Environmental Monitoring Systems Laboratory Office of Research and Development, U.S. Environmental Protection Agency, Las Vegas, NV 89193-3478.
2. Gamma Design Software GS+ v. 3.06.5 beta. 1998: Geostatistics for the environmental sciences.
3. Pannatier Y. 1994: Variowin 2.1. Program for geostatistical analysis. University of Lousanne.
4. Turski R., Uziak S., Zawadzki S. 1993: Środowisko przyrodnicze Lubelszczyzny – Gleby. LTN, Lublin, 1-107.
5. Webster R. 1985: Quantitative Spatial Analysis of Soil in the Field. *Advances in Soil Sci.* 3, 1-70.

## BIODEGRADATION OF ORGANIC CHEMICALS IN SOIL IN THE PRESENCE OF ACTIVATED CARBON

*Vasilyeva G.K., Strijakova E.R., Subocheva S.A., Nikolaeva S.N.*

### INTRODUCTION

One of the reasons for low effectiveness of soil bioremediation is the high toxicity of chemical contaminants to microbes and plants. The amendment to soil with some natural adsorbents can reduce chemical toxicity. Activated carbon (AC) is one of the best adsorbents for many organic chemicals because of its hydrophobicity, high specific surface, and microporous structure.

The objective of this research is to demonstrate the reduction in toxicity of three classes of pollutants (chloroanilines, polynitroaromatics and polychlorinated biphenyls) and to study mechanisms of their accelerated biodegradation and detoxification in soil in the presence of activated carbon.

### RESULTS AND DISCUSSION

Laboratory experiments with 3,4-dichloroanilines (DCA), 2,4,6-trinitrotoluene (TNT) and polychlorinated biphenyls (PCB) were conducted with several types of soil from Russia and the USA. Soil samples were artificially or naturally contaminated with these chemicals with the initial concentrations from 500 to 15000 mg/kg. Some samples were inoculated with microorganisms able to degrade these chemicals (e.g. *Pseudomonas aeruginosa* reducing TNT and some commercial rhizosphere microorganisms degrading PCB) or with strains able to use these chemicals as a sole source of carbon, nitrogen and energy (*Pseudomonas denitrificans* and other strains growing on DCA). A fractionated analysis of the soil was carried out to determine water extractable, solvent extractable and unextractable (bound) fractions of the chemicals. HPLC, GC and chromatomass-spectrometer were used for analytical determination of the chemicals and their metabolites in soil.

It was demonstrated that these microorganisms could grow in highly contaminated soils and transformed the chemicals only after soil amendment with appropriate brand and dose of activated carbon. The adsorbent maintained low toxic concentrations of the chemicals in soil solution to degrading microorganisms and plants. Meantime the adsorbed chemicals were mostly available to degrading microorganisms, however the rates of degradation of the chemical residues were slower than those at the beginning of the process. Nevertheless the toxicity of the

adsorbed chemicals to microorganisms, plants and biotest-organisms (*Daphnia magna*) remained very low. Mechanisms of the chemical degradation in the AC-amended soil were different.

*Biodegradation of DCA.* Only a minor reduction in DCA ( $C_0=15000$  mg/kg) was found in the untreated control soil after several months and the main DCA reduction was due to its binding (up to 27%) to soil matrix. Disappearance of DCA in the treated soil was sharply accelerated. The DCA was microbially degraded almost totally, that was confirmed by stoichiometric release of chloride-ion and low accumulation of bound DCA (up to 4%). In spite of some initial population decreases (from  $10^5$  to 1 cells/g just after inoculation), the number of the inoculated strain in soil began increasing and finally reached  $10^6$  cells/g by 60 d of incubation. Only trace concentrations of tetrachloroazobenzene were registered in the contaminated soil after bioremediation, while remarkable amount of the toxic and persistent metabolite is usually accumulated in DCA contaminated soil. Biotests with *Daphnia magna* demonstrated the absence of sharp and chronic toxicity of this soil after bioremediation. This approach has been successfully applied for bioremediation of highly contaminated soil after accidental leakage of herbicide propanil (3,4-dichloro-propylanilide) [1,2].

*Degradation and binding of TNT.* Disappearance of TNT ( $C_0=500-2000$  mg/kg) was also accelerated after mixing soil with activated carbon, and the largest effect was at the highest TNT concentration. Within 6 h after AC-amendment, extractable TNT decreased from 2000 to 1200 in the amended soil compared to 1800 mg/kg in unamended soil (40 and 10% decrease, respectively). After about 7 d, the process slowed but continued until only 4% of the initially added TNT was detected in the amended soil by 120 d. The final content of total extractable  $^{14}\text{C}$  (including [ $^{14}\text{C}$ ]TNT and its  $^{14}\text{C}$ -products) in the amended and unamended soils were 134 and 793 mg/kg, respectively. The content of water-extractable TNT in the soil sharply decreased to 3% just after AC introduction while its content in the control was 35%. The initial TNT concentrations in soil solution of the amended and control soils were 5 and 80 mg/l. The maximum accumulation of TNT reduction products in amended and unamended soils was similar (about 3% of the initially added TNT). However, in amended soil they were formed faster (maximum by 24 d) and finally decreased to 1%, while their concentration in control remained constant until the end of the incubation. In contrast, the accumulation of oxidation products in unamended soil was negligible (<0.2%) compared to amended soil where their total concentration reached 3.5% and diminished to 2% by the end of the incubation period.

Only minor amounts of  $^{14}\text{C}$ -TNT (1-2%) were mineralized to  $^{14}\text{CO}_2$  in both treatments. Almost all the disappeared extractable  $^{14}\text{C}$ -TNT was detected as bound  $^{14}\text{C}$ . However, the process of TNT binding occurred much faster and was more extensive in the AC-amended soil compared to the control. The bound  $^{14}\text{C}$ -products were very resistant to solvent extraction. Practically no  $^{14}\text{C}$ -products were released from the amended soil after 3 or 4 sequential extractions with acetonitrile. Plant tissues contained no more than 0.5% of the initially added  $^{14}\text{C}$ , demonstrating low accumulation of TNT and its products in corn plants growing in contaminated soil amended with AC.

Microbial toxicity of TNT was indicated by a greater than 50% decrease in plateable heterotrophic microorganisms in soils containing 1000 or 2000 mg TNT/kg. Similarly, the activated carbon reduced the phytotoxicity of TNT in the soil. While corn plant growth was severely inhibited in TNT-contaminated soil, their growth characteristics in AC-amended soil (TNT contaminated or uncontaminated) were similar to the uncontaminated control. The results corresponded to minimal phytotoxic concentration of TNT in solution in experiments with corn and tall fescue seedlings growing in hydroponics culture at presence of TNT. Their growth began to decline negligibly at 5 mg TNT/l while growth was inhibited or the seedling died at a higher concentration [3].

The next mechanism of accelerated detoxification of TNT in the AC-amended soil was suggested. The activated carbon promoted strong binding of TNT to soil matrix in two steps. First, some of the adsorbed TNT was quickly bound to AC through catalytic oxidation and polymerization of the oxidized products. Then the remaining TNT that was reversibly adsorbed to AC was microbially (and chemically) transformed to reduction products, which were bound to soil humus and likely polymerized with the TNT oxidation products. TNT oxidation in the amended soil presents evidences of strong oxidative properties of AC. It probably plays the role of catalyst that promotes formation of active oxygen containing species (OH-radical and others) on the AC surface including its intraporous spaces. The suggested mechanism of TNT binding in AC-amended soil is presented in [4]. The bound TNT products were shown to be nontoxic to heterotrophic soil microorganisms and plants.

*Detoxification of PCB.* First positive results have been received when adsorptive bioremediation was applied for soils highly contaminated with polychlorinated biphenyls (PCB) ( $C_0=200-4000$  mg/kg). Amendment of PCB contaminated soil with activated carbon sharply decreased their concentration and soil toxicity. Bio- and phytotoxicity of the treated soil reduced to minimal levels after 2 month' incubation, while low reduction of PCB concentration and toxicity

were detected in the untreated soil. Mechanism of PCB transformation in soil at presence of activated carbon is being studied.

## CONCLUSIONS

AC introduced to soil in adequate dose reduced concentration of DCA, TNT and probably PCB or its metabolites in soil solution to low toxicity to degrading microorganisms and plants; AC promoted total biodegradation of DCA accompanied by almost stoichiometric release of chloride-ions; AC promoted microbial reduction of TNT nitro-groups and simultaneously catalyzed chemical oxidation of its methyl-group that resulted in accelerated transformation of TNT to products of low toxicity that were strongly bound to the soil-carbon matrix. Mechanism of accelerated PCB detoxification in soil at presence of activated carbon is being studied.

**Acknowledgements.** This research was partly supported by RFBR and Moscow oblast' grant № 01-05-97006. We thank Dr. Pat Shea and J-M. Bollag for valuable discussions and use of laboratory facilities.

## REFERENCES

1. Bakhaeva LP, Vasilyeva GK, Surovtseva EG, Mukhin VM (2001) Microbial degradation of 3,4-dichloroaniline adsorbed to activated carbon. *Microbiology* 70: 277-284
2. Vasilyeva GK, Bakhaeva LP, Surovtseva EG (1996) The use of *in situ* soil adsorptive bioremediation following an accidental spill of propanil in the Krasnodar region of Russia. *Land Contam Reclam* 4: 263-268
3. Vasilyeva GK, Kreslavski VD, Shea PJ, Oh B-T (2001) Potential of activated carbon to decrease 2,4,6-trinitrotoluene toxicity and accelerate soil decontamination. *Environ Toxicol Chem* 20: 965-971
4. Vasilyeva GK, Kreslavski VD, Shea PJ, Bollag J-M (2002) Accelerated transformation and binding of 2,4,6-trinitrotoluene in soil amended with activated carbon. In: Violante A, Huang PM, Bollag JM, and Gianfreda L (eds) *Soil Mineral-Organic Matter - Microorganism Interactions and Ecosystems Health*. Ser. Development in Soil Science 28 B. Amsterdam and others, Elsevier. Pp. 157-168

## DETERMINATION OF WATER CHARACTERISTICS OF POLISH MINERAL SOILS WITH TDR METHOD APPLICATION

*Walczak R. T., Sławiński C., Witkowska-Walczak B.*

The water retention, saturated and unsaturated hydraulic conductivity coefficients are the basic hydrophysical characteristics of the soil. The correct determination of those characteristics is indispensable to obtain the required accuracy of the used models of water transport in soil profile. Therefore, the methods of measurement and estimation of these characteristics are extensively developed.

Unsaturated hydraulic conductivity is one of the most important physical soil characteristics. Applying TDR techniques and the instantaneous profile method (IPM) the measurement of hydraulic conductivity coefficient  $k(\psi)$  and also dynamic retention curve  $\theta(\psi)$  has become much faster and effective. It was demonstrated, that this method gives accurate results for various initial and boundary conditions applied to the soil sample. The instantaneous profile method (IPM) rest on simultaneously measurements of water content and water potential dynamic in the process of drying or wetting the soil column (see Fig.1, 2).

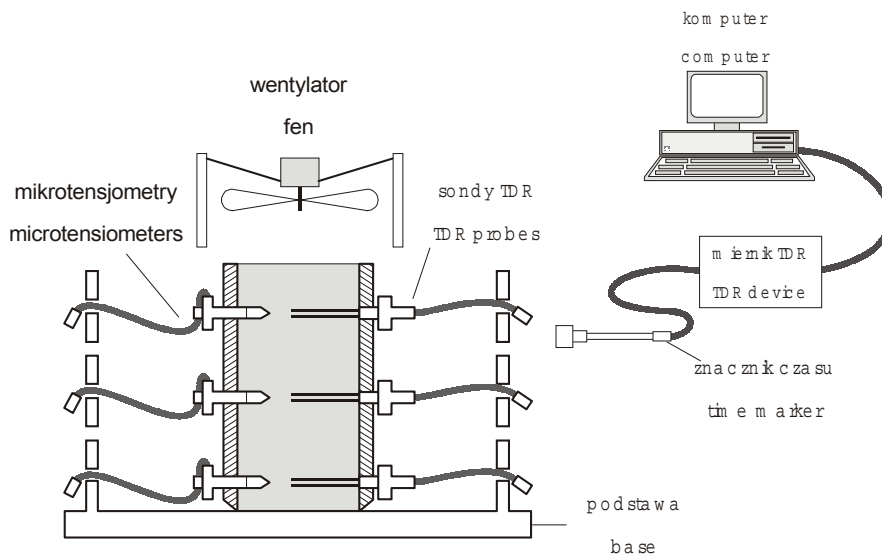


**Fig. 1.** TDR set-up for water content and water potential dynamic measurements in evaporation process

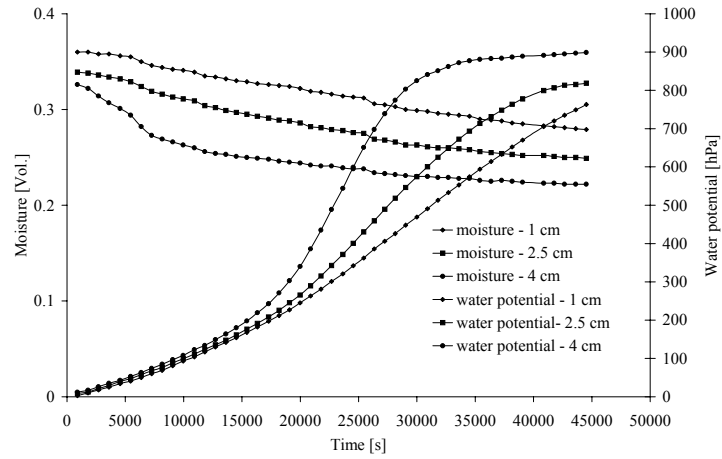


**Fig. 2.** Water content and water potential dynamic in soil column evaporation process

Assuming that the process of water transport takes place under isothermal conditions and is one-dimensional, the Darcy's law is valid for the proposed experimental conditions. The water flow can be described with the use of the following equation:

$$q(z, t) = -k(\psi) \left( \frac{\partial \psi(z, t)}{\partial z} - 1 \right) \quad (1)$$

Alternatively the flux can be calculated from the equation:

$$q(z, t) = - \int_{z=z_0}^z \frac{\partial \theta(z, t)}{\partial t} dz \quad (2)$$

Comparing these equations it is possible to calculate the hydraulic conductivity  $k(\psi)$  from the equation:

$$k(\psi) = \frac{\int_{z=z_0}^z \frac{\partial \theta(z, t)}{\partial t} dz}{\left( \frac{\partial \psi(z, t)}{\partial z} - 1 \right)} \quad (3)$$

Using this method it is possible to determine relationship between hydraulic conductivity coefficient and water potential (see Fig. 3) and so called dynamic retention curve (see Fig. 4).

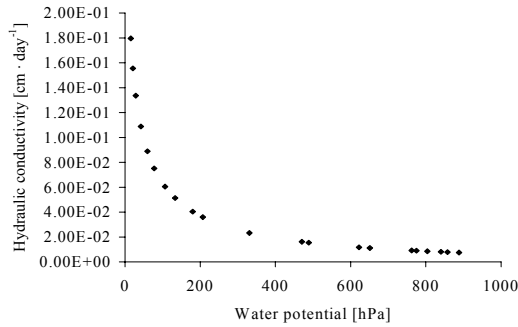


**Fig. 3.** Hydraulic conductivity coefficient as a function of water potential

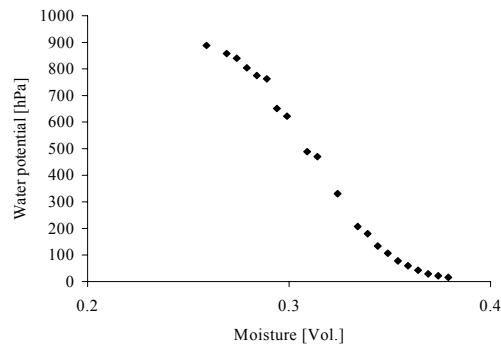


**Fig. 4.** Dynamic retention curve

Using TDR laboratory set-up and applying instantaneous profile methods (IPM) the hydraulic conductivity coefficients as a function of water potential and dynamic retention curve for minerals soil of Poland were determined. Also using Richard's chambers the static retention curves were measured. Results of mentioned investigations are documented by two qualities:

- average numerical values of chosen soil hydrophysical characteristics set in tabular form,
- cartographic presentation of the variability and differentiation of soil cover of arable lands according to the values of these characteristics.

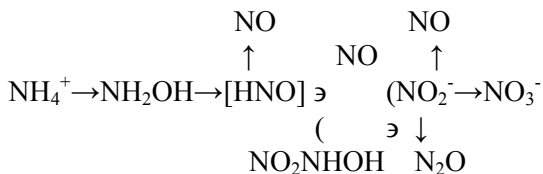
## NITROUS OXIDE EMISSION FROM SOILS

*Włodarczyk T., Kotowska U.*

Soils are important sources of number of greenhouse gases such as water vapour, CO<sub>2</sub>, CH<sub>4</sub> and N<sub>2</sub>O. In general, most N<sub>2</sub>O is formed from denitrification in oxygen deficient environment, although it can also be produced from chemolithotrophic nitrification in aerobic conditions (*Martikainen et al., 1993, Rice and Rogers 1993*).

N<sub>2</sub>O production is affected by many physical and biochemical factors, such as nitrate concentration, redox potential, organic matter content, temperature, soil pH and soil moisture content (*Horn et al., 1994, Yu et al., 2001*).

**NITRIFICATION** Although nitrification is understood to be an aerobic process there is strong evidence that it can also occur under anaerobic conditions. Nitrifying bacteria have been shown to produce NO and N<sub>2</sub>O. Nitrate reduction is now thought to be the major process involved in those gaseous emissions, with NH<sub>4</sub><sup>+</sup> oxidation providing the electrons for this denitrification process.



According to *Groffman* (1991) two processes are responsible for N<sub>2</sub>O formation from nitrification:

1. Ammonium oxidisers can use NO<sub>2</sub><sup>-</sup> as an alternative electron acceptor when O<sub>2</sub> is limiting and produce N<sub>2</sub>O. This process is called nitrifier denitrification.
2. Intermediates between NH<sub>4</sub><sup>+</sup> and NO<sub>2</sub><sup>-</sup>, or NO<sub>2</sub><sup>-</sup> itself, can chemically decompose to N<sub>2</sub>O, especially under acidic conditions (a type of chemodenitrification).

Nitrification is often considered to be the dominant source of N<sub>2</sub>O in "aerobic" soils (*Bremner and Blackmer, 1978*).

**ASSIMILATORY REDUCTION OF NITRATE** In nitrate assimilation, the first step is the reduction to nitrite, which is accomplished by the enzyme nitrate reductase. Subsequently, the nitrite is reduced to hydroxylamine by the enzyme nitrite reductase to finally be reduced to ammonia (*Payne, 1973*). The net reaction is shown in following equation:

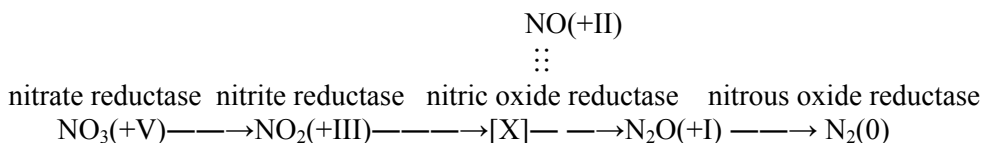




where  $\text{N}_2\text{O}$  rather than  $\text{N}_2$  may be produced as a by-product from the indicated intermediate (hyponitrite). The reaction shown is essentially the same as that which occurs during  $\text{NO}_3^-$  reduction to  $\text{NH}_4^+$  and involves the same precursor of,  $\text{N}_2\text{O}$  again probably hyponitrite (Frenay et al., 1979; Mosier et al., 1983).

**DISSIMILATORY REDUCTION OF NITRATE** When dissimilative reduction produces the gaseous dinitrogen or nitrous oxide compounds, the process is termed **denitrification**.

**Biological denitrification** is the last step in the N-cycle, where N is returned to the atmospheric pool of  $\text{N}_2$ . It is an anaerobic process. Biological denitrification is a respiratory process in which N-oxides (electron acceptors) are enzymatically reduced under anaerobic conditions to nitrous oxide and dinitrogen for ATP production by organisms that normally use  $\text{O}_2$  for respiration. The process of denitrification (including rhizobial denitrification) can be presented as follows:



### CONDITIONS AFFECTING NITROUS OXIDE PRODUCTION IN SOILS

*Oxygen* The oxygen status in soil, which is inversely, proportional to the amount of soil moisture, appears in many studies to be one of the key factors influencing nitrous oxide production (McKenney et al., 2001), (Fig.1 Włodarczyk, 2000).

*Redox potential* Changes in soil redox potential are related to changes in oxygen levels. The occurrence of a variety of microbial processes is related to specific redox potential. The highest  $\text{N}_2\text{O}$  emission from Eutric Cambisol was observed at 200 mV (Fig. 2 Włodarczyk, 2000).

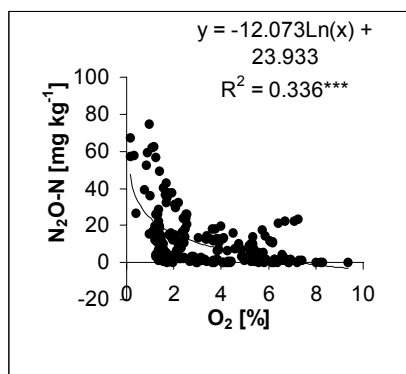


**Fig. 1.**  $N_2O$  emission vs.  $O_2$  content for the day of maximum emission.

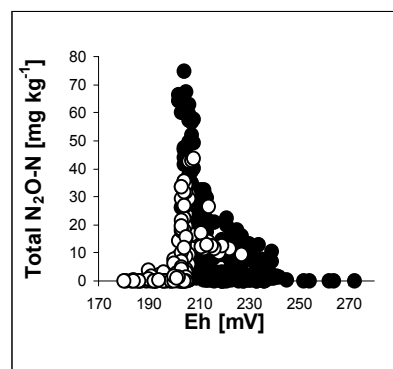


**Fig. 2.**  $N_2O$  emission as a function of Eh value (●emission ○absorption).

**Organic matter availability** Denitrification is a respiratory process, which requires an easily oxidisable organic substrate. The presence of readily metabolize organic matter and the availability of water soluble organic matter are closely correlated with the rate biological denitrification and hence the potential production of  $N_2O$  from soil. There is observed very high correlation between  $N_2O$  emission and organic matter content (Fig. 3 Włodarczyk, 2000).

**Dehydrogenases** These enzymes conduct a broad range of oxidative activities that are responsible for degradation, i.e., dehydrogenation, of organic matter. The amount of nitrous oxide formed due to denitrification showed high positive correlation with dehydrogenase activity (Fig. 4 Włodarczyk et al., 2001).

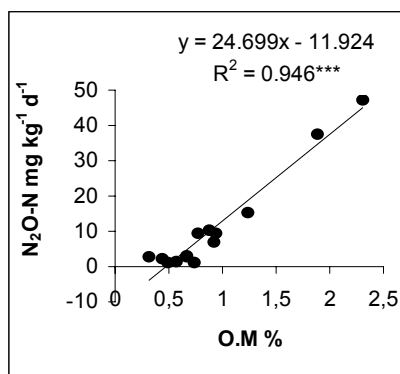


**Fig.3**  $N_2O$  emission as a function of organic matter content.

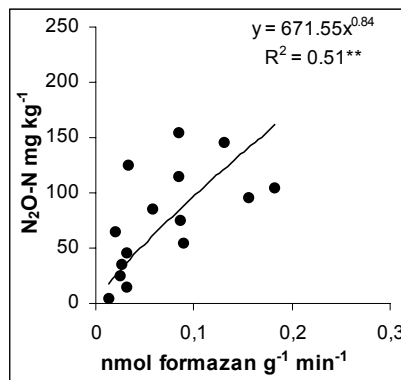


**Fig.4**  $N_2O$  emission as a function of dehydrogenase activity.

**pH** Under conditions where  $\text{NO}_3^-$  concentrations do not limit potential denitrification, the overall rates of both denitrification and nitrification decline with decreasing pH from optima of about pH 7.5 (Fig. 5 Włodarczyk 2000).

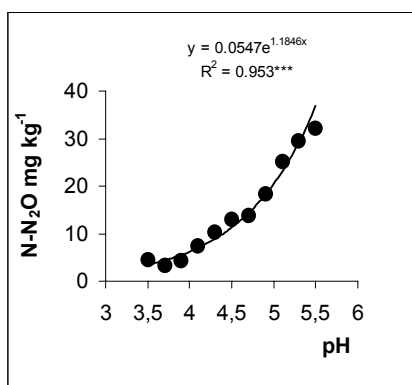


**Fig.5** Average of  $\text{N}_2\text{O}$  emission as a function of pH for the day of maximum emission.

**Nitrate concentrations** Total denitrification fluxes ( $\text{N}_2\text{O}$  plus  $\text{N}_2$ ) are directly proportional to soil  $\text{NO}_3^-$  concentrations when the other important component, a readily metabolizable organic substrate, is also present and non rate-limiting. When a lack of metabolizable organic matter limits potential denitrification,  $\text{N}_2$  plus  $\text{N}_2\text{O}$  fluxes do not increase with increasing  $\text{NO}_3^-$  concentration (Sahrawat and Keeney, 1986).

**Soil texture** The soil texture and particle size distribution significantly affected the production of  $\text{N}_2\text{O}$  (Fig. 6). Nitrous oxide production from heavier-textured soils exceeds that from coarse-textured soils up to 6-times (Włodarczyk, 2000).

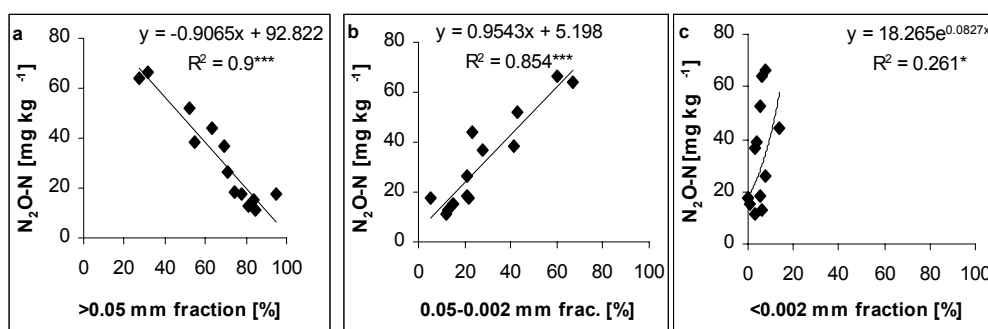


**Fig. 6**  $\text{N}_2\text{O}$  emission as a function of granulometric composition.

## LITERATURE

1. Bremner, J.M., Blackmer, A.M. (1978) Nitrous oxide: emission from soils during nitrification of fertiliser nitrogen. *Science* 199:295-296.
2. Freney, J.R.; Denmead, O.T., Simpson, J.R. (1979) Nitrous oxide emission from soils at low moisture contents. *Soil Biology and Biochemistry* 11:167-173
3. Groffman, P.M. (1991) Ecology of Nitrification and denitrification in soil evaluated at scales relevant to atmospheric chemistry. In Rogers, J.E. and Whitman, W.B. (eds) *Microbial production and consumption of greenhouse gases: methane, nitrogen oxides, and halomethanes*. American Society for Microbiology, Washington D.C. 201-217
4. Horn R., Stepniewski W., Włodarczyk T., Walenzik G., Eckhard F.E.W.: Denitrification rate and microbial distribution within homogenous model soil aggregates. *Int. Agrophysics*, 8, 65-74, 1994
5. Martikainen, P.J. De Boer, W. (1993) Nitrous oxide production and nitrification in an acidic soil from a Dutch coniferous forest. *Soil Biol. Biochem.* 25:343-347
6. McKenney, D.J., C.F. Drury, S.W. Wang. 2001. Effect of oxygen on denitrification inhibition, repression, and depression in soil columns. *Soil Sci. Soc. Am. J.* 65:126-132.
7. Mosier, A.R.; Parton, W.J.; Hutchinson, G.L. (1983) Modelling nitrous oxide evolution from cropped and native soils. In Hallberg, R. (ed) *Environmental biogeochemistry*. *Ecol. Bull. (Stockholm)* 35:229-241
8. Payne, W.J. (1973) Reduction of nitrous oxides by micro-organisms. *Bacteriological Reviews* 37: 409-452
9. Sahrawat, K.L., Keeney, D.R. (1986) Nitrous oxide emission from soils In Stewart, B.A. (ed.) (1986) *Advances in soil science volume 4*, Springer-Verlag, New York pp. 103-148
10. Rice, C.W., K.L. Rogers. 1993. Denitrification in subsurface environments: potential source for atmospheric nitrous oxide. p. 121-132. In D.E. Rolston et al. (eds) *Agricultural ecosystems effects on trace gases and global climate change*. ASA special publication 55.
11. Włodarczyk T.: N<sub>2</sub>O emission and absorption against a background of CO<sub>2</sub> in Eutric Cambisol under different oxidation-reduction conditions. Monography. *Acta Agrophysica*, No 28. 131-132, 2000.
12. Włodarczyk T. Stepniewski, W., Brzezińska, M. 2001
13. Yu K.W., Z. P. Wang, A. Vermoesen, W. H. Patrick Jr, O. Van Cleemput. 2001. Nitrous oxide and methane emission from different soil suspensions: effect of soil redox status. *Biol. Fertil. Soils* 34:25-30.

## CARBON CYCLING IN RHIZOSPHERE AND BULK SOIL AFTER <sup>13</sup>C PULSE-CHASE LABELING

*Yevdokimov I., Ruser R., Buegger F., Marx M., Goerke K.,  
Schneider D., Munch J.C.*

### OBJECTIVES

Complex interactions in *plant roots – microorganisms – soil* system depend on partitioning of assimilated C between plant roots, microbes, and CO<sub>2</sub> respired by microorganisms and roots. Besides, they are strongly determined by the turnover rates of C in roots and different soil carbon pools, especially of the most labile pools of microbial biomass and dissolved organic carbon (DOC). In this connection the objectives of our investigation were to determine:

- i) <sup>13</sup>C partitioning between roots, soil carbon pools and CO<sub>2</sub> emission after pulse chase labeling;
- ii) Kinetic characteristics of microbial populations in rhizosphere and bulk soil during all the period of plant growth.

### EXPERIMENTAL DESIGN AND METHODOLOGICAL APPROACHES

Dynamics of total and labeled carbon in roots and the main C pools of soil and rhizosphere were studied periodically during the first 80 – 90 h after the <sup>13</sup>C pulse-chase labeling (duration 5 h) in greenhouse experiment with oats (*Avena sativa L.*, day 47 after emergence, shooting growth stage). Soil (Cambisol, 1.4±0.2% C, 0.14±0.01% N, pH<sub>KCl</sub> 5.9±0.2, with sand, silt and clay fractions of 42%, 30% and 28% respectively) was sampled near Munich, Germany. Before starting the greenhouse experiment, soil was sieved (5 mm) and air-dried. To isolate rhizosphere from bulk soil, plants seedlings were put into special nylon bags filled with soil and placed in the center of pots.

Kinetic characteristics of microbial populations in bulk soil and rhizosphere were determined by *kinetic method* (Panikov and Sizova, 1996). The method involves simulation of both lag and exponential phases of microbial growth after addition of the excess quantities of readily decomposable C substrate using the following equations (Blagodatsky et al., 2000):

$$\begin{aligned}v(t) &= v_u + v_c \times \exp(\mu_{\max} \times t) \\x_0 &= (v_c \times 0.9 \times Y_{x/p}) / (r_0 \times \mu_{\max}) \\r_0 &= (v_c \times 0.1) / (v_u + v_c \times 0.1) \\x' &= x_0 \times r_0\end{aligned}$$

where  $v(t)$  -  $\text{CO}_2$  production rate;  $t$  - time;  $x_0$  - microbial biomass before addition of C substrate,  $x'$  - active microbial biomass;  $r_0$  - fraction of the “active” microbial biomass;  $v_C$  - coupled respiration rate;  $v_U$  - uncoupled respiration rate;  $\mu_{\max}$  - maximal specific growth rate;  $Y_{x/p}$  - yield factor equal to 1.5 (Blagodatsky et al., 2000).

Mixed soil samples prepared from 5 sub-samples (5 pots with plants) were used for all the analysis for each sampling time. Total and labeled C in roots and soil carbon pools are the mean of 5 replicates, kinetic parameters are the mean of 3 replicates. The kinetics of microbial growth was studied after addition of four C substrates – 1) glucose, 2) mixture of amino acids, organic acids, sugars (“organic mixture” simulating natural root exudates), 3) roots extract, and 4) sterilized soil. Kinetic parameters in soil after addition of glucose and “organic mixture” were determined weekly in the course of all the period of the greenhouse experiment (before and after pulse-chase labeling). The rest two substrates were used for bulk soil and rhizosphere only at the shooting growth stage. All the substrates were concentrated to reach 4 – 6 mg substrate C added per 1 g of bulk or rhizosphere soil.

## RESULTS AND DISCUSSION

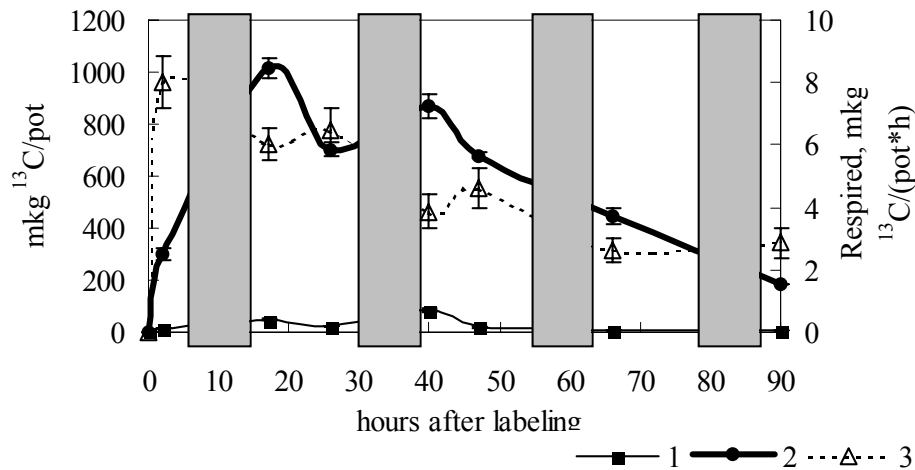


**Fig. 1.**  $^{13}\text{C}$  dynamics (mean  $\pm$  SE) in rhizosphere after pulse-labeling: 1 -  $^{13}\text{C}$  in DOC; 2 -  $^{13}\text{C}$  in microbial biomass; 3 -  $^{13}\text{C}\text{-CO}_2$  (respired by roots and microorganisms of soil and rhizosphere). Gray area indicates nighttime.

The dynamics of  $^{13}\text{C}$  in rhizosphere microbial C and DOC were opposite to that for  $\text{CO}_2 - ^{13}\text{C}$  fluxes from soil with plants immediately after the pulse-labeling (Fig.1): minimums in microbial C and DOC coincided with the maximums in  $\text{CO}_2$  emissions, and vice versa.  $^{13}\text{C}$  values in the carbon pools oscillated periodically depending on day – night changes (i.e. on activity of the processes of photo-assimilation and translocation of photo-assimilates to roots and rhizosphere): maximums in  $^{13}\text{C}$  in DOC and microbial biomass in rhizosphere were revealed after nighttime. After 66 h this tendency was smoothed over because of decrease in total  $^{13}\text{C}$  content in soil (Fig.1, 2).

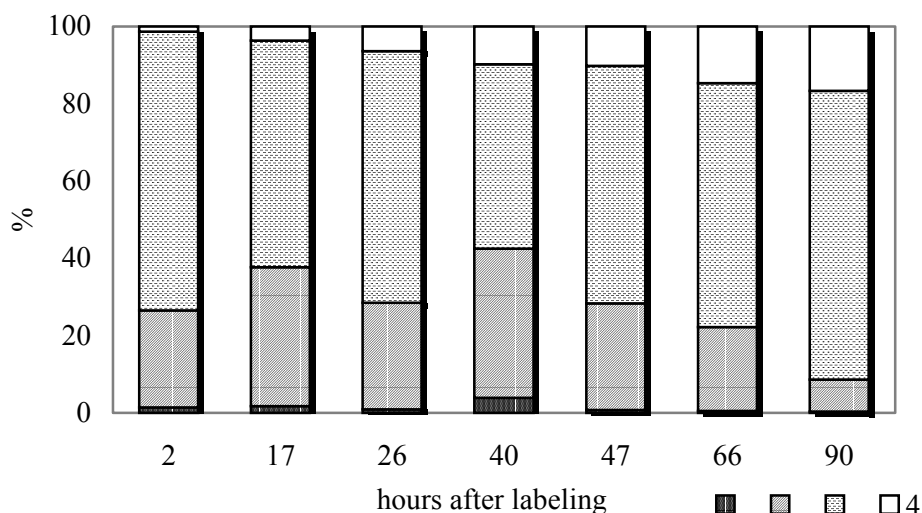


**Fig .2.** Partitioning of  $^{13}\text{C}$  in rhizosphere between DOC (1), microbial biomass (2), roots (3) and  $\text{CO}_2$  respired (4)

Considerable part of  $^{13}\text{C}$  translocated (about  $\frac{1}{4}$  of total  $^{13}\text{C}$  below-ground translocation) was found in biomass of rhizosphere microorganisms as soon as by 2h after pulse labeling (Fig. 2). Sum of  $^{13}\text{C}$  in microbial biomass and DOC was approximately equal to the total  $^{13}\text{C}$  pool in rhizosphere soil till the sampling at 90 h when sufficient incorporation of  $^{13}\text{C}$  to soil organic matter was revealed. It might be explained in two ways: i) only low-molecular substances readily decomposable by rhizosphere microorganisms were exuded in first 3 – 4 days after pulse labeling; ii) no sufficient microbial synthesis of high-molecular substances on the base of freshly exuded components took place on this period. Thus, close inter-relations between  $^{13}\text{C}$  dynamics in C pools in rhizosphere and plant activity were revealed in a short-term (hrs or few days) scale for rhizosphere of oats. Freshly – exuded

*carbon was involved mainly into microbial biomass, and sufficient incorporation into soil organic matter was revealed only by 90 h after pulse labeling.*

Microbial populations of bulk soil and rhizosphere were found to have similar values of maximal specific growth rates ( $0.2 - 0.3 \text{ h}^{-1}$ ), with weak fluctuations during the period of the greenhouse experiment. It means that fast immobilization of newly exuded  $^{13}\text{C}$ -containing substances by rhizosphere microorganisms cannot be explained only by more intensive growth of micro biota in rhizosphere compare to bulk soil. At the same time, larger pools of total and active microbial biomass were found in rhizosphere. Percentage of active microbial biomass in rhizosphere averaged for all the period of samplings was 1.5 and 2.5 times higher that that for bulk soil for C substrates glucose and “organic mixture”, respectively.

Among four C substrates tested, “organic mixture” and roots extract were found the best for the microbial populations of rhizosphere and bulk soil. Kinetics of  $\text{CO}_2$  formation after addition of roots extract gave lower values of total and active microbial biomass C than after application of “organic mixture”. However, soil enriched with roots extract showed highest specific growth rates among all four substrates tested. *Thus, short – term interactions in plant roots – microorganisms – soil system were indicated by  $^{13}\text{C}$  dynamics in roots, C pools of bulk and rhizosphere soil, and  $\text{CO}_2$  emissions. These interactions are the subject for the further simulations by more sophisticated models, taking into account kinetic characteristics of microbial populations in bulk soil and rhizosphere after addition of different C substrates.*

**Acknowledgements** This research was supported by Alexander von Humboldt Foundation, Russian Foundation for Basic Research (projects 02-04-48623 and 02-04-49843) and by Russian Ministry of Industry and Science (contract 43.016.11.1625).

## REFERENCES

1. Blagodatsky, S.A., Heinemeyer, O., Richter, J, 2000. Estimating the active and total soil microbial biomass by kinetic respiration analysis. *Biology & Fertility of Soils* 32, 73-81.
2. Panikov, N.S., Sizova, M.V., 1996. A kinetic method for estimating the biomass of microbial functional groups in soil. *Journal of Microbiological Methods* 24, 219-230.

## **AUTHORS:**

<i>Abashina Nadejda MSc</i>	<i>IPBPSS*, Laboratory of Physicochemistry of Soils abashina@issp.serpukhov.su</i>
<i>Abramichev Alexey MSc</i>	<i>Institute of Basic Biological Problems RAS alex@stack.net</i>
<i>Alekseev Andry PhD</i>	<i>IPBPSS, Laboratory of Geochemistry and Soil Mineralogy alekseev@issp.serpukhov.su</i>
<i>Alekseeva Tatiana PhD</i>	<i>IPBPSS, Laboratory of Geochemistry and Soil Mineralogy alekseeva@issp.serpukhov.su</i>
<i>Alekseeva Veronika PhD</i>	<i>Moscow State University, Russia, Geography Faculty, Department of Geomorphology and Palaeogeography valekseeva@rambler.ru</i>
<i>Balakhnina Tamara PhD</i>	<i>Institute of Basic Biological Problems RAS, Puschino</i>
<i>Banach Artur MSc</i>	<i>Catholic University Lublin</i>
<i>Benicelli Ricardo PhD</i>	<i>Catholic University Lublin</i>
<i>Besse Pascale PhD</i>	<i>Universite Blaise Pascal, Aubiere Cedex, France Laboratoire de Synthese Et Etude de Systemes Interet Biologique besse@chisg1.univ-bpclermont.fr</i>
<i>Bieganski Andrzej PhD</i>	<i>IA**, Department of Hydrotermophysics of Soil Environment and Agricultural Materials biegan@demeter.ipan.lublin.pl</i>
<i>Binet Françoise PhD</i>	<i>Universite de Rennes I, Rennes Cedex, France Laboratoire Fonctionnement des Ecosystemes et Biologie de la Conservation fbinet@mailhost.univ-rennes1.fr</i>
<i>Borisov Alexander PhD</i>	<i>IPBPSS, Laboratory of Archaeological Soil Science a.v.borisov@rambler.ru</i>
<i>Buegger F. PhD</i>	<i>Institute of Soil Ecology, GSF- Research Center, Neuherberg, Germany</i>
<i>Davies Geoffrey PhD</i>	<i>Barnett Institute, Northeastern University Department of Chemistry, Boston, MA, 02115, USA</i>
<i>Delort Anne-Marie Prof</i>	<i>Université Blaise Pascal, Aubiere Cedex, France Laboratoire de Synthese Et Etude de Systemes Interet Biologique amdelort@chimtp.univ-bpclermont.fr</i>
<i>Demkina Tatiyana PhD</i>	<i>IPBPSS, Laboratory of Soil Microbiology demkina@issp.psn.ru</i>

<i>Demkin Vitaliyy DrSc</i>	<i>IPBPSS, Laboratory of Archaeological Soil Science demkin@issp.serpukhov.su</i>
<i>Dmitrakov Leonid PhD</i>	<i>IPBPSS, Laboratory of Physicochemistry of Soils pinsky@issp.serpukhov.su</i>
<i>Dmitrakova Ludmila PhD</i>	<i>IPBPSS, Laboratory of Physicochemistry of Soils pinsky@issp.serpukhov.su</i>
<i>Elzov Maxim MSc</i>	<i>IPBPSS, Laboratory of Archaeological Soil Science m_eltsov@mail.ru</i>
<i>Farkas Csilla PhD</i>	<i>Institute for Soil Science and Agricultural Chemistry of HAS, Budapest, Hungary csilla@rissac.hu</i>
<i>Forano Claude PhD</i>	<i>Universite Blaise Pascal, Aubicre Cedex, France, Laboratoire des Materiaux Inorganiques forano@chimsrv1.univ-bpclermont.fr</i>
<i>Ghabbour Elham A. PhD</i>	<i>Barnett Institute, Northeastern University Department of Chemistry, Boston, MA, 02115, USA</i>
<i>Goerke K. PhD</i>	<i>Institute of Soil Ecology, GSF- Research Center, Neuherberg, Germany</i>
<i>Hajnos Mieczysław DrSc</i>	<i>IA, Department of Physical Chemistry of Agricultural Materials mhajnos@demeter.ipan.lublin.pl</i>
<i>Horabik Józef Prof</i>	<i>IA, Laboratory of Physics of Plant Granular Solids jhorabik@demeter.ipan.lublin.pl</i>
<i>Józefaciuk Grzegorz DrSc</i>	<i>IA, Department of Physical Chemistry of Agricultural Materials jozefaci@demeter.ipan.lublin.pl</i>
<i>Kerjentzev Anatolyi DrS</i>	<i>Institute of Basic Biological Problems RAS, Puschino</i>
<i>Khokhlova Olga PhD</i>	<i>IPBPSS, Laboratory of Geochemistry and Soil Mineralogy olgakhl@issp.serpukhov.su</i>
<i>Koptsik Galina PhD</i>	<i>Moscow State University koptsik@skop.phys.msu.su</i>
<i>Korsunskaja Ludmila PhD</i>	<i>IPBPSS, Soil-Ecological Station</i>
<i>Kossowski Jan PhD</i>	<i>IA, Department of Hydrotermophysic of Soil Environment and Agricultural Materials j.kossowski@demeter.ipan.lublin.pl</i>
<i>Kotowska Urszula MSc</i>	<i>IA, Department of Aeration and Gas Exchange in Soil Environment and Agricultural Materials ukot@demeter.ipan.lublin.pl</i>
<i>Księżopolska Alicja PhD</i>	<i>IA, Department of Physical Chemistry of Agricultural Materials aksiezo@demeter.ipan.lublin.pl</i>

<i>Kudeyarova Agniya DrSc</i>	<i>IPBPSS, Laboratory of Geochemistry and Soil Mineralogy vnk@issp.serpukhov.su</i>
<i>Kudeyarov Valery Prof</i>	<i>IPBPSS, Institute Director,</i>
<i>Kurochkina Galina PhD</i>	<i>IPBPSS, Laboratory of Physicochemistry of Soils pinsky@issp.serpukhov.su</i>
<i>Lamorski Krzysztof MSc</i>	<i>IA, Department of Hydrotermophysics of Soil Environment and Agricultural Materials lamorski@demeter.ipan.lublin.pl</i>
<i>Lukina Natalia PhD</i>	<i>Institute of North Environmental Problems nikonov@cepl.rssi.ru</i>
<i>Maher Barbara Prof</i>	<i>Lancaster University, Centre for Environmental Magnetism and Paleomagnetism, Department of Geography, UK.</i>
<i>Marx M. PhD</i>	<i>Institute of Soil Ecology, GSF- Research Center, Neuherberg, Germany</i>
<i>Matyka-Sarzyńska Dorota PhD</i>	<i>IA, Department of Physical Chemistry of Agricultural Materials dmatyka@demeter.ipan.lublin.pl</i>
<i>Mikhailov Alexei MSc</i>	<i>IPBPSS, Laboratory of Modelling of Ecosystems alexei_mikhailov@mail.ru</i>
<i>Molenda Marek DrSc</i>	<i>IA, Laboratory of Physics of Plant Granular Solids mmolenda@demeter.ipan.lublin.pl</i>
<i>Munch J.PhD</i>	<i>Institute of Soil Ecology, GSF- Research Center, Neuherberg, Germany</i>
<i>Nikonov Vyacheslav PhD</i>	<i>Institute of North Environmental Problems nikonov@cepl.rssi.ru</i>
<i>Oleynik Sergey PhD</i>	<i>IPBPSS, Laboratory of Geochemistry and Soil Mineralogy olgakhl@issp.serpukhov.su</i>
<i>Pachepsky Yakov Prof</i>	<i>USDA-ARS Environmental Microbial Safety Laboratory, Beltsville MD, USA ypachepsky@anri.barc.usda.gov</i>
<i>Pampura Tamara PhD</i>	<i>IPBPSS, Laboratory of Physicochemistry of Soils pinsky@issp.serpukhov.su</i>
<i>Piekarz Jarosław MSc</i>	<i>IA, Department of Agrophysical Bases of Soil Environment Management buli@demeter.ipan.lublin.pl</i>
<i>Pinsky David DrSc</i>	<i>IPBPSS, Laboratory of Physicochemistry of Soils pinsky@issp.serpukhov.su</i>

<i>Priputina Irina PhD</i>	<i>IPBPSS, Laboratory of Modelling of Ecosystems pripulina@issp.serpukhov.su</i>
<i>Rudko Tadeusz PhD</i>	<i>IA, Laboratory of Physical Properties of Crop rudko@demeter.ipan.lublin.pl</i>
<i>Ruser R. PhD</i>	<i>Institute of Soil Ecology, GSF- Research Center, Neuherberg, Germany</i>
<i>Rutgers Michiel PhD</i>	<i>Institute of Public health and the Environment (RIVM), Bilthoven, Netherlands Michiel.Rutgers@rivm.nl</i>
<i>Sancelme Martine PhD</i>	<i>Universite Blaise Pascal, Aubiere Cedex, France Laboratoire de Synthèse Et Etude de Systemes Interet Biologique besse@chisg1.univ-bpclermont.fr</i>
<i>Schneider D. PhD</i>	<i>Institute of Soil Ecology, GSF- Research Center, Neuherberg, Germany</i>
<i>Shein Evgeni Prof</i>	<i>Moscow State University, Department of Physics and Melioration of Soils, Soil Science Faculty</i>
<i>Shirshova Ludmila PhD</i>	<i>IPBPSS, Laboratory of Mass- and Energy Transfer in Soils shirshova@issp.serpukhov.su</i>
<i>Skierucha Wojciech PhD</i>	<i>IA, Department of Hydrotermophysics of Soil Environment and Agricultural Materials skieruch@demeter.ipan.lublin.pl</i>
<i>Sławiński Cezary PhD</i>	<i>IA, Department of Hydrotermophysics of Soil Environment and Agricultural Materials cslawin@demeter.ipan.lublin.pl</i>
<i>Sokolowska Zofia Prof</i>	<i>IA, Department of Physical Chemistry of Agricultural Materials sokolows@demeter.ipan.lublin.pl</i>
<i>Stepniewska Zofia Prof</i>	<i>IA, Department of Aeration and Gas Exchange in Soils and Agricultural Materials stepniews@demeter.ipan.lublin.pl</i>
<i>Stepniewski Witold Prof</i>	<i>Lublin University of Technology stepw@fenix.pol.lublin.pl</i>
<i>Strizhakova Elena MSc</i>	<i>IPBPSS, Laboratory of Physicochemistry of Soils helene@issp.psn.ru</i>
<i>Subocheva Svetlana PhD</i>	<i>Moscow State University, Chemical Department</i>
<i>Świeboda Ryszard PhD</i>	<i>Medical Academy Lublin, Department of Pharmacy rysio@eskulap.am.lublin.pl</i>
<i>Szajnocha Katarzyna MSc</i>	<i>Catholic University Lublin</i>

<i>Szatanik-Kloc Alicja PhD</i>	<i>IA, Department of Physical Chemistry of Agricultural Materials akloc@demeter.ipan.lublin.pl</i>
<i>Usowicz Bogusław DrSc</i>	<i>IA, Department of Hydrotermophysics of Soil Environment and Agricultural Materials usowicz@demeter.ipan.lublin.pl</i>
<i>Vasilyeva Galina PhD</i>	<i>IPBPSS, Laboratory of Physicochemistry of Soils vasilyeva@issp.serpukhov.su</i>
<i>Walczak Ryszard Prof</i>	<i>IA, Institute Director, Department of Hydrotermophysics of Soil Environment and Agricultural Materials rwalczak@demeter.ipan.lublin.pl</i>
<i>Wilczek Andrzej MSc</i>	<i>IA, Department of Hydrotermophysics of Soil Environment and Agricultural Materials awilczek@demeter.ipan.lublin.pl</i>
<i>Witkowska-Walczak Barbara DrSc</i>	<i>IA, Department of Hydrotermophysics of Soil Environment and Agricultural Materials bwitwal@demeter.ipan.lublin.pl</i>
<i>Włodarczyk Teresa PhD</i>	<i>IA, Department of Aeration and Gas Exchange in Soil Environment and Agricultural Materials teresa@demeter.ipan.lublin.pl</i>
<i>Wolińska Agnieszka MSc</i>	<i>Catholic University Lublin</i>
<i>Yevdokimov Il'ya PhD</i>	<i>IPBPSS, Laboratory of Soil Cycles of Nitrogen and Carbon</i>

\* *IPBPSS*      *Institute of Physicochemical and Biological Problems in Soil Science, Russian Academy of Sciences*  
Pushchino Moscow region 142292 RUSSIA

\*\* *IA*            *Institute of Agrophysics, Polish Academy of Sciences*  
ul. Doświadczalna 4, 20-290 Lublin POLAND